UNIVERSITY OF CALIFORNIA,
IRVINE

Unraveling the role of *Toxoplasma gondii*'s mitochondrial superoxide dismutase

DISSERTATION

Submitted in partial satisfaction of the requirements
for the degree of

DOCTOR OF PHILOSOPHY

In Biomedical Sciences

By

James Alexander Tirtorahardjo

Dissertation Committee:
Assistant Professor Rosa M. Andrade, Chair
Professor Ming Tan
Professor Alan Barbour
Professor Melissa B. Lodoen
Associate Professor Naomi Morrissette

2023

TABLE OF CONTENTS

LIST OF FIGURES

LIST OF TABLES

ACKNOWLEDGEMENTS

To my committee chair and PI, Rosa Andrade: Thank you for taking me into your lab and granting me the opportunity to research these little monsters. Rosa's hard work has ensured that I could complete this story, and for that I am extremely grateful. Her mentorship and support will serve as an inspiration for my continued growth as a scientist.

To my dissertation committee, Alan Barbour, Ming Tan, Naomi Morrissette, and Melissa Lodoen: Thank you for your expertise, time, and guidance through these years.

To my former mentors, Michele Kempik and Shahrdad Lotfipour: Thank you for setting me down this path of research. My time in your labs convinced me that I should pursue graduate studies and push the boundaries of human knowledge.

Christopher Ma: Your mentorship was absolutely critical to the completion of this work. You've taught me everything I know about tissue culture and the finer points of genetic engineering. Our discussions over the years have been insightful and helped me grow into who I am now.

Additional thanks to my undergraduate students: Sakura Schweizer, Yanmiao Du, Shaw Rosario, Jerry Zhang, Noor Elbershawi, Zian Fang, Cindy Huang, Brian Sun, Tom Park, and Daniel Marquez. Thank you for your assistance in running the various experiments and procedures in the Andrade Lab. Mentoring all of you has been a pleasure. I'm looking forward to all the things you will do.

To my friends, cabin mates, party members, guildmates, and crew: Thank you for reminding me that there's life outside of lab, being sporting recipe test subjects, and taking me on all manner of adventures. Whether we met as cadets, or somewhere later along the way, I would not have completed this work without all of you. Special thanks to Aliza Le for her guidance through the dissertation writing process.

To my family: my mom (Suzana), dad (Budi), and brothers (Jason and Ethan). Thank you for supporting me through this journey. Thank you for the meals, infinite patience, and advice throughout the years. I hope I can continue to make you all proud.

Financial Support: I thank the Graduate Division Completion Fellowship.

A portion of text from Chapter 2 is a reprint of the material as it appears in Auranofin Resistance in *Toxoplasma gondii* Decreases the Accumulation of Reactive Oxygen Species but Does Not Target Parasite Thioredoxin Reductase, published by Frontiers from Frontiers in Cellular and Infection Microbiology, accessible at https://doi.org/10.3389/fcimb.2021.618994. The co-authors included Christopher I. Ma, James A.Tirtorahardjo, Sharon Jan, Sakura S. Schweizer, Shawn A. C. Rosario, Yanmiao Du, Jerry J. Zhang, Naomi S. Morrissette, and Rosa M. Andrade. Christopher I. Ma directed and supervised research which forms the basis for the dissertation.

VITA

James Alexander Tirtorahardjo

EDUCATION

2015 Bachelors of Science, Biological Sciences, University of California, Irvine

2023 Doctor of Philosophy, Biomedical Sciences, University of California, Irvine
Advisor: Rosa M. Andrade, Assistant Professor, Department of Microbiology and Molecular Genetics

HONORS & AWARDS

2022 Graduate Division Completion Fellowship

PUBLICATIONS (* indicates co-authorship)

*Christopher Ma, **James Tirtorahardjo**, Sakura Schweizer, Jerry Zhang, Zian Fang, Li Xing, Mingjie Xu, David Herman, Michael Kleinman, Brandon Mccullough, Amy Barrios, and Rosa Andrade (2023). Gold(I) ion and the phosphine ligand are necessary for the anti-*Toxoplasma gondii* activity of Auranofin. Microbiol. Spectr.

*Christopher Ma, **James Tirtorahardjo**, Sharon Jan, Sakura Schweizer, Shawn Rosario, Yanmiao Du, Jerry Zhang, Naomi Morrissette, and Rosa Andrade (2021). Auranofin resistance in *Toxoplasma gondii* decreases the accumulation of reactive oxygen species but does not target parasite thioredoxin reductase. Front. Cell. Infect. Microbiol. 11:618994.

*Shahrdad Lotfipour, Celina Mojica, Sakura Nakauchi, Marcela Lipovsek, Sarah Silverstein, Jesse Cushman, **James Tirtorahardjo**, Andrew Poulos, Ana Belén Elgoyhen, Katumi Sumikawa, Michael S. Fanselow, and Jim Boulter (2017). α2* Nicotinic acetylcholine receptors influence hippocampus-dependent learning and memory in adolescent mice. Learn. Mem. 24: 231-244

MEETING PRESENTATIONS

James Tirtorahardjo, Christopher Ma, Rosa Andrade. Elucidating the role of *Toxoplasma gondii*'s mitochondrial superoxide dismutase. Talk presented at: SCEP 2023. Proceedings of the 13th Southern California Eukaryotic Pathogen Symposium; 2023 Nov. 8; Riverside, CA.

Christopher Ma, **James Tirtorahardjo**, Sharon Jan, Sakura Schweizer, Xi Li, Rosa Andrade. *Toxoplasma gondii* acquires auranofin resistance without mutations in the thioredoxin reductase gene. Poster presented at: SCEP 2018. Proceedings of the 8th Southern California Eukaryotic Pathogen Symposium; 2018 Nov. 28; Riverside, CA.

ABSTRACT OF THE DISSERTATION

Unraveling the role of *Toxoplasma gondii*'s mitochondrial superoxide dismutase

By

James Alexander Tirtorahardjo

Doctor of Philosophy in Biomedical Sciences

University of California, Irvine, 2023

Assistant Professor Rosa M. Andrade, Chair

Toxoplasma gondii is the only apicomplexan parasite known to possess a well-developed reactive oxygen species (ROS) scavenging system which includes an endogenous catalase and complete glutathione and thioredoxin pathways. Compared against other apicomplexan parasites, *T. gondii* is uniquely equipped with a wide array of ROS scavenging systems. These ROS scavenging enzymes are key to neutralizing both endogenous and host cell generated ROS. By virtue of having more ROS scavenger systems, *T. gondii* may be capable of tolerating a wider variety of intracellular conditions, which is then reflected in its wide host cell tropism. Conversely, these ROS scavenging systems may also be the key to eliminating parasitic infections as their components are unique to the parasite. Several treatment options are able to selectively inhibit the activity of parasite ROS scavengers, and thereby treat various apicomplexan parasitic infections.

Of ROS scavenger targeting therapeutic strategies, auranofin was thought to specifically inhibit pathogen thioredoxin reductase. To determine if thioredoxin reductase is still the target of auranofin in *T. gondii*, we isolated drug resistant mutants. Auranofin resistant *T. gondii* parasites, harbor mutations in *T. gondii*'s mitochondrial superoxide dismutase (TgSOD2). These parasites showed reduced accumulation of ROS upon exposure to auranofin. However, the L201P mutation of TgSOD2 is not sufficient to confer resistance to auranofin. Our work indicated that auranofin likely induces parasite death by apoptosis: evidenced by parasite

shrinkage and exposure of phosphatidylserine (PS) residues on the parasite surface detected by Annexin V.

To understand the role of TgSOD2 throughout the parasite's life, we generated inducible knockdown mutants using an auxin-inducible degron system that allowed us to explore the role of TgSOD2 in parasite replication and replication fitness (*Chapter Three*). During stages of extracellular stress, TgSOD2 transcription is upregulated. TgSOD2 depletion leads to reduction in replication fitness as these parasites showed decreased plaque formation when compared to their parental line. At the mitochondrial level, depletion of TgSOD2 results in aberrant mitochondrial morphology as well as reduction of the parasite's mitochondrial membrane potential. Through a proximal biotinylation approach, we found that TgSOD2 localizes adjacent to complexes IV and V of *T. gondii* mitochondrial electron transport chain, suggesting that these may be sites of ROS generation or ROS sensitive enzyme subunits. Our studies are the first ones to demonstrate the role of TgSOD2 in parasite life and mitochondrion maintenance.

Lastly, *Chapter Four* describes the future lines of inquiry opened by the findings presented in *Chapters Two and Three*. Based on the studies presented, TgSOD2 is likely implicated in the formation or maintenance of the ATP synthase complex. Furthermore, inhibition of TgSOD2 may sensitize the parasite to further ROS damage. Future studies ought to investigate the link between TgSOD2 and ATP synthase, then evaluate the viability of dual inhibition as a therapeutic strategy for *T. gondii* infection clearance.

CHAPTER ONE: Introduction and Overview of the Dissertation

Mitochondrial metabolism in *T. gondii*

Toxoplasma gondii is an obligate intracellular apicomplexan parasite responsible for toxoplasmosis. While felines are this parasite's definitive host, *T. gondii* can still infect other warm-blooded creatures such as mammals and birds. This parasite can infect an extremely wide range of host cells: namely, any nucleated cell of said warm-blooded animal. These infections have two distinct phases: the acute phase, marked by the presence of rapidly dividing tachyzoites; and the chronic phase, which includes bradyzoite encystation within neurons and muscles. These tissue cysts are highly persistent, with the cyst wall preventing access of drugs or immune cells to the sheltered bradyzoites. When conditions permit, these cysts can undergo reactivation, releasing rapidly dividing tachyzoites in these sensitive tissues. Reactivations can induce grievous tissue damage, inflicting headaches, loss of motor coordination, blindness, seizures, and death. These reactivations tend to occur in immunocompromised or immunosuppressed patients. Given this parasite's prevalence throughout the global human population, and its degree of pathogenicity, it is important to study its basic biology to find treatment strategies against it.

Unlike some other eukaryotic organisms, apicomplexans bear a single, tubular mitochondrion in each of their cells (Berná et al., 2021). Apicomplexans are single celled eukaryotes, some of which are pathogenic intracellular parasites. This phylum includes notable parasites such as: *Plasmodium falciparum*, the causative agent of malaria, *Toxoplasma gondii*, responsible for toxoplasmosis, and *Cryptosporidium parvum*, which causes cryptosporidiosis. Within apicomplexans, there are further variations in mitochondria. For instance, *Plasmodium falciparum* has a single, short, tubular mitochondrion while *Toxoplasma gondii*'s mitochondrion resembles a lasso encircling its nucleus (Melo et al., 2000). At the extreme end, *Cryptosporidium* lacks a traditional mitochondrion, instead containing a mitosome responsible for iron-sulfur cluster synthesis. These differences in mitochondrial structure are also

accompanied by a rearrangement of the mitochondrial genome. Apicomplexans tend to have smaller mitochondrial genomes, as a large portion of typically mitochondrial-encoded genes have been integrated into the nuclear genome or outright lost (Berná et al., 2021). Interestingly, this has led apicomplexans to contain the smallest mitochondrial genomes among all organisms (Gray et al., 2004). Unlike other eukaryotes, apicomplexan mitochondrial genomes do not encode for mitochondrial tRNA; *T. gondii* imports tRNA from its own cytosol for mitochondrial translation (Esseiva et al., 2004). For comparison, a human mitochondrial genome encodes 37 genes across 16,000 base pairs (Taanman, 1999) while the *T. gondii* mitochondrial genome encodes 3 genes across 6,000 base pairs (Berná et al., 2021). This minimal set of mitochondrial proteins and genes may allow apicomplexans to minimize their exposure to host cell defenses, boosting their success as parasites (Seeber et al., 2008). Although the apicomplexan mitochondrial genome is drastically reduced and simplified compared to other eukaryotes, it remains a critical organelle to the survival of the organism. Drugs interfering with mitochondrial function have been effective in combatting apicomplexan parasite infections (Mather et al., 2007).

Despite these unusual features, the apicomplexan mitochondrion (when present) is still a major metabolic site responsible for ATP generation via oxidative phosphorylation. Similar to other eukaryotes, the apicomplexan mitochondrion is responsible for the biosynthesis of iron-sulfur clusters (Seeber, 2002; Lill et al., 2012). Additionally, respiratory chains, such as the electron transport chain, are still localized to the mitochondrion of apicomplexans (Hayward and van Dooren, 2019). These components of the electron transport chain are distinguishable against those of other eukaryotes. Notably, all apicomplexans lack a discrete, membrane bound complex I, opting instead to express NADH dehydrogenases within the mitochondrial matrix (Krungkrai et al., 2002; Saleh et al., 2007). Furthermore, apicomplexan versions of cytochrome C oxidase (Complex IV) and ATP synthase are larger and contain more subunits than other eukaryotic counterparts (Maclean et al., 2022). At the extreme end, *Cryptosporidium parvum*

completely lacks a mitochondrial genome, as well as both cytochrome C and cytochrome C oxidase, substituting the latter enzymes with an alternative oxidase (Roberts et al., 2004)

As the principal site of aerobic respiration, mitochondria are one of the major sources of reactive oxygen species (ROS) within the eukaryotic cell. Prior studies have identified complexes I and III as the main generators of ROS in the form of superoxide anions (Brand et al., 2004). While not normally a producer of superoxide anions, mutations of complex IV can also lead to increased superoxide content in eukaryotes (Turrens, 2003; Reichart et al., 2019). While apicomplexans lack complex I, they still contain complexes III and IV, which generate superoxide. It is thought that the loss of complex I was beneficial to reduce overall superoxide burden (Fisher et al., 2007). Superoxide anions are highly reactive, capable of oxidizing biomolecules and generating other ROS, such as hydrogen peroxide. Unwanted changes to a biomolecule's redox status may interfere with its function. This reactive metabolic byproduct must be tightly controlled to ensure cell health.

Reactive oxygen species scavenging systems in *T. gondii*

Throughout aerobic environments, organisms must be able to address the presence of ROS altering the redox status of their biomolecules. In these conditions, cell metabolism produces highly reactive oxygen radicals such as the superoxide anion or hydrogen peroxide. These ROS are not innately harmful to organisms; in fact, controlled levels of ROS may stimulate cell proliferation (Ray et al., 2012). On the other hand, excessive or mislocalized ROS can cause damage to necessary biomolecules and lead to cell death (Ray et al., 2012). In this scenario, these ROS will carry out uncontrolled oxidation of sensitive biomolecules, altering their function. It is proposed that cells have three main lines of defense against ROS damage: i) small molecule antioxidants such as uric acid, citric acid, or glutathione can directly scavenge ROS, ii) antioxidant enzymes such as superoxide dismutase, catalase, or peroxiredoxins can neutralize ROS into less reactive species, and iii) the cell can resynthesize or repair ROS

damaged biomolecules (Lei et al., 2016). These defenses also contribute to maintaining redox homeostasis within the cell. As intracellular parasites, ROS homeostasis is essential to apicomplexan survival. These parasites must be able to regulate their own ROS by-products in addition to ROS generated by their host cell's metabolism and immune system.

Superoxide dismutases are a critical enzyme in ROS scavenging systems. This broad family of metalloenzymes was initially purified from bovine erythrocytes and are solely responsible for the dismutation of superoxide anions into hydrogen peroxide (McCord and Fridovich, 1969). All superoxide dismutase (SOD) enzymes require multi-subunit arrangements to function, contain a metal cofactor, and catalyze the same reaction. To differentiate between the different types of SOD, these enzymes can be classified by their preferred metal cofactor. Superoxide dismutase enzymes can use iron, manganese, zinc, copper, or nickel as an oxygen interacting metal cofactor. Of these enzymes, Mn/FeSOD are thought to be the most ancient, with Cu/Zn SOD being a more recently developed enzyme (Smith and Doolittle, 1992). Between MnSOD and FeSOD, FeSOD is likely the ancestral SOD, giving rise to cambialistic (capable of using multiple metal cofactors) and MnSODs via mutation (Case, 2017). Furthermore, these enzymes are multimers with at least 2 subunits for function. FeSODs tend to form dimers, but some bacterial FeSODs require a tetrameric structure to function (Sheng et al., 2014). The resulting multimers exhibit an extremely rapid rate of electron transfer from their substrates along with to a high degree of stability even when exposed to wide thermal variations, urea, or other stressors (Bowler et al., 1992).

In *T. gondii*, there are three distinct superoxide dismutases (TgSOD), all of which are iron-dependent (Sibley et al., 1986; Odberg-Ferragut et al., 2000; Kwok et al., 2004). TgSOD1 is the sole cytosolic superoxide dismutase, consistently expressed throughout parasite life (Odberg-Ferragut et al., 2000). TgSOD2 has dual localization between the parasite's apicoplast and mitochondrion; it is also expressed through all parasite life stages (Pino et al., 2007). TgSOD3 is a strictly mitochondrial superoxide dismutase and is only expressed in the oocyst

form of the parasite (Kwok et al., 2004). As with other iron-dependent SODs, TgSOD is still susceptible to inhibition by peroxide or azide, but not cyanide (Sibley et al., 1986). Previous attempts to delete TgSOD1 or TgSOD2 have been unsuccessful (Odberg-Ferragut et al., 2000), verifying their predicted fitness conferring status (Sidik et al., 2016). Interestingly, vaccines targeting TgSOD1 confer partial immunity to acute toxoplasmosis in BALB/c mice (Liu et al., 2017).

Catalase and peroxiredoxins metabolize the hydrogen peroxide generated by superoxide dismutation. Catalase reactions produce H_2O and O_2 (Loew, 1900), whereas peroxiredoxin can generate H_2O from hydrogen peroxide but is also capable of catalyzing other peroxidase reactions (Karplus, 2015). Together, these enzymes maintain the levels of peroxides within the cell; this peroxide balance is crucial to cell survival. Hydrogen peroxide activity is shown to be upregulated in key survival pathways such as inhibition of pre-death phosphatases, and activation of ROS-sensitive transcription factors (Groeger et al., 2009). Conversely, excess peroxide concentrations have shown anti-parasitic effects (Tang et al., 2004).

T. gondii is one of the few apicomplexans, alongside *Eimeria tenella* and *Neospora caninum*, to express catalase along (Kwok et al., 2004). Despite this distinction, catalase is predicted to be dispensable (Sidik et al., 2016), and has been successfully knocked out at the expense of *in vivo* virulence (Kwok et al., 2004). While this enzyme is often found within peroxisomes, the presence of peroxisomes in *T. gondii* is debated (Ding et al., 2000; Kaasch and Joiner, 2000). Reports from two groups agree that catalase would not be found within the parasite mitochondrion (Ding et al., 2000; Kaasch and Joiner, 2000), whether it is dissolved in the cytosol or contained within discrete peroxisomes requires further study. Moving to peroxiredoxins, *T. gondii* encodes three peroxiredoxins, two are cytosolic (TgPrx1 and TgPrx2) with TgPrx3 localizing to the parasite mitochondrion (Kwok et al., 2004).

Downstream of the SODs, catalase, and peroxiredoxins are the glutathione and thioredoxin pathways. These pathways use NADPH as an intermediate to regulate redox

homeostasis within the cell (Case, 2017). Oxidized proteins, hydrogen peroxide, or other peroxides can be neutralized by the activity of these pathways. This is especially critical as not all superoxide anions are dismutated via SOD activity (Fridovich, 1983). Some will undergo spontaneous dismutation, resulting in the oxidation of essential proteins and other biomolecules (Winterbourn, 2020). These oxidized biomolecules can then be restored to normal redox status through activity of the glutathione or thioredoxin pathways (Carmel-Harel and Storz, 2000). As these pathways perform similar functions, it is no surprise that there is evidence of crosstalk between the thioredoxin and glutathione systems. Glutathionylation of thioredoxin leads to a decrease in its enzymatic activity, likely shifting the cell to a glutathione-dominant state (Casagrande et al., 2002). It is unclear whether this crosstalk exists in other eukaryotes.

T. gondii contains intact glutathione and thioredoxin pathways (Kwok et al., 2004). Parasites tolerate the loss of glutaredoxin, but show impaired ROS clearance and virulence (Li et al., 2023). Similar defects (decreased ROS clearance and virulence) were observed in thioredoxin deletion mutants (Xue et al., 2017). These studies align with the prediction that both glutaredoxin and thioredoxin reductase are dispensable (Sidik et al., 2016); this strongly suggests a compensatory mechanism between these parallel pathways. It may be the case that targeted simultaneous disruptions of both the thioredoxin and glutaredoxin pathways would lead to fatal accumulation of oxidized biomolecules. Compared against other apicomplexans, *T. gondii* boasts an extensively developed ROS scavenging system (**Figure 1.1**). Its redox scavenger system development may contribute to its wide host cell range. Notably, tachyzoites can infect ROS producing phagocytes. Bradyzoites on the other hand, are capable of encystation within neurons, which produce ROS during their activity. Both of these cell types pose unique challenges to parasite ROS scavenging, which could be addressed by a well-developed ROS scavenging system.

	Cryptosporidium	*Plasmodium*	*Babesia*	*Toxoplasma*
Superoxide Dismutase	1	2	Putative	3
Peroxiredoxin	Putative	5	Putative	3
Thioredoxin Reductase	1	1	Putative	1
Glutathione Reductase	1	0	0	1
Catalase	0	0	0	1

Figure 1.1: Table of ROS scavengers present in select human apicomplexan pathogens, and diagrams of their notable niches (intestinal epithelial cell, red blood cell, and neuron shown for *Cryptosporidium*, *Plasmodium* and *Babesia*, and *Toxoplasma* respectively). ROS scavenger gene counts from EuPathDB (Warrenfeltz et al., 2018). Created with BioRender.com

Treatment strategies against *T. gondii*

Currently, the standard of care for toxoplasmosis is a cocktail of pyrimethamine and sulfadiazine initially proposed in 1953 (Eyles and Coleman, 1953). This treatment interferes with folate metabolism, and because parasites cannot scavenge host folates, preventing DNA synthesis in affected parasites. As an intracellular parasite, *T. gondii* relies upon its host to reduce 4-aminobenzoic acid into usable folinic acid; sulfadiazine blocks the conversion of 4-aminobenzoic acid into folic acid, pyrimethamine then blocks the conversion of folic acid into folinic acid (Frenkel and Hitchings, 1957). In fact, administration of 4-aminobenzoic acid during pyrimethamine and sulfadiazine treatment leads to premature death of infected mice (Eyles and Coleman, 1960). As this treatment disrupts folate synthesis in host cells, it poses significant host cell cytotoxicity, causing bone marrow toxicity, anemia, and gastrointestinal disturbances as a side effect (Ben-Harari et al., 2017). Thus, pyrimethamine and sulfadiazine are often prescribed

alongside folate supplements to mitigate against hematologic adverse effects (Holliman, 1989). In addition to bone marrow toxicity, this drug combination is a potent teratogen, prohibiting use with pregnant patients (Remington, 1964). Unfortunately, pyrimethamine and sulfadiazine are also unable to penetrate the cyst wall, which precludes their use in treating chronic *T. gondii* infections (Gormley et al., 1998). Given these shortcomings, it is imperative to find new therapeutic strategies against *T. gondii*.

To address the need for new treatments for other diseases, many labs have resorted to repurposing previously FDA approved drugs. This approach would expedite the process of implementing effective treatments; novel drug development often requires roughly $2-3 billion USD; conversely, repurposing a drug can be done with $300 million USD (Nosengo, 2016). Recent studies have demonstrated that interference with dopamine and estrogen signaling via pimozide and tamoxifen, respectively, inhibit parasite growth (Dittmar et al., 2016). Pimozide, a dopamine receptor antagonist, has been used for treatment of Tourette syndrome tics (Shapiro and Shapiro, 1984) and schizophrenia (Chouinard and Annable, 1982). Tamoxifen, an estrogen modulator, is notably used in the treatment of breast cancer and other estrogen receptor positive malignancies (Haddow et al., 1944). While the mechanistic actions of the repurposed therapies are wildly varied, there is evidence that disruption of mitochondrial metabolism is a highly potent antiparasitic strategy.

Intracellular parasites have evolved minimal sets of metabolic pathways which are highly divergent compared against their host organisms (Goodman et al., 2017). Having a limited set of highly essential enzymes, and minimal similarities to host metabolic enzymes make the apicomplexan electron transport chain an attractive drug target (Jacot et al., 2016). Another drug approved for treatment of acute toxoplasmosis, atovaquone, inhibits parasitic cytochrome C, part of its electron transport chain (Korsinczky et al., 2000). The resulting stress to the mitochondrion leads to a decrease in its mitochondrial membrane potential, a collapse of its mitochondrion, and eventual parasite death (Srivastava et al., 1997). Continuing along this path

of mitochondrial interference, several promising drug development or repurposing projects have been undertaken.

Monensin, an ionophore used to treat veterinary coccidian infections (Fitzgerald and Mansfield, 1973) was shown to be effective against *T. gondii* infections (Lawrence, 1988). Further investigations in *T. gondii* demonstrate that it generates ROS, which leads to impaired mitochondrial activity (Charvat and Arrizabalaga, 2016) and death by autophagy (Lavine and Arrizabalaga, 2012). Among the repurposed treatments for toxoplasmosis, auranofin is thought to induce ROS stress by inhibition of thioredoxin reductase (Pessetto et al., 2013). This drug is effective against *Entamoeba histolytica* (Debnath et al., 2012), *Streptococcus suis* (Lu et al., 2021), *Schistosoma masoni* (Angelucci et al., 2009), *Trypanosoma cruzi* and *Leishmania tropica* (Yıldırım et al., 2023). Furthermore, auranofin treatment completely prevents death of chick embryos infected with *T. gondii* (Andrade et al., 2014). Relatedly, inorganic metal nanoparticles are also thought to generate ROS, impairing mitochondrial membrane potential and leading to parasite death (Adeyemi et al., 2017).

The accumulated evidence above highlights not only the vital nature of antioxidant systems to intracellular parasites, but also the viability of redox homeostasis disruption as a possible anti-parasitic mechanism of action. In this dissertation, we will explore how the antioxidant systems in *T. gondii* respond to various stressors, and how the parasite's mitochondrion reacts to depletion of a necessary ROS scavenger. Altogether, this dissertation aims to elucidate the role of *T. gondii*'s mitochondrial superoxide dismutase.

This dissertation will address the following questions on *T. gondii* and ROS scavenging:

- Auranofin's mechanism for efficacy against *T. gondii*
- The development of resistance to auranofin treatment
- Consequences of TgSOD2 depletion in *T. gondii*
- TgSOD2's placement within the mitochondrial microenvironment

References

Adeyemi, O. S., Murata, Y., Sugi, T., and Kato, K. (2017). Inorganic nanoparticles kill Toxoplasma gondii via changes in redox status and mitochondrial membrane potential. *International journal of nanomedicine* 12, 1647–1661. doi: 10.2147/IJN.S122178.

Andrade, R. M., Chaparro, J. D., Capparelli, E., and Reed, S. L. (2014). Auranofin is highly efficacious against Toxoplasma gondii in vitro and in an in vivo experimental model of acute toxoplasmosis. *PLoS Neglected Tropical Diseases* 8, e2973. doi: 10.1371/journal.pntd.0002973.

Angelucci, F., Sayed, A. A., Williams, D. L., Boumis, G., Brunori, M., Dimastrogiovanni, D., et al. (2009). Inhibition of Schistosoma mansoni thioredoxin-glutathione reductase by auranofin: structural and kinetic aspects. *The Journal of Biological Chemistry* 284, 28977–28985. doi: 10.1074/jbc.M109.020701.

Ben-Harari, R. R., Goodwin, E., and Casoy, J. (2017). Adverse Event Profile of Pyrimethamine-Based Therapy in Toxoplasmosis: A Systematic Review. *Drugs R D* 17, 523–544. doi: 10.1007/s40268-017-0206-8.

Berná, L., Rego, N., and Francia, M. E. (2021). The Elusive Mitochondrial Genomes of Apicomplexa: Where Are We Now? *Front Microbiol* 12, 751775. doi: 10.3389/fmicb.2021.751775.

Bowler, C., Montagu, M. V., and Inze, D. (1992). Superoxide dismutase and stress tolerance. *Annu Rev Plant Physiol Plant Mol Biol* 43, 83–116. doi: 10.1146/annurev.pp.43.060192.000503.

Brand, M. D., Affourtit, C., Esteves, T. C., Green, K., Lambert, A. J., Miwa, S., et al. (2004). Mitochondrial superoxide: production, biological effects, and activation of uncoupling proteins. *Free Radical Biology and Medicine* 37, 755–767. doi: 10.1016/j.freeradbiomed.2004.05.034.

Carmel-Harel, O., and Storz, G. (2000). Roles of the glutathione- and thioredoxin-dependent reduction systems in the Escherichia coli and saccharomyces cerevisiae responses to oxidative stress. *Annu Rev Microbiol* 54, 439–461. doi: 10.1146/annurev.micro.54.1.439.

Casagrande, S., Bonetto, V., Fratelli, M., Gianazza, E., Eberini, I., Massignan, T., et al. (2002). Glutathionylation of human thioredoxin: A possible crosstalk between the glutathione and thioredoxin systems. *Proceedings of the National Academy of Sciences* 99, 9745–9749. doi: 10.1073/pnas.152168599.

Case, A. J. (2017). On the Origin of Superoxide Dismutase: An Evolutionary Perspective of Superoxide-Mediated Redox Signaling. *Antioxidants (Basel)* 6. doi: 10.3390/antiox6040082.

Charvat, R. A., and Arrizabalaga, G. (2016). Oxidative stress generated during monensin treatment contributes to altered Toxoplasma gondii mitochondrial function. *Scientific Reports* 6, 22997. doi: 10.1038/srep22997.

Chouinard, G., and Annable, L. (1982). Pimozide in the treatment of newly admitted schizophrenic patients. *Psychopharmacology* 76, 13–19. doi: 10.1007/BF00430747.

Debnath, A., Parsonage, D., Andrade, R. M., He, C., Cobo, E. R., Hirata, K., et al. (2012). A high-throughput drug screen for Entamoeba histolytica identifies a new lead and target. *Nature Medicine* 18, 956–960. doi: 10.1038/nm.2758.

Ding, M., Clayton, C., and Soldati, D. (2000). Toxoplasma gondii catalase: are there peroxisomes in toxoplasma? *Journal of Cell Science* 113 (Pt 13), 2409–2419.

Dittmar, A. J., Drozda, A. A., and Blader, I. J. (2016). Drug Repurposing Screening Identifies Novel Compounds That Effectively Inhibit Toxoplasma gondii Growth. *mSphere* 1, 10.1128/msphere.00042-15. doi: 10.1128/msphere.00042-15.

Esseiva, A. C., Naguleswaran, A., Hemphill, A., and Schneider, A. (2004). Mitochondrial tRNA Import in Toxoplasma gondii. *Journal of Biological Chemistry* 279, 42363–42368. doi: 10.1074/jbc.M404519200.

Eyles, D. E., and Coleman, N. (1953). Synergistic effect of sulfadiazine and daraprim against experimental toxoplasmosis in the mouse. *Antibiot Chemother (Northfield)* 3, 483–490.

Eyles, D. E., and Coleman, N. (1960). The effect of metabolites on the antitoxoplasmic action of pyrimethamine and sulfadiazine. *Am J Trop Med Hyg* 9, 277–283. doi: 10.4269/ajtmh.1960.9.277.

Fisher, N., Bray, P. G., Ward, S. A., and Biagini, G. A. (2007). The malaria parasite type II NADH:quinone oxidoreductase: an alternative enzyme for an alternative lifestyle. *Trends in Parasitology* 23, 305–310. doi: 10.1016/j.pt.2007.04.014.

Fitzgerald, P. R., and Mansfield, M. E. (1973). Efficacy of Monensin Against Bovine Coccidiosis in Young Holstein-Friesian Calves*. *The Journal of Protozoology* 20, 121–126. doi: 10.1111/j.1550-7408.1973.tb06014.x.

Frenkel, J. K., and Hitchings, G. H. (1957). Relative reversal by vitamins (rho-aminobenzoic, folic, and folinic acids) of the effects of sulfadiazine and pyrimethamine on Toxoplasma, mouse and man. *Antibiot Chemother (Northfield)* 7, 630–638.

Fridovich, I. (1983). Superoxide Radical: An Endogenous Toxicant. *Annu. Rev. Pharmacol. Toxicol.* 23, 239–257. doi: 10.1146/annurev.pa.23.040183.001323.

Goodman, C. D., Buchanan, H. D., and McFadden, G. I. (2017). Is the Mitochondrion a Good Malaria Drug Target? *Trends in Parasitology* 33, 185–193. doi: 10.1016/j.pt.2016.10.002.

Gormley, P. D., Pavesio, C. E., Minnasian, D., and Lightman, S. (1998). Effects of drug therapy on Toxoplasma cysts in an animal model of acute and chronic disease. *Investigative Ophthalmology & Visual Science* 39, 1171–1175.

Gray, M. W., Lang, B. F., and Burger, G. (2004). Mitochondria of protists. *Annu Rev Genet* 38, 477–524. doi: 10.1146/annurev.genet.37.110801.142526.

Groeger, G., Quiney, C., and Cotter, T. G. (2009). Hydrogen Peroxide as a Cell-Survival Signaling Molecule. *Antioxidants & Redox Signaling* 11, 2655–2671. doi: 10.1089/ars.2009.2728.

Haddow, A., Watkinson, J. M., Paterson, E., and Koller, P. C. (1944). Influence of Synthetic Oestrogens on Advanced Malignant Disease. *Br Med J* 2, 393–398.

Hayward, J. A., and van Dooren, G. G. (2019). Same same, but different: Uncovering unique features of the mitochondrial respiratory chain of apicomplexans. *Molecular and Biochemical Parasitology* 232, 111204. doi: 10.1016/j.molbiopara.2019.111204.

Holliman, R. E. (1989). Folate Supplements and the Treatment of Cerebral Toxoplasmosis. *Scandinavian Journal of Infectious Diseases* 21, 475–476. doi: 10.3109/00365548909167456.

Jacot, D., Waller, R. F., Soldati-Favre, D., MacPherson, D. A., and MacRae, J. I. (2016). Apicomplexan Energy Metabolism: Carbon Source Promiscuity and the Quiescence Hyperbole. *Trends in Parasitology* 32, 56–70. doi: 10.1016/j.pt.2015.09.001.

Kaasch, A. J., and Joiner, K. A. (2000). Targeting and Subcellular Localization of Toxoplasma gondii Catalase: IDENTIFICATION OF PEROXISOMES IN AN APICOMPLEXAN PARASITE *. *Journal of Biological Chemistry* 275, 1112–1118. doi: 10.1074/jbc.275.2.1112.

Karplus, P. A. (2015). A primer on peroxiredoxin biochemistry. *Free Radical Biology and Medicine* 80, 183–190. doi: 10.1016/j.freeradbiomed.2014.10.009.

Korsinczky, M., Chen, N., Kotecka, B., Saul, A., Rieckmann, K., and Cheng, Q. (2000). Mutations in Plasmodium falciparumCytochrome b That Are Associated with Atovaquone Resistance Are Located at a Putative Drug-Binding Site. *Antimicrobial Agents and Chemotherapy* 44, 2100–2108. doi: 10.1128/aac.44.8.2100-2108.2000.

Krungkrai, J., Kanchanarithisak, R., Krungkrai, S. R., and Rochanakij, S. (2002). Mitochondrial NADH Dehydrogenase from Plasmodium falciparum and Plasmodium berghei. *Experimental Parasitology* 100, 54–61. doi: 10.1006/expr.2001.4674.

Kwok, L. Y., Schlüter, D., Clayton, C., and Soldati, D. (2004). The antioxidant systems in Toxoplasma gondii and the role of cytosolic catalase in defence against oxidative injury. *Molecular Microbiology* 51, 47–61. doi: 10.1046/j.1365-2958.2003.03823.x.

Lavine, M. D., and Arrizabalaga, G. (2012). Analysis of monensin sensitivity in Toxoplasma gondii reveals autophagy as a mechanism for drug induced death. *Plos One* 7, e42107. doi: 10.1371/journal.pone.0042107.

Lawrence, K. (1988). Use of monensin sodium against Toxoplasma. *Vet Rec* 123, 323. doi: 10.1136/vr.123.12.323-a.

Lei, X. G., Zhu, J.-H., Cheng, W.-H., Bao, Y., Ho, Y.-S., Reddi, A. R., et al. (2016). Paradoxical Roles of Antioxidant Enzymes: Basic Mechanisms and Health Implications. *Physiological Reviews* 96, 307–364. doi: 10.1152/physrev.00010.2014.

Li, T.-T., Zhao, D.-Y., Liang, Q.-L., Elsheikha, H. M., Wang, M., Sun, L.-X., et al. (2023). The antioxidant protein glutaredoxin 1 is essential for oxidative stress response and pathogenicity of Toxoplasma gondii. *The FASEB Journal* 37, e22932. doi: 10.1096/fj.202201275R.

Lill, R., Hoffmann, B., Molik, S., Pierik, A. J., Rietzschel, N., Stehling, O., et al. (2012). The role of mitochondria in cellular iron–sulfur protein biogenesis and iron metabolism. *Biochimica et Biophysica Acta (BBA) - Molecular Cell Research* 1823, 1491–1508. doi: 10.1016/j.bbamcr.2012.05.009.

Liu, Y., Cao, A., Li, Y., Li, X., Cong, H., He, S., et al. (2017). Immunization with a DNA vaccine encoding Toxoplasma gondii Superoxide dismutase (TgSOD) induces partial immune protection against acute toxoplasmosis in BALB/c mice. *BMC Infectious Diseases* 17, 403. doi: 10.1186/s12879-017-2507-5.

Loew, O. (1900). A NEW ENZYME OF GENERAL OCCURRENCE IN ORGANISMIS. *Science* 11, 701–702. doi: 10.1126/science.11.279.701.

Lu, H., Lu, W., Zhu, Y., Wang, C., Shi, L., Li, X., et al. (2021). Auranofin Has Advantages over First-Line Drugs in the Treatment of Severe Streptococcus suis Infections. *Antibiotics* 10, 26. doi: 10.3390/antibiotics10010026.

Maclean, A. E., Hayward, J. A., Huet, D., van Dooren, G. G., and Sheiner, L. (2022). The mystery of massive mitochondrial complexes: the apicomplexan respiratory chain. *Trends Parasitol* 38, 1041–1052. doi: 10.1016/j.pt.2022.09.008.

Mather, M. W., Henry, K. W., and Vaidya, A. B. (2007). Mitochondrial Drug Targets in Apicomplexan Parasites. *Current Drug Targets* 8, 49–60. doi: 10.2174/138945007779315632.

McCord, J. M., and Fridovich, I. (1969). Superoxide Dismutase: AN ENZYMIC FUNCTION FOR ERYTHROCUPREIN (HEMOCUPREIN). *Journal of Biological Chemistry* 244, 6049–6055. doi: 10.1016/S0021-9258(18)63504-5.

Melo, E. J., Attias, M., and De Souza, W. (2000). The single mitochondrion of tachyzoites of Toxoplasma gondii. *J Struct Biol* 130, 27–33. doi: 10.1006/jsbi.2000.4228.

Nosengo, N. (2016). Can you teach old drugs new tricks? *Nature* 534, 314–316. doi: 10.1038/534314a.

Odberg-Ferragut, C., Renault, J. P., Viscogliosi, E., Toursel, C., Briche, I., Engels, A., et al. (2000). Molecular cloning, expression analysis and iron metal cofactor characterisation of a superoxide dismutase from Toxoplasma gondii. *Molecular and Biochemical Parasitology* 106, 121–129. doi: 10.1016/S0166-6851(99)00211-X.

Pessetto, Z. Y., Weir, S. J., Sethi, G., Broward, M. A., and Godwin, A. K. (2013). Drug Repurposing for Gastrointestinal Stromal Tumor. *Molecular Cancer Therapeutics* 12, 1299–1309. doi: 10.1158/1535-7163.MCT-12-0968.

Pino, P., Foth, B. J., Kwok, L.-Y., Sheiner, L., Schepers, R., Soldati, T., et al. (2007). Dual targeting of antioxidant and metabolic enzymes to the mitochondrion and the apicoplast of Toxoplasma gondii. *PLoS Pathogens* 3, e115. doi: 10.1371/journal.ppat.0030115.

Ray, P. D., Huang, B.-W., and Tsuji, Y. (2012). Reactive oxygen species (ROS) homeostasis and redox regulation in cellular signaling. *Cellular Signalling* 24, 981–990. doi: 10.1016/j.cellsig.2012.01.008.

Reichart, G., Mayer, J., Zehm, C., Kirschstein, T., Tokay, T., Lange, F., et al. (2019). Mitochondrial complex IV mutation increases reactive oxygen species production and reduces lifespan in aged mice. *Acta Physiol (Oxf)* 225, e13214. doi: 10.1111/apha.13214.

Remington, J. S. (1964). TOXOPLASMA AND CHRONIC ABORTION. *Obstet Gynecol* 24, 155–157.

Roberts, C. W., Roberts, F., Henriquez, F. L., Akiyoshi, D., Samuel, B. U., Richards, T. A., et al. (2004). Evidence for mitochondrial-derived alternative oxidase in the apicomplexan parasite Cryptosporidium parvum: a potential anti-microbial agent target. *International Journal for Parasitology* 34, 297–308. doi: 10.1016/j.ijpara.2003.11.002.

Saleh, A., Friesen, J., Baumeister, S., Gross, U., and Bohne, W. (2007). Growth inhibition of Toxoplasma gondii and Plasmodium falciparum by nanomolar concentrations of 1-hydroxy-2-dodecyl-4(1H)quinolone, a high-affinity inhibitor of alternative (type II) NADH dehydrogenases. *Antimicrob Agents Chemother* 51, 1217–1222. doi: 10.1128/AAC.00895-06.

Seeber, F. (2002). Biogenesis of iron–sulphur clusters in amitochondriate and apicomplexan protists. *International Journal for Parasitology* 32, 1207–1217. doi: 10.1016/S0020-7519(02)00022-X.

Seeber, F., Limenitakis, J., and Soldati-Favre, D. (2008). Apicomplexan mitochondrial metabolism: a story of gains, losses and retentions. *Trends Parasitol* 24, 468–478. doi: 10.1016/j.pt.2008.07.004.

Shapiro, A. K., and Shapiro, E. (1984). Controlled Study of Pimozide vs. Placebo in Tourette's Syndrome. *Journal of the American Academy of Child Psychiatry* 23, 161–173. doi: 10.1097/00004583-198403000-00007.

Sheng, Y., Abreu, I. A., Cabelli, D. E., Maroney, M. J., Miller, A.-F., Teixeira, M., et al. (2014). Superoxide dismutases and superoxide reductases. *Chemical Reviews* 114, 3854–3918. doi: 10.1021/cr4005296.

Sibley, L. D., Lawson, R., and Weidner, E. (1986). Superoxide dismutase and catalase in Toxoplasma gondii. *Molecular and Biochemical Parasitology* 19, 83–87. doi: 10.1016/0166-6851(86)90069-1.

Sidik, S. M., Huet, D., Ganesan, S. M., Huynh, M.-H., Wang, T., Nasamu, A. S., et al. (2016). A Genome-wide CRISPR Screen in Toxoplasma Identifies Essential Apicomplexan Genes. *Cell* 166, 1423-1435.e12. doi: 10.1016/j.cell.2016.08.019.

Smith, M. W., and Doolittle, R. F. (1992). A comparison of evolutionary rates of the two major kinds of superoxide dismutase. *J Mol Evol* 34, 175–184. doi: 10.1007/BF00182394.

Srivastava, I. K., Rottenberg, H., and Vaidya, A. B. (1997). Atovaquone, a Broad Spectrum Antiparasitic Drug, Collapses Mitochondrial Membrane Potential in a Malarial Parasite *. *Journal of Biological Chemistry* 272, 3961–3966. doi: 10.1074/jbc.272.7.3961.

Taanman, J.-W. (1999). The mitochondrial genome: structure, transcription, translation and replication. *Biochimica et Biophysica Acta (BBA) - Bioenergetics* 1410, 103–123. doi: 10.1016/S0005-2728(98)00161-3.

Tang, Y., Dong, Y., and Vennerstrom, J. L. (2004). Synthetic peroxides as antimalarials. *Medicinal Research Reviews* 24, 425–448. doi: 10.1002/med.10066.

Turrens, J. F. (2003). Mitochondrial formation of reactive oxygen species. *J Physiol* 552, 335–344. doi: 10.1113/jphysiol.2003.049478.

Warrenfeltz, S., Basenko, E. Y., Crouch, K., Harb, O. S., Kissinger, J. C., Roos, D. S., et al. (2018). EuPathDB: the eukaryotic pathogen genomics database resource. *Methods Mol Biol* 1757, 69–113. doi: 10.1007/978-1-4939-7737-6_5.

Winterbourn, C. C. (2020). Biological chemistry of superoxide radicals. *ChemTexts* 6, 7. doi: 10.1007/s40828-019-0101-8.

Xue, J., Jiang, W., Chen, Y., Gong, F., Wang, M., Zeng, P., et al. (2017). Thioredoxin reductase from Toxoplasma gondii: an essential virulence effector with antioxidant function. *The FASEB Journal* 31, 4447–4457. doi: 10.1096/fj.201700008R.

Yıldırım, A., Özbilgin, A., and Yereli, K. (2023). Antiprotozoal activity of auranofin on Trypanosoma cruzi, Leishmania tropica and Toxoplasma gondii: in vitro and ex vivo study. *Trans R Soc Trop Med Hyg* 117, 733–740. doi: 10.1093/trstmh/trad040.

CHAPTER TWO: Investigation of *T. gondii* death by auranofin, and the development of auranofin resistance

Abstract

Auranofin, an FDA-approved drug for rheumatoid arthritis, has emerged as a promising antiparasitic medication in recent years. It induces the accumulation of reactive oxygen species (ROS) in parasites, including *Toxoplasma gondii*. Herein, we demonstrated that auranofin, inhibited the growth of *T. gondii in vitro*. We found that auranofin affected the *T. gondii* biological cycle (lytic cycle) by inhibiting *T. gondii's* invasion and triggering its egress from the host cell. However, auranofin could not prevent parasite replication once *T. gondii* resided within the host. Auranofin treatment induced apoptosis in *T. gondii* parasites, as demonstrated by its reduced size and elevated phosphatidylserine externalization (PS). We generated auranofin resistant *T. gondii* lines through chemical mutagenesis to identify the molecular target of this drug. Resistant clones were confirmed with a competition assay using wild-type *T. gondii* expressing yellow fluorescence protein (YFP) as a reference strain. The predicted auranofin target, thioredoxin reductase, was not mutated in any of our resistant lines. Subsequent whole genomic sequencing analysis (WGS) did not reveal a consensus resistance locus, although many have point mutations in genes encoding redox-relevant proteins such as superoxide dismutase (TgSOD2) and ribonucleotide reductase. We investigated the SOD2 L201P mutation and found that it was not sufficient to confer resistance when introduced into wild-type parasites. Resistant clones accumulated less ROS than their wild type counterparts. Our results demonstrate that resistance to auranofin in *T. gondii* enhances its ability to abate oxidative stress through diverse mechanisms. This evidence supports a hypothesized mechanism of auranofin anti-parasitic activity as disruption of redox homeostasis.

Introduction

For more than 50 years, treatment of toxoplasmosis has relied upon a combination of sulfadiazine and pyrimethamine. This cocktail is effective at treating acute toxoplasmosis, clearing rapidly dividing tachyzoites from the patient. However, it fails to inhibit encysted parasites as the medications cannot penetrate the cyst wall; this leaves treated patients with encysted parasites capable of reactivation at a later time point. To make matters worse, this therapeutic strategy has significant bone marrow toxicity and is teratogenic. It is clear that new treatments must be discovered which can treat all forms of *Toxoplasma gondii*, while also avoiding the pitfalls of unwanted side effects. To expedite drug discovery for this neglected parasitic disease, we propose repurposing existing FDA-approved drugs. For instance, auranofin, previously approved for treating rheumatoid arthritis, has demonstrated efficacy against infections of other apicomplexans such as *Plasmodium falciparum* (Sannella et al., 2008), *Schistosoma mansoni* (Angelucci et al., 2009), *Leishmania infantum* (Ilari et al., 2012), and *Entamoeba histolytica* (Debnath et al., 2012), as well as other parasites with public health significance (Martínez-González et al., 2010; Debnath et al., 2013; Bulman et al., 2015; da Silva et al., 2016; Hopper et al., 2016; Peroutka-Bigus and Bellaire, 2019). While auranofin has a promising spectrum of anti-parasitic effects, its mechanism of action on parasites is unknown. Prior studies have implicated auranofin as an inhibitor of thioredoxin reductase, a notable member of the redox homeostasis system.

Thioredoxin reductase is an essential conserved enzyme found in archaea, bacteria, and eukaryotes; it maintains the oxidation status of thioredoxin and, indirectly, NADPH as well. The thioredoxin system is critical to protecting cells from oxidative stress, engaging in redox signaling, and maintaining oxygen metabolism (Myers and Myers, 2009). Given the wide variety of critical functions thioredoxin reductase is involved in, it is no surprise that it is generally essential to survival. In humans, inhibition of thioredoxin reductase induces expression of heme oxygenase-1, which in turn, reduces inflammation (Kobayashi et al., 2006). Thioredoxin

reductase related disorders in humans can manifest as conditions such as chronic inflammation (Becker et al., 2000), cancer (Selenius et al., 2010), and neurodegenerative disease (Cimini et al., 2013).

Treatment of *Entamoeba histolytica* with auranofin resulted in the accumulation of oxidized proteins, which are canonically reduced by thioredoxin reductase. Buildup of these oxidized molecules suggests inhibition of thioredoxin reductase (Shaulov et al., 2020). While auranofin is thought to underlie this inhibition, its exact mechanism is unclear. Auranofin is rapidly metabolized to release monovalent gold; which then interacts with other molecules (Debnath et al., 2012). One possibility is that the released gold binds to the catalytic domains of the enzyme, thus decreasing the speed at which it catalyzes reactions (Parsonage et al., 2016). However, this reduced catalytic rate could also reflect the drug's disruption of thioredoxin reductase's substrate (Parsonage et al., 2016). Chapter Two will further investigate auranofin's mechanism of action on *T. gondii*, specifically how it inhibits parasite growth and pathways for drug resistance development, which could help identify the molecular target of auranofin in *T. gondii*.

T. gondii contains endogenous thioredoxin reductase, thus making auranofin an attractive therapeutic strategy against anti-toxoplasmosis. Furthermore, treatment with this drug has been shown to increase survival of *T. gondii* infected chicken embryos (Andrade et al., 2014). Additional studies are needed to identify auranofin's specific mechanism of action. In this section, we propose to examine auranofin-resistant mutants to identify the direct target of auranofin in *T. gondii* and thus improve our understanding of auranofin's anti-parasitic properties.

Results

Auranofin affects parasite lytic cycle progression:

Our experiments showed that auranofin exerts its anti-*T. gondii* effect while the parasite is in the extracellular stages. As an obligate intracellular parasite, *T. gondii* is more susceptible to drug treatment while removed from its parasitophorous vacuole. We have used invasion assays in order to measure the ability of the parasite to enter into host cells. This assay was carried out by counting both invaded and uninvaded parasites following exposure to uninfected host cells. Notably, without pre-treatment, there is no significant difference in percentage of *T. gondii* invasion between control and auranofin treatment groups (59% vs. 60% respectively; $p>0.05$) (**Figure 2.1A**). Pre-treatment of extracellular tachyzoites with auranofin caused a significant decrease in invasion compared to controls (18% vs. 35% respectively; $p<0.05$) (**Figure 2.1B**).

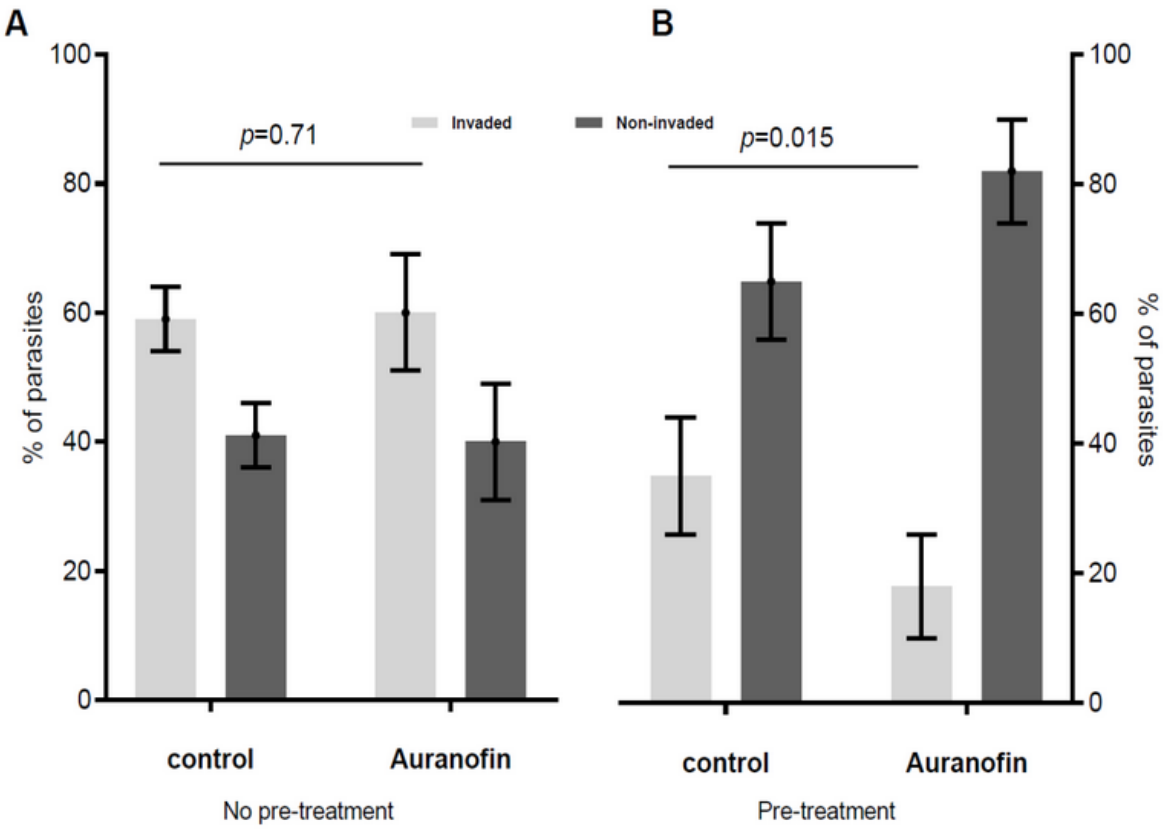

Figure 2.1. Evaluation of the effect of auranofin during *T. gondii* invasion of host cells: A) Invasion rates of HFF in control and treatment groups without pre-treatment of *T. gondii* with auranofin before invasion ($p>0.05$). **B)** Invasion rates of HFF with parasites pre-treated with auranofin before invasion ($p<0.05$). Results from three independent experiments. Error bars for standard deviations are shown.

To interrogate parasite replication, we infected host cells with *T. gondii* before treatment with auranofin. Once *T. gondii* invaded the host cell, 24-hour treatment of auranofin did not inhibit parasite replication, as numbers of parasites per parasitophorous vacuole (PV) were similar in control and treated monolayers (**Figure 2.2A**). This effect was not associated with abnormalities of the host cells as the monolayer did not show changes in its integrity following 24 hours of auranofin treatment (*data not shown*).

The last stage of *T. gondii*'s lytic cycle corresponds to host cell egress, and thus we measured lactate dehydrogenase (LDH) concentration as an indicator of egress-induced host cell death (Schultz and Carruthers, 2018). For our egress assays, both zaprinast and A23187

were included as positive controls. Zaprinast, a phosphodiesterase inhibitor, induces egress by activating parasite protein kinase G (Lourido et al., 2012). A23187 is a calcium ionophore that triggers parasite motility, thereby inducing egress (Endo et al., 1982). After 30 hours of replication, infected monolayers were treated with each pharmacological agent for 40 minutes to induce parasite egress. While A23187 was a more potent egress inducer than auranofin (LDH concentrations: 0.4533 ±0.01148 vs. 0.2768±0.03435; $p<0.01$), auranofin and zaprinast released similar LDH concentrations (0.3272 ± 0.009 vs. 0.2768± 0.034; $p>0.05$) (**Figure 2.2B**). While auranofin does not induce dramatic egress like A23187, it does induce similar amounts of egress as zaprinast. These compounds were selected to show a range of egress induction from host cells, both of which are greater than untreated parasites. Altogether, auranofin modestly induces parasite egress from infected host cells.

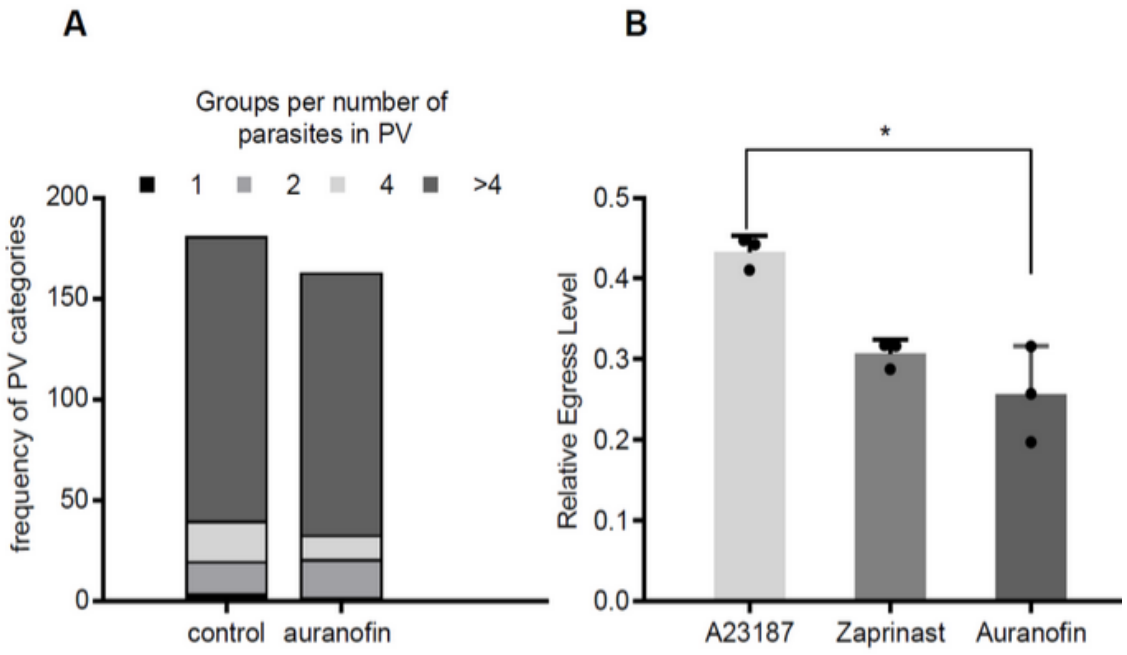

Figure 2.2. Evaluation of the effect of auranofin on *T. gondii* replication and egress: A) Replication assays: Monolayers of HFF were infected with *T. gondii* for 1 hour, then washed and D10 or D10 containing auranofin (2.5 μM) was added back for 24 hours. Data shown as parasites per vacuole following 24hrs replication, no significant difference between groups (Chi-square test $p>0.05$). Results from three independent experiments. **B)** Egress assays: HFF were infected with *T. gondii* for 30 hours before exposure to A23187(5 μM), zaprinast (57 μM), auranofin (5 μM) and DMSO (solvent) for 40 minutes. Student's t-test ($p<0.01$). Results from three independent experiments. Error bars for standard deviations are shown.

Auranofin likely induced apoptosis in *T. gondii:*

Previous experiments suggest that pre-treatment of extracellular parasites with auranofin prevents invasion, but the exact mechanism is unknown. A pilot study showed that auranofin treated parasites are smaller compared to controls (*data not shown*). To validate our observation, we filter purified *T. gondii* parasites before exposing them to auranofin for 24 hours. The treated parasite size was then measured via flow cytometry by forward scattering (FSC-H). Auranofin treatment significantly decreased parasite size compared to untreated parasites (152.7 ± 8.225 vs. 201.2± 4.064; $p<0.01$). Extended (48hr) treatment with auranofin yielded similar significant decreases in cell size (auranofin vs. control 123.5± 7.339 vs. 169.9 ± 66.25 $p<0.05$) (**Figure 2.3B**). This reduction in size is suggestive of apoptosis, and thus we also measured phosphatidylserine externalization via Annexin V staining. Increased phosphatidylserine externalization is another feature of cells likely undergoing apoptosis. Auranofin treatment caused increases Annexin V staining in compared to controls (29.16± 3.615 vs. 11.2± 2.937; $p<0.05$) at 24 hours (**Figure 2.3C**). Annexin V measurements following 48 hours of treatment were not performed due to low parasite recovery. In combination with the reductions in cell size, it may be the case that auranofin induces apoptosis in treated parasites.

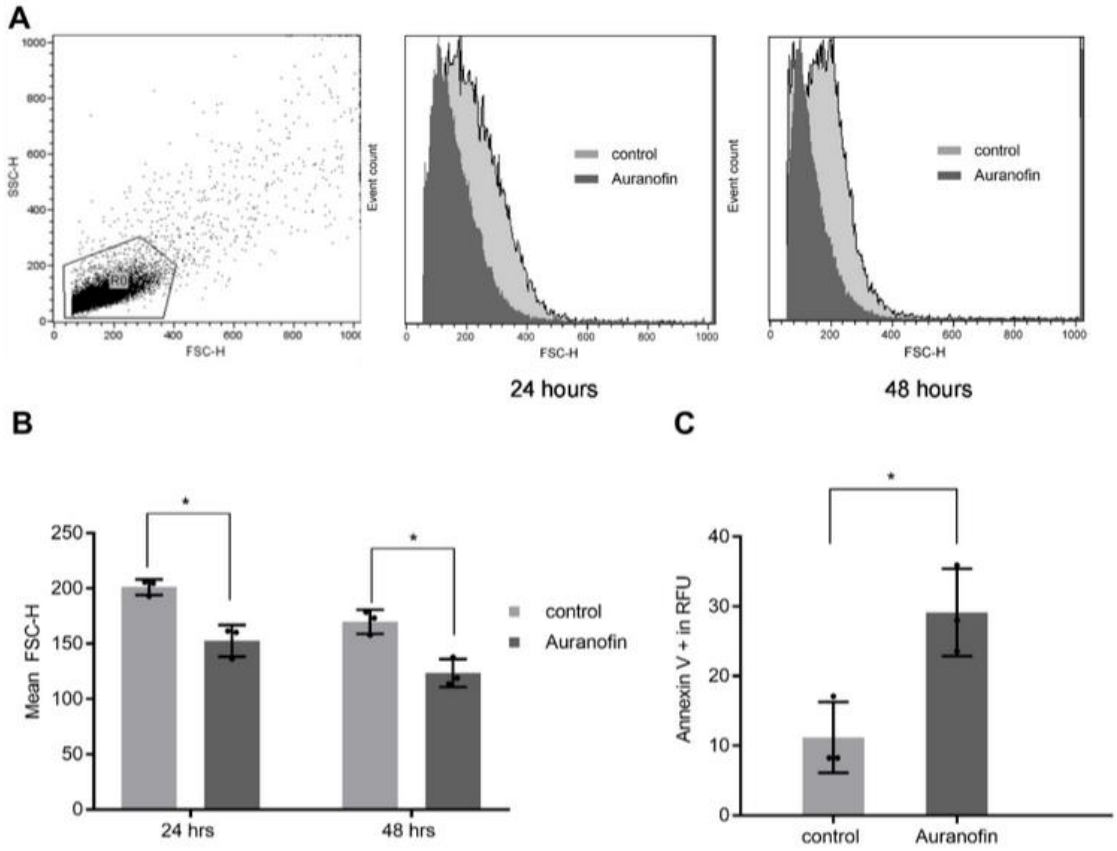

Figure 2.3. Apoptosis of *T. gondii* by auranofin: Purified *T. gondii* parasites were exposed to auranofin for 24 hours or 48 hours before preparing them for flow cytometry. **A)** Size of *T. gondii* parasites as determined by FSC-H: Gating strategy of parasites (left); Representative histograms for FSC-H for control (light gray) and auranofin-treated parasites (dark gray) at 24 hours (center) and 48 hours (right). **B)** Evaluation of *T. gondii* parasite size: Auranofin-treated parasites were smaller than those in the control group at 24 hours ($p<0.01$) and 48 hours ($p<0.01$). **C)** Phosphatidylserine externalization (PS) as demonstrated by Annexin V assay and presented as relative fluorescent units: auranofin-treated parasites show higher PS than control ($p<0.05$). Student's t-test. Results from three independent experiments. Error bars for standard deviations are shown.

Aur^R *T. gondii* lines have a growth advantage over wild type parasites:

To identify molecular targets of auranofin in *T. gondii*, we selected for auranofin-resistant (Aur^R) parasites after chemical mutagenesis and performed competition assays between wild-type parasites and clonal resistant lines. Resistant clone selection was carried out under the highest dose of auranofin (3mM) tolerated by the host cell monolayer. During competition assays, either wild-type parasites or Aur^R *T. gondii* lines were grown in competition with an equivalent amount of YFP-expressing RH strain *T. gondii*; the starting inoculum was verified by flow cytometry to ensure that the relative populations were in balance. These mixed populations were then measured by flow cytometry after each lytic cycle to determine relative fitness. If a parasite line were to exceed 50% of the population, this would be indicative of a growth advantage over the line it is growing in opposition to. In the absence of selective pressure, most of the Aur^R *T. gondii* lines grew as well as the YFP-RH line, with 1 of the 4 lines being outperformed by the controls (**Figure 2.4A**). On the other hand, addition of selective pressure (3µM auranofin) caused all of the Aur^R *T. gondii* lines to completely replace the YFP-RH line within 6 days of inoculation (**Figure 2.4B**). Together, these observations demonstrate that Aur^R *T. gondii* lines have a general growth advantage over wild-type parasites. Furthermore, these experiments also show that 6 days post inoculation is an optimal time to observe differences in growth advantage between populations. With this observation in mind, we measured the relative fitness of a larger set of 10 Aur^R *T. gondii* lines against YFP RH parasites, 6 days after inoculation. This larger screen of Aur^R *T. gondii* lines showed that 9 of the 10 resistant lines outperformed the wild-type parasites under selective pressure (**Figure 2.5**). Interestingly, one of the auranofin-resistant lines (line 6) showed a growth defect in both auranofin-containing media and normal media, suggesting that protracted replication may allow it to evade auranofin-mediated parasite clearance.

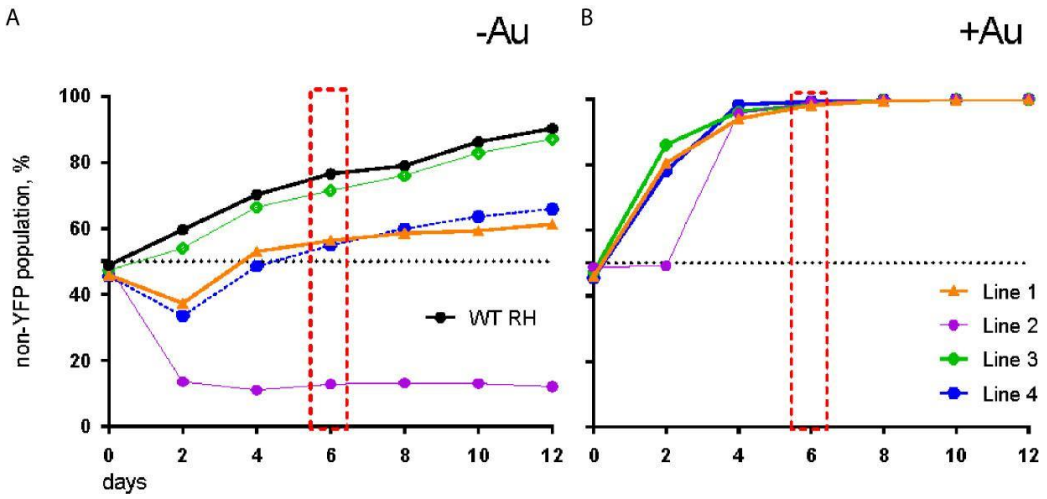

Figure 2.4 Growth competition assay of representative AurR lines under auranofin selection. (A) In the absence of auranofin (Au), individual resistant lines (colored) grow as well or less well than the parental RH strain (black). **(B)** In the presence of 3 µM auranofin, wild-type parasites are eliminated by day 6 (red box). Single representative experiment.

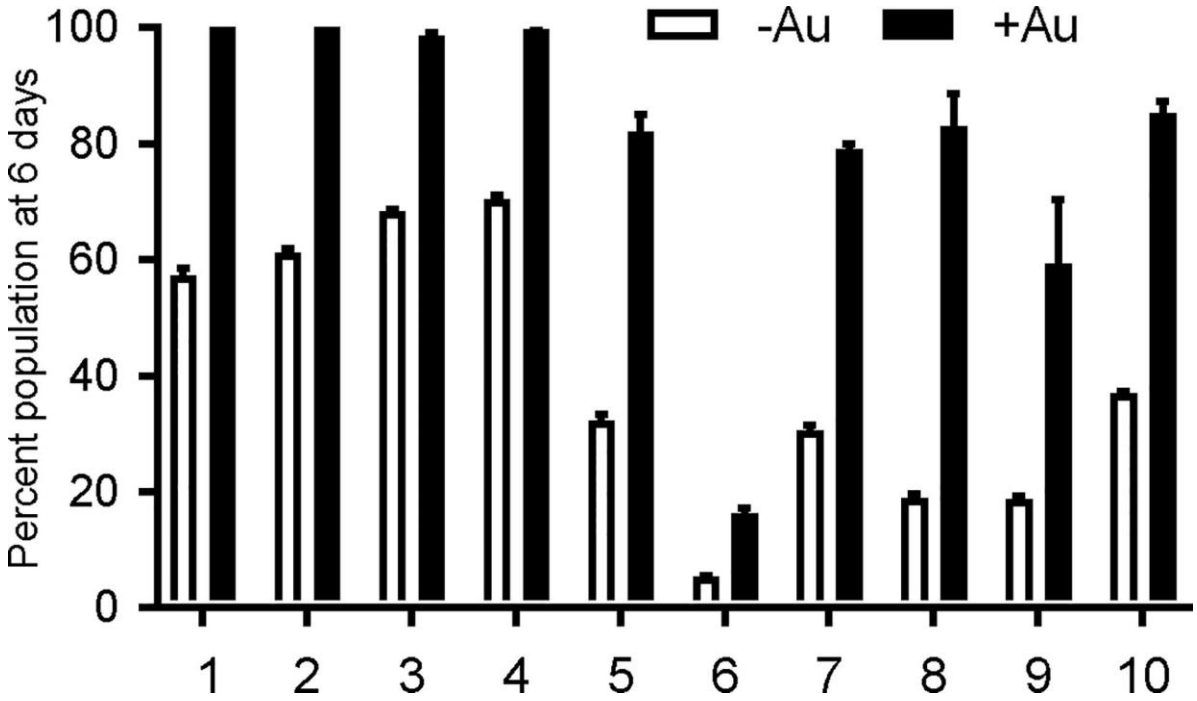

Figure 2.5 Growth competition assay of additional AurR lines under selective pressure with auranofin. Aur^R lines are represented as percentage of the total population of parasites after 6 days in competition with YFP-expressing wild type (sensitive) parasites in, media without drug (white) or 2.5 µM auranofin (black). Mean difference between parasite population in the absence of auranofin and in the presence of auranofin: 40.6; SD 14.6; two-tailed unpaired t-test $p < 0.001$. Results from three independent experiments.

Aur^R lines do not harbor mutations in the thioredoxin reductase gene:

Prior studies have proposed thioredoxin reductase as the target of auranofin; we had predicted that auranofin resistance would arise from mutations in the single parasite thioredoxin reductase gene. To test this prediction, we amplified and sequenced the thioredoxin reductase gene in 53 Aur^R *T. gondii* lines derived from independent parallel selections (*data not shown*). Mutations of thioredoxin reductase were not found in the sequencing of these lines, indicating that auranofin resistance arose through alternative methods.

Following specific gene sequencing, we performed whole genome sequencing (WGS) analysis of a subset (10) of these Aur^R *T. gondii* lines to identify possible commonalities between lines. This WGS analysis was restricted to coding single nucleotide variants (SNVs) with 100% SNV frequency and at least 50-fold coverage within each line. WGS analysis revealed a profile of ~5 SNVs per analyzed line, which were then verified by amplification of the mutated gene and Sanger sequencing (**Table 2.1**). Within the analyzed lines, Aur^R line 8 is of notable importance due to its greater degree of mutation (12 coding SNVs which result in amino acid substitutions) compared against the other lines. Subsequent analysis reveals mutations in highly fitness-conferring genes responsible for encoding superoxide dismutase (TgSOD2, TGGT1_316330) and ribonuclease reductase (RNR, TGGT1_294640). Both of these genes are expressed within the tachyzoites and are well-conserved across various species. It is not clear how these amino acid substitutions would affect protein function, but it is unlikely that the SNVs would result in a loss of function while maintaining parasite survival. Both of these genes are predicted to be essential to parasite survival; loss of function mutations in either of these genes would likely result in a gross survival defect in the mutant parasites.

Delving deeper into the specific function of these genes, RNR catalyzes the formation of deoxyribonucleosides from nucleoside diphosphates through the removal of a hydroxyl group from the ribose ring. On the other hand, TgSOD2 is a mitochondrial enzyme which is the sole enzyme capable of the dismutation of superoxide anions into hydrogen peroxide. This is one of

T. gondii's three SOD enzymes, all of which are iron-dependent and form homodimers to function but vary in terms of their localization and expression pattern. TgSOD1 and TgSOD2 are constitutively expressed but are sequestered to the cytoplasm and mitochondrion respectively. SOD3 expression is limited to feline oocysts. TgSOD2 itself bears some resemblance to its human counterpart, with a predicted homology of roughly 39% to human SOD. Examining the specific mutation unique to the Aur^R line 8, L201P introduces a proline to an α-helix near the iron coordinating residues (H111, E249, and H260). This mutation could lead to bending of the helix, which may alter enzyme functionality. Between these two genes, TgSOD2 is more likely to contribute to developing auranofin resistance as it can neutralize reactive oxygen species generated by auranofin-induced redox stress. Furthermore, its specific localization to the mitochondrion localizes it to an organelle sensitive to redox stress (Ghosh et al., 2012; Charvat and Arrizabalaga, 2016).

Rank	Mutation	Locus	Predicted protein	CRISPR	*RNA-seq	Motif	Index
1	*L201P*	TGGT1_316330	Superoxide dismutase SOD2	–4.09	76.99	SOD motif	2.50
2	*L166Q*	TGGT1_294640	Ribonucleoside-diphosphate reductase	–4.79	40.9	R1 subunit, ribonucleotide reductase	2.29
3	*Y95C*	TGGT1_233460	SAG-related sequence SRS29B	–0.07	1809.46	Major surface antigen p30	2.10
4	*Y637H*	TGGT1_268870	Tetracopeptide repeat-containing	–1.66	38.52	Predicted dehydrogenase	1.81
5	*P1357-S1358Δ*	TGGT1_310350	PGAP1 family protein	–2.41	11.67	Alpha/beta-hydrolase/PGAP1-like protein	1.45
6	*D487G*	TGGT1_289820	TBC domain-containing protein	–1.14	15.49	Rab-GTPase-TBC domain	1.25
7	*L606L*	TGGT1_271290	Hypothetical protein	–2.02	8.1	Alternative splicing regulator	1.21
8	*F424L*	TGGT1_234250	Hypothetical protein	–2.02	6.39	SWAP/MAEBL	1.11
9	*A574G*	TGGT1_290910	Hypothetical protein	–1.39	7.63	No putative conserved domain	1.03
10	*D1983del*	TGGT1_211310	Hypothetical protein	–0.69	12.86	RCC1 repeat	0.95
11	*F563S*	TGGT1_260490	Hypothetical protein	–1.62	5.34	Herpes BLLF1	0.94
12	*P66P*	TGGT1_225340	Hypothetical protein	0.73	24.06	No putative conserved domain	N/A

**Transcriptome Gregory series at 2 h RH (log 2 FPKM+1). FPKM, fragments per kilobase of exon per million fragments mapped; N/A: not calculated due to dispensable (positive) CRISPR phenotype index.*

index Formula = Sum of Log10 of (–CRISPR phenotype index)+log10 (RNAseq expression).

Table 2.1 SNVs in AurR line 8.

Aur^R lines accumulate less reactive oxygen species (ROS):

As auranofin treatment induces ROS accumulation (Lee et al., 2019), we have tested the ROS scavenging abilities of a subset of the Aur^R *T. gondii* lines. Briefly, four representative Aur^R *T. gondii* lines were exposed to hydrogen peroxide for 30 minutes and then ROS accumulation was measured via dichloro-fluorescein (DCF). This subset included line 8, which harbors the TgSOD2 L201P mutation. All the Aur^R *T. gondii* lines surveyed showed greater ROS clearance than the parental RH line ($p<0.05$). These differences in ROS accumulation persisted in the presence of auranofin treatment as well (**Figure 2.6**). It would follow that auranofin treatment results in ROS generation, therefore, increased ROS scavenging ability protects parasites from auranofin treatment.

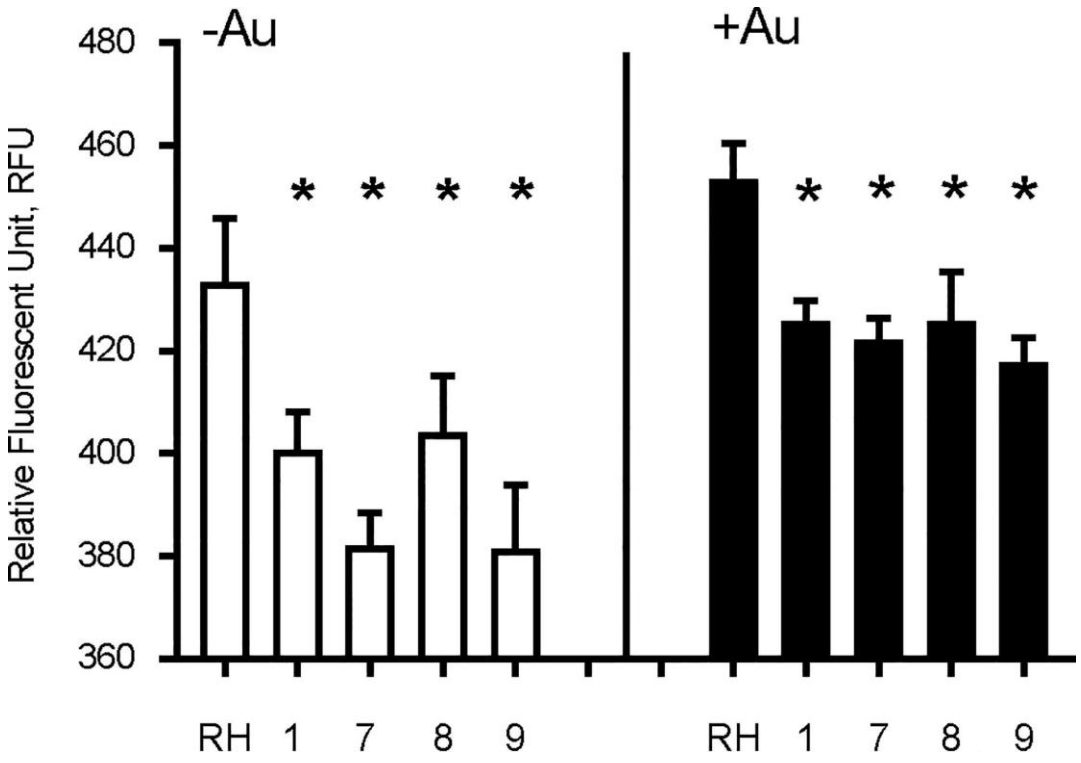

Figure 2.6 ROS accumulation of AuR parasite lines. Freshly lysed wild-type parasites were treated with 500 µM hydrogen peroxide (H_2O_2) for 30 min and accumulation of reactive oxygen species (ROS) was assayed with dichloro-fluorescein H_2DCDFC. Auranofin-resistant clones accumulated less ROS after H_2O_2 treatment compared to the wild-type RH parasites in the presence of H_2O_2 (white) or H_2O_2 + 1 µM auranofin (black). (*) $p < 0.05$ when compared to RH or to RH+ Auranofin (Au). Results from three independent experiments.

Resistance to auranofin is not conferred by an isolated mutation in TgSOD2:

As our previous mutagenesis created Aur^R *T. gondii* lines with multiple mutations, we wanted to investigate if a single mutation was sufficient to confer auranofin resistance. Of the mutations found in Aur^R line 8, the L201P TgSOD2 mutation is the most promising candidate for a resistance driver mutation as it could alter the redox capabilities of the mutated parasites. Unlike the other affected genes, TgSOD2 is a bona fide enzymatic ROS scavenger, and the sole mitochondrial superoxide dismutase in *T. gondii* tachyzoites. To investigate this mutation in isolation, we have generated a new mutant *T. gondii* with a C-terminal YFP-tagged L201P TgSOD2, and one without the YFP tag. Once these lines were verified by sequencing and microscopy, the SNV mutants were subjected to competition assays to evaluate their replication fitness. In the absence of auranofin, the L201P lines outperformed Aur^R line 8, but are less fit than TgSOD2-YFP wild type lines (**Figure 2.7B**). With auranofin, the L201P mutants fail to grow, unlike Aur^R line 8 (**Figure 2.7B**). This indicates that L201P is insufficient to confer auranofin resistance. Furthermore, ROS scavenging assays with these L201P mutants also show scavenging activity consistent with wild-type parasites, rather than the increased ROS scavenging profile of Aur^R line 8 (**Figure 2.7C**). Together, these results suggest that additional mutations are necessary for the development of auranofin resistance and increased ROS scavenging activity. These additional mutations are unlikely to interact with TgSOD2 directly, as there is no evidence for TgSOD2 interacting with other enzymes. Moreover, these results also suggest that the L201P mutation is a neutral or at least minor gain of function. Given that TgSOD2 has been previously predicted to be highly fitness conferring but does not have increased ROS scavenging activity, the L201P mutation cannot be a loss of function mutation.

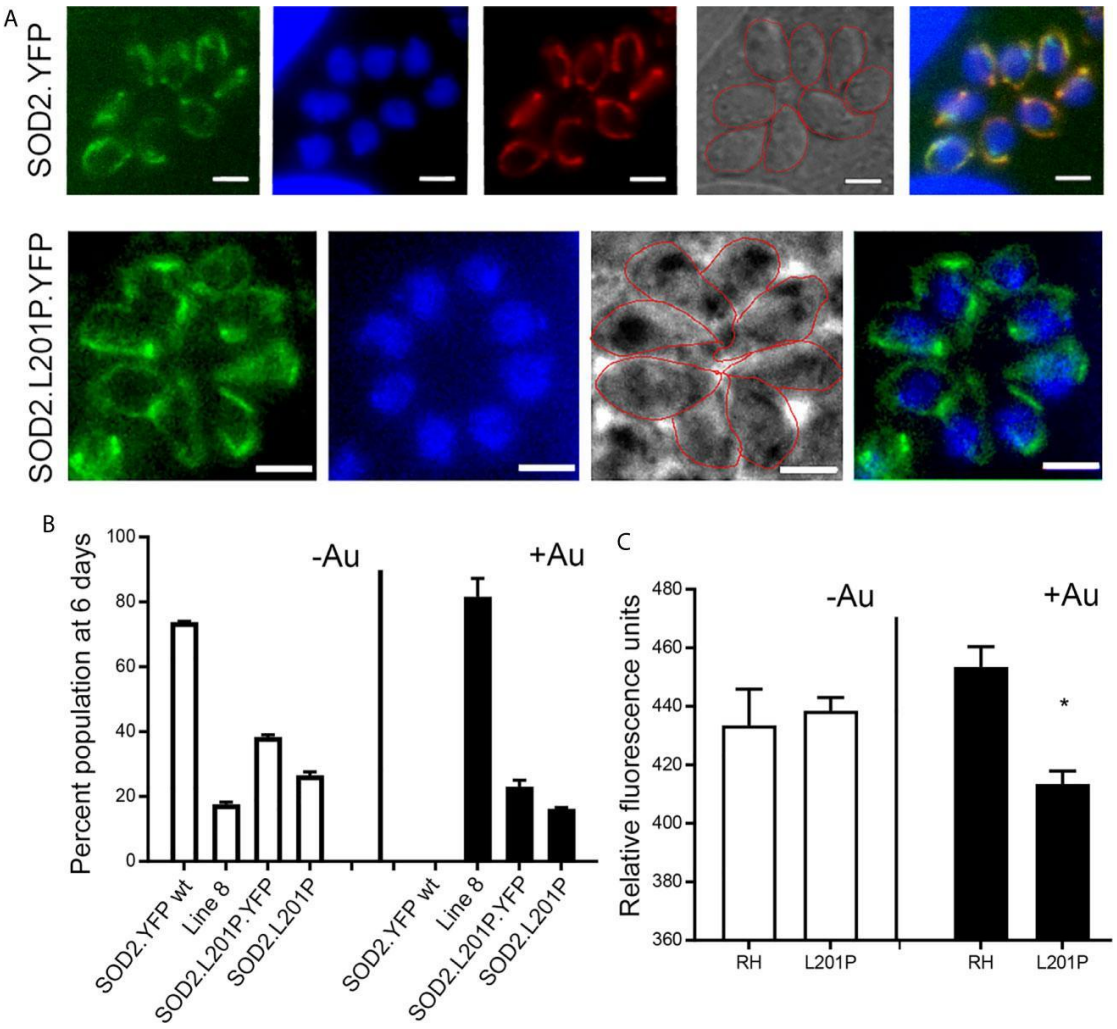

Figure 2.7 TgSOD2 localization, competition under auranofin selection, and ROS accumulation of L201P mutant parasites. (A) Wild type and mutant SOD2-YFP exhibit a mitochondrial distribution. Mitochondrion was stained red with the anti-F1B ATPase. Scale bar: 5 µm. **(B)** Growth competition assays indicate that the L201P mutation is associated with reduced fitness in the absence of auranofin (control conditions, white bars). In the presence of auranofin (black bars), only line 8 shows growth advantage, indicating that the single L201P mutation to TgSOD2 does not confer resistance. **(C)** In the absence of auranofin, the SOD2.L201P line accumulated ROS similarly to wild type parasites, consistent with its auranofin-sensitive growth; however, it accumulated less ROS in the presence of auranofin. *p < 0.05 when compared to RH in auranofin (+Au).

Discussion

Auranofin is an effective treatment for *in vitro* toxoplasmosis: it impairs extracellular parasites' ability to invade new host cells and, in intracellular parasites, induces egress from infected hosts. Once exposed to the drug, the parasites likely undergo apoptosis, which may be

a consequence of ROS accumulation. This aligns with our previous work which demonstrated *in vivo* inhibition of toxoplasmosis following auranofin treatment (Andrade et al., 2014). While its efficacy is clear, the direct molecular target of auranofin in toxoplasma has not been identified. Prior studies in *Entamoeba* suggest that the drug inhibits thioredoxin reductase in this parasite (Parsonage et al., 2016). To identify auranofin's target in *T. gondii*, we generated auranofin-resistant mutants. While no mutations in thioredoxin reductase were identified, we did observe mutations in TgSOD2. This TgSOD2 Aur^R mutant exhibited decreased ROS accumulation auranofin treatment. Interestingly, the TgSOD2 L201P mutation was not sufficient to confer auranofin resistance. While these results suggest that TgSOD2 is not the direct target of auranofin, *Toxoplasma* thioredoxin reductase remains a possible direct molecular target of the drug.

Auranofin, a gold-containing anti-inflammatory drug, has shown promising activity against a wide variety of parasitic infections (Sannella et al., 2008; Angelucci et al., 2009; Ilari et al., 2012; Sharlow et al., 2014; da Silva et al., 2016; Hopper et al., 2016; Leitsch, 2017) in addition to *Toxoplasma*, as we have previously demonstrated (Andrade et al., 2014; Ma et al., 2020). Auranofin's chemical structure includes a gold(I) ion, a 2,3,4,6-tetra-O-acetyl-1-thio-β-D-glucopyranose ligand, and a triethylphosphine ligand. Of these features, it is thought that auranofin's delivery of gold to dithiol groups, such as those in thioredoxin domain containing proteins, is responsible for its anti-parasitic activity (Chircorian and Barrios, 2004; Saccoccia et al., 2014). Based on our findings, auranofin is capable of impairing parasite invasion (**Figure 2.1**), inducing egress (**Figure 2.2B**), and possibly inducing apoptosis (**Figure 2.3**), without effect on parasite replication (**Figure 2.2A**). These findings are consistent with the phenotype presented by auranofin treatment of *Leishmania*, where treatment also induces parasite apoptosis (Sharlow et al., 2014). During these extracellular stages of the lytic cycle, the parasite is more vulnerable to ROS stress (Camps and Boothroyd, 2001). This could be attributed to a shift in parasite metabolism to rely more upon mitochondrial oxidative phosphorylation while

extracellular (MacRae et al., 2012). Given that ROS is generated as a byproduct of oxidative phosphorylation (Tahara et al., 2009) ROS accumulates, which then sensitizes the parasite to further treatment-induced disruptions of ROS homeostasis. Prior studies have demonstrated that auranofin induces ROS accumulation in mammalian cells (Lee et al., 2019) and *T. gondii* (**Figure 2.6**) (Ma et al., 2020). While *T. gondii* is able to neutralize host ROS bursts during invasion (Wilson et al., 1980) it is still susceptible to ROS damage while extracellular (Camps and Boothroyd, 2001).

Our studies with Aur^R *T. gondii* mutants allowed us to test whether they can scavenge ROS better than wild-type counterparts. Drug resistant mutant screens are a method of determining the direct targets of a given drug of interest. It is assumed that resistance to a drug may arise from a mutation in the drug's direct target, thereby rendering the mutant resistant to its effects. In generating Aur^R mutants, no mutations of thioredoxin reductase were captured, but these parasite lines did display increased fitness under auranofin treatment (**Figures 2.4-2.5**). Rather, it is likely the case that their resistance is a product of increased ROS scavenging activity under auranofin stress (**Figure 2.6**); this would allow the mutant parasites to compensate for additional ROS generated as a result of auranofin treatment. One specific mutation (TgSOD2 L201P) was sufficient to confer increased ROS scavenging activity under auranofin treatment, but not auranofin resistance (**Figure 2.7**). Compared against the other Au^R mutants generated by ENU mutagenesis and auranofin selection, the TgSOD2 L201P mutant line was generated through targeted insertion into the TgSOD2 gene. This approach allowed us to focus on the contribution of the TgSOD2 L201P mutation in isolation whereas the original Au^R mutant contained additional mutations (**Table 2.1**). It is likely the case that at least one of those additional mutations is necessary for auranofin resistance in combination with TgSOD2 L201P. Future studies could determine the minimal necessary mutation set required for auranofin resistance.

Overall, the previously described experiments and findings provide striking insight into how auranofin interacts with *T. gondii*; but these experiments are not without limitations. The treatment induced size reduction and an increase phosphatidylserine translocation to the parasite cell surface, suggesting an apoptosis-related mechanism of killing. Confirmation of apoptosis is needed to support this conclusion; data such as increased transcription of apoptotic markers would be an acceptable addition. Unfortunately, the presented extracellular treatment paradigm results in drastic loss of parasites over time, preventing effective harvest of RNA at corresponding time points (*data not shown*). An effective antibiotic treatment may induce apoptosis, which would result in a loss of RNA via degradation (Thomas et al., 2015). It may be interesting to interrogate the transcriptome of parasites which survive extended antibiotic treatment, but it would not be informative of which genes are upregulated during the process of cell death. Rather, transcriptomic assays following extended antibiotic treatment may reveal methods of antibiotic resistance in surviving parasites.

Instead, we generated auranofin resistant parasites through chemical ENU mutagenesis, probed their genome for SNVs which would alter coding regions of genes. This limitation in scope prevents us from identifying non-coding mutations which could alter regulatory patterns. The characterization of these resistant lines was also limited. Future studies should probe whether Aur^R lines display changes in lytic cycle assays, or other behavioral differences. Given the wide variety of mutations captured in the Aur^R lines, it is likely that the mutants display differences amongst each other if subjected to invasion, replication, or egress assays. Additional investigations into thioredoxin reductase expression patterns of other ENU mutagenized auranofin resistant lines could reveal changes in splicing or overall transcription or translation.

This is the first demonstration that auranofin inhibits parasite growth by inducing apoptosis of extracellular parasites thereby preventing invasion into host cells. Furthermore, resistant mutant screens demonstrate that TgSOD2 mutations confer increased ROS

scavenging activity, which, in combination with other mutations, results in auranofin resistance. These findings highlight both the viability of ROS homeostasis disruption as a therapeutic strategy and the mechanisms by which parasites can adapt to treatment regimens. While we did not confirm if auranofin targets thioredoxin reductase in *T. gondii*, the results suggest that the drug achieves anti-parasitic action through ROS accumulation-induced apoptosis. Future studies should investigate the viability of auranofin in combination with additional treatments. We have demonstrated that auranofin alone is capable of partial parasite inhibition, but a combination therapy strategy may be able to completely inhibit parasite growth. Additionally, studies should evaluate the use of auranofin during chronic infections; elimination of *T. gondii* cysts remains an elusive therapeutic goal.

Materials and Methods

Host Cell and Parasite Cultures

Parasite clones and human foreskin fibroblasts (HFF) were grown and maintained in Dulbecco's modified Eagle's medium supplemented with 10% fetal bovine serum (Hyclone), penicillin and streptomycin (50 mg/ml each) and 200 mM L-glutamine, this media will hereby be referred to as D10. *T. gondii* were maintained by serial passage in HFF monolayers at 37°C in a humid 5% CO_2 atmosphere, including RH parasites (National Institutes of Health AIDS Reference and reagent Repository, Bethesda, MD), RH tachyzoites expressing cytoplasmic yellow fluorescent protein (YFP) (kindly provided by M.J. Gubbels, Boston College, Boston, Massachusetts) (Gubbels et al., 2003) and Ku80 knock-out parasites (DKu80, kindly provided by V. Carruthers, University of Michigan Medical School Dexter, Michigan) (Fox et al., 2009; Huynh and Carruthers, 2009).

Invasion assays

Invasion assays with or without pre-treatment of *T. gondii* tachyzoites with auranofin were modified from previously described assays (Nagel and Boothroyd, 1989; Stokkermans et al., 1996; Kafsack et al., 2004; Sweeney et al., 2010). We performed a modified invasion assay using 2.5 $x10^6$ parasites freshly lysed YFP+ RH parasites (Nagel and Boothroyd, 1989; Gubbels et al., 2003) that were filtered and centrifuged before each assay as follows:

Invasion assay without pre-treatment of *T. gondii* with auranofin: Confluent monolayers of HFF in an 8-chamber slide were inoculated with YFP+ RH parasites in D10 with DMSO (control) or auranofin at 3 µM in D10 for 30 minutes at 37°C and 5% CO_2. The chamber slide was kept warm throughout the invasion assay by immersing it in a container with 37°C water.

Invasion assay with pre-treatment of *T. gondii* with auranofin: Similarly, freshly filtered YFP+ RH parasites were centrifuged and resuspended in either D10 with DMSO (control) or auranofin at 3 µM in D10 for 30 min before the invasion assay. Upon 30 min pre-treatment with auranofin, a confluent monolayer of HFF was inoculated with these pre-treated parasites for 30 min as described above.

After the 30-minute invasion, chamber slides were washed with PBS and fixed with 4% paraformaldehyde prior to blocking with 3% bovine serum albumin. Extracellular parasites were stained with anti-SAG-1 antibody (DG52) (David Sibley, Washington University in St. Louis) for 1 hour, followed by staining with goat anti-mouse IgG conjugated to Alexa-594 fluorophore (A19069, Thermo Fisher). To quantify invasion, 8 randomly selected fields of view with at least 300 parasites were scored for each sample. Uninvaded parasites were double labeled with mouse anti-SAG1 in addition to their endogenous YFP signal (extracellular YFP+/SAG1+). Intracellular parasites, YFP+/SAG1-, remained green. The invasion rate was calculated by dividing the number of intracellular parasites by the total number of parasites counted.

A paired t-test was used to determine the statistical difference between control or auranofin treatment from three independent experiments. Slides were imaged on Zeiss Axioskop with Axiovision camera and software.

Parasite Replication Assay

$5x10^5$ YFP expressing parasites were used to invade a confluent 12mm coverslip of human fibroblasts at an MOI of 5 in standard D10 media. The infected coverslip returned to the incubator for 1 hour to allow for invasion, then rinsed with PBS to remove non-adherent parasites. Following the rinse, new media was added to begin auranofin (2.5 µM) treatment. Twenty four hours later, coverslips were fixed and stained with DAPI to visualize nuclei. Parasites were counted across 10 random fields of view per coverslip and individual vacuoles were scored as containing: 1, 2, 4, or ≥8 parasites per vacuole. Data shown as the sum of all vacuoles counted across 3 independent experiments, for a total of 30 quantified fields of view. Slides were imaged on Zeiss Axioskop with Axiovision camera and software.

Egress assay

The presented egress assay was modified from prior studies to measure lactate dehydrogenase (LDH) release by parasite egress from host cells (Fruth and Arrizabalaga, 2007; Schultz and Carruthers, 2018). Confluent HFF monolayers in a 24-well plate were infected with $5x10^5$ filtered parasites (3 µm filter) for 30 hours prior to drug treatment in three technical replicates. Infected HFF monolayers were rinsed with 37°C Ringer's solution (Ward's Science) 3 times and supplied with 5 µM calcium ionophore A23187 (ACROS), 57 µM Zaprinast (Alfa Aesar), 5 µM auranofin (Enzo Life Sciences) or DMSO control (all in 5 µl) for 40 minutes in 5% CO_2 and 37°C to induce egress. Supernatant from treated cells was collected and centrifuged at 4°C and 500 g for 5 minutes. The supernatant was kept at 4°C and assayed immediately for the LDH content. Absorbance at 490ʎ (A490) is indicative of LDH content and was measured using a multimode microplate plate reader (Molecular Devices Spectramax i5, SoftMax Pro 7.0.2

Software). The readings were compared against a standard curve of known LDH quantities to determine absolute LDH quantities (CytoTox 96™ Nonradioactive Cytotoxicity Assay, Promega). Absolute LDH values were then normalized against a DMSO control by subtracting absolute levels of LDH induced by drug-absolute levels of LDH induced by DMSO alone (DMSO is the solvent for all drugs in this assay). Student's t-test was used to determine the statistical difference between the relative egress triggered by auranofin and A23187 or auranofin and Zaprinast from three independent experiments. Slides were imaged on Zeiss Axioskop with Axiovision camera and software.

Acute Treatment with Auranofin in Extracellular Parasites

A confluent T175 was infected with fresh parasites and allowed 24 hours of undisturbed incubation in standard D10 media. The parasites were forcefully released from host cells by scraping. Differential centrifugation was used to separate released parasites from host cell debris (Lüder et al., 1999). Briefly, host cell debris was isolated via centrifugation at 35xG for 5 minutes; the resulting supernatant was then centrifuged at 1350xG for 10 minutes to pellet the extracellular parasites. The parasite pellet was then resuspended in PBS for counting. Afterwards, $2.7x10^7$ parasites were placed into each well of a 12 well plate into 1ml of drug containing D10 media. The plate was left undisturbed for 24-48 hours at normal tissue culture conditions prior to collection for flow cytometry. For flow cytometry, $1x10^5$ parasites were resuspended in 1 ml of PBS, and then parasite size was analyzed via forward scattering.

Assessment of Apoptosis

In addition to measurements of parasite size following auranofin treatment, Annexin V assays were carried out in order to quantify the amount of apoptosis induced by drug treatment. Treated parasites were collected following 24 hours of treatment in a host cell free environment. Parasites were washed with PBS to remove remaining media. Washed parasites were

resuspended at a concentration of 10^6 parasites per mL in annexin binding buffer (10 mM HEPES, 140 mM NaCl, and 2.5 mM $CaCl_2$, pH 7.4). 100µl of this parasite suspension was stained with 5µl of annexin V-Alexa fluor conjugate for 15 minutes at room temperature. After staining, 400µl of additional annexin binding buffer was added, and the stained parasites were placed on ice prior to flow cytometry analysis.

Generation of *T. gondii* Clones Resistant to Auranofin

T. gondii ENU mutagenesis was carried out as previously described (Pfefferkorn and Pfefferkorn, 1979; Nagamune et al., 2007). Briefly, approximately $1.5x10^7$ wild-type RH strain tachyzoites were mutagenized with ENU (N-Ethyl-N-nitrosourea, N3385-1G, Sigma Aldrich; 100–200 µg/ml) in DMEM without FBS for 2 h at 37°C. Mutagenized parasites were washed with PBS, then inoculated into a new confluent HFF monolayer for auranofin selection (2.5 mM-3 mM). Once mutant parasites had regained normal replication speed (roughly 2 weeks after mutagenesis), they were single cell cloned under 2 mM auranofin selective pressure. The isolated clones were propagated under 1 mM auranofin pressure while minimizing host cell cytotoxicity (*data not shown*). This process was carried across 10 independently generated pools of mutagenized parasites, resulting in 10 independent resistant clones. A modified tachyzoite growth competition assay was used to measure auranofin resistance (Ma et al., 2008). Confluent monolayers of HFF cells were inoculated with both ENU-mutagenized parasites and YFP-expressing wild-type RH parasites at a 1:1 ratio ($2x10^6$ of each strain). Once the monolayer was lysed, 0.25 ml of mixed lysed parasites would be used to inoculate a new T25 flask with a confluent monolayer. 0.25 ml of lysed parasites would be subjected to population tracking via flow cytometry as resistant parasites do not bear a YFP signal. Relative population distribution was recorded over serial passages. Both total parasite number and the YFP+ parasite number were quantified using a FACSCalibur flow cytometer (Becton Dickinson)

and analyzed with FlowJo (Tree Star). Parametric paired t-tests were used to analyze three independent experiments. A two-tailed p-value $p<0.05$ was considered statistically significant.

Identification of Mutations in Auranofin-Resistant *T. gondii* Clones

Genomic DNA (gDNA) was extracted from auranofin resistant parasite lines using the DNeasy Blood and Tissue kit (Qiagen). The thioredoxin reductase gene (TGGT1_309730, ToxoDB.org) was amplified from gDNA samples as two PCR fragments ~3.7 kb each. Both amplification and sequencing primers can be found in supplementary table 1.

To determine the presence of other SNVs in the coding region of our *T. gondii* auranofin resistant clones, gDNA from 10 resistant clones and wild-type RH parasites was submitted for library construction and whole genome sequencing at the Genomic High Throughput Facility at University of California, Irvine. Briefly, genomic DNA (gDNA) was initially quantified with a Qubit DNA High Sensitivity kit. One hundred nanograms of gDNA was sheared to <300–500> bp in size using a Covaris S220 ultrasonicator (shearing conditions: duty Cycle 10%, Cycles/burst 200 and treatment time 55 sec) (Covaris, MA). The size and the quality of the resulting DNA fragments were analyzed with an Agilent DNA High Sensitivity chip. Ten nanograms of each sample's fragmented DNA was end-repaired, polyadenylated and ligated to a 6bp DNA barcodes (Bioo Scientific NextFlex DNA barcodes) using a PrepX Complete ILMN DNA Library kit (Takara Bio, CA). The genomic library was built using the Apollo 324 system (Takara Bio, CA) to generate 520 bps inserts. To enrich the DNA libraries, 8 cycles of PCR amplification using a Kapa library amplification kit was used (cycling conditions: 98°C for 45 s, 8 cycles of 98°C for 15 sec, 60°C for 30 s 72° C for 30 s and then 72°C for 1 min) in an Apollo 324 system. The ultimate DNA concentration was calibrated using Qubit 2.0 dsDNA HS Assay kit and analyze with an Agilent DNA High Sensitivity chip. DNA libraries were quantified prior to sequencing using a KAPA Library Quantification kit for Illumina platforms (Roche). Each library was normalized to 2nM and then pooled equimolar amounts in the final multiplex library that

was sequenced on the Illumina HiSeq 4000. The ten auranofin resistant *T. gondii* clones and wild-type RH *T. gondii* were sequenced with HiSeq 4000 paired end 100 reads, quality analyzed, adapter and quality trimmed before alignment with the annotated reference genome of GT1 strain from ToxoDB.org (published 7/19/2013) (Gajria et al., 2008). After initial quality control with FASTQC, reads were trimmed using Illumina adapter sequences with the error probability of 0.05 and reads shorter than 20 bases were discarded. Single Nucleotide Variant (SNV) calling for the haploid genome had a coverage threshold of >5 fold. Each of the 10 mutant clones was compared to wild-type RH variant track and shared variants were filtered out. Only SNVs in the coding regions of the 10 mutant clones are reported. Only genes containing SNVs with 100% frequency and ≥50% of read count and read coverage were considered in the final analysis. Genomic DNA from each mutant clone was used to amplify the targeted SNV region of interest. The resulting amplicons ranged between 1.7–4.5 kbp in size. PCR amplicons were purified prior to sequencing via a QiaQuick PCR Purification Kit (Qiagen 28106). Amplicons were sequenced by Sanger sequencing (Genewiz), using sequencing primers targeted to the SNV region (Table S1). Genomic sequences for all 10 mutant lines can be accessed by NCBI, under the Bioproject PRJNA679812.

Generation of Modified TgSOD2 Lines

A *T. gondii* mutant line expressing TgSOD2 with a 3' YFP tag was generated via homologous recombination of a ligation independent cloning vector (Huynh and Carruthers, 2009). Verification of the mitochondrial localization of mutant TgSOD2 was achieved through immunofluorescence studies using an anti-F1B ATPase antibody (gift from Peter Bradley at UCLA). In addition to mitochondrial localization, apicoplastic localization was verified through immunofluorescence studies using an anti-ATRx antibody (gift from Peter Bradley at UCLA). CRISPR-Cas9 was used in order to induce the L201P point mutation into the YFP-tagged mutant line. A sgRNA/CAS9 expressing plasmid was transfected into the mutant parasites, the

plastid pSAG1::CAS9-U6::sgUPRT was used as the scaffold (Shen et al., 2014); Addgene # 54467. The endogenous SAG1 directed gRNA was replaced with two gRNA sequences (cggtataccggacagatccg and TAGTTTCGCCCAGTTCAAGG) directed against TgSOD2. Benchling was used in gRNA selection (Benchling.com).

The homology directed repair oligo was amplified from the plasmid used for TgSOD2 YFP tagging, using the following primers: GATAGTGTGTGAAGAGCAGC and CTGCCGTTACCAACATGG. Site directed mutagenesis via the Q5-Site Directed Mutagenesis kit (New England Bio Labs) was used to introduce the L201P mutation into the homology directed repair oligo. Additionally, novel restriction endonuclease sites were introduced into the oligo to enable clone screening; these novel site generations are both silent mutations: AflI on Leucine 180 (CTC->CTT) and XcmI on Serine 208 (TCA->TCT). Lastly, site directed mutagenesis was used to abolish the PAM sequence and prevent unwanted CAS9 activity on successfully mutated DNA. The sequence AGAGACCCGGCGG (including the PAM sequence cgg) was deleted on the HDR sequence corresponding to gRNA #1, and sequence CACTTAACAGAGGGTC (including the PAM sequence agg) was deleted on the HDR sequence corresponding to gRNA #2.

Transfection of both the sgRNA/CAS9 plasmid and homology directed repair oligo was used to induce the L201P point mutation in the TgSOD2-YFP tagged line(Figure S1) (Shen et al., 2014). Minor modifications were made to the transfection protocol: 10^7 of freshly lysed TgSOD2-YFP parasites were filtered and spun down at 400xg and 18℃ for 10 min. The pellet was resuspended with Cytomix buffer (10 mM KPO_4, 120 mM KCl, 5 mM $MgCl_2$, 25 mM HEPES, 2 mM EDTA, 2 µM ATP and 5 µM glutathione) up to 800 µl, including 7.5 µg of gRNA/CAS9 plasmid and 1.5 µg of homology directed repair oligo. The mixture was transfected using the ECM 630 Electro Cell Manipulator (BTX). Transfected parasites were used to infect T25 flasks and switched to 2 mM pyrimethamine selection 24 hours later. Pyrimethamine selection lasted for 3 days leading up to single cell cloning; transfectant pools were switched to

pyrimethamine free D10 media for 24 hours before single cell cloning in 96-well plates. Genomic DNA from isolated clones was harvested via DNeasy Blood and Tissue kit (Qiagen) then screened via PCR amplification of TgSOD2 and XcmI digestion.

Measurement of ROS Accumulation in T. gondii

To measure ROS accumulation and clearance, $5x10^4$ freshly lysed parasites were harvested and treated with 500 mM hydrogen peroxide (H2O2) for 30 min at 37°C, 5% CO_2, with or without 1 mM auranofin. Dichlorofluores cin diacetate (1 μM H_2DCDFC, Invitrogen) was used to detect ROS presence after incubation. The resulting fluorescent signal was measured via Spectramax i5, (Molecular Devices California US; multimode microplate reader SoftMax Pro 7.0.2 Software) multimode microplate reader (excitation 494 nm; emission 522 nm) at 37°C for 15 min. For excitation, a single flash from a UV Xenon lamp was used for each well, and emission signals were recorded as relative fluorescence units with a sensitivity setting of 100. Analysis was done via two-tailed unpaired t-test across three independent experiments, and $p<0.05$ was considered statistically significant. ROS accumulation was measured in all of the representative auranofin resistant lines and compared against a wild-type control line.

References

Andrade, R. M., Chaparro, J. D., Capparelli, E., and Reed, S. L. (2014). Auranofin is highly efficacious against Toxoplasma gondii in vitro and in an in vivo experimental model of acute toxoplasmosis. *PLoS Negl. Trop. Dis.* 8, e2973. doi: 10.1371/journal.pntd.0002973.

Angelucci, F., Sayed, A. A., Williams, D. L., Boumis, G., Brunori, M., Dimastrogiovanni, D., et al. (2009). Inhibition of Schistosoma mansoni thioredoxin-glutathione reductase by auranofin: structural and kinetic aspects. *J. Biol. Chem.* 284, 28977–28985. doi: 10.1074/jbc.M109.020701.

Becker, K., Gromer, S., Schirmer, R. H., and Müller, S. (2000). Thioredoxin reductase as a pathophysiological factor and drug target. *Eur. J. Biochem. FEBS* 267, 6118–6125. doi: 10.1046/j.1432-1327.2000.01703.x.

Bulman, C. A., Bidlow, C. M., Lustigman, S., Cho-Ngwa, F., Williams, D., Alberto A. Rascón, J., et al. (2015). Repurposing Auranofin as a Lead Candidate for Treatment of Lymphatic Filariasis and Onchocerciasis. *PLoS Negl. Trop. Dis.* 9, e0003534. doi: 10.1371/journal.pntd.0003534.

Camps, M., and Boothroyd, J. C. (2001). Toxoplasma gondii: selective killing of extracellular parasites by oxidation using pyrrolidine dithiocarbamate. *Exp. Parasitol.* 98, 206–214. doi: 10.1006/expr.2001.4636.

Charvat, R. A., and Arrizabalaga, G. (2016). Oxidative stress generated during monensin treatment contributes to altered Toxoplasma gondii mitochondrial function. *Sci. Rep.* 6, 22997. doi: 10.1038/srep22997.

Chircorian, A., and Barrios, A. M. (2004). Inhibition of lysosomal cysteine proteases by chrysotherapeutic compounds: a possible mechanism for the antiarthritic activity of Au(I). *Bioorg. Med. Chem. Lett.* 14, 5113–5116. doi: 10.1016/j.bmcl.2004.07.073.

Cimini, A., Gentile, R., Angelucci, F., Benedetti, E., Pitari, G., Giordano, A., et al. (2013). Neuroprotective effects of PrxI over-expression in an in vitro human Alzheimer's disease model. *J. Cell. Biochem.* 114, 708–715. doi: 10.1002/jcb.24412.

da Silva, M. T. A., Silva-Jardim, I., Portapilla, G. B., de Lima, G. M. A., Costa, F. C., Anibal, F. de F., et al. (2016). In vivo and in vitro auranofin activity against Trypanosoma cruzi: Possible new uses for an old drug. *Exp. Parasitol.* 166, 189–193. doi: 10.1016/j.exppara.2015.05.012.

Debnath, A., Ndao, M., and Reed, S. L. (2013). Reprofiled drug targets ancient protozoans. *Gut Microbes* 4, 66–71. doi: 10.4161/gmic.22596.

Debnath, A., Parsonage, D., Andrade, R. M., He, C., Cobo, E. R., Hirata, K., et al. (2012). A high-throughput drug screen for Entamoeba histolytica identifies a new lead and target. *Nat. Med.* 18, 956–960. doi: 10.1038/nm.2758.

Endo, T., Sethi, K. K., and Piekarski, G. (1982). Toxoplasma gondii: Calcium Ionophore A23187-mediated exit of trophozoites from infected murine macrophages. *Exp. Parasitol.* 53, 179–188. doi: 10.1016/0014-4894(82)90059-5.

Fox, B. A., Ristuccia, J. G., Gigley, J. P., and Bzik, D. J. (2009). Efficient Gene Replacements in Toxoplasma gondii Strains Deficient for Nonhomologous End Joining. *Eukaryot. Cell* 8, 520–529. doi: 10.1128/ec.00357-08.

Fruth, I. A., and Arrizabalaga, G. (2007). Toxoplasma gondii: induction of egress by the potassium ionophore nigericin. *Int. J. Parasitol.* 37, 1559–1567. doi: 10.1016/j.ijpara.2007.05.010.

Gajria, B., Bahl, A., Brestelli, J., Dommer, J., Fischer, S., Gao, X., et al. (2008). ToxoDB: an integrated Toxoplasma gondii database resource. *Nucleic Acids Res.* 36, D553-6. doi: 10.1093/nar/gkm981.

Ghosh, D., Walton, J. L., Roepe, P. D., and Sinai, A. P. (2012). Autophagy is a cell death mechanism in Toxoplasma gondii. *Cell. Microbiol.* 14, 589–607. doi: 10.1111/j.1462-5822.2011.01745.x.

Gubbels, M.-J., Li, C., and Striepen, B. (2003). High-Throughput Growth Assay for Toxoplasma gondii Using Yellow Fluorescent Protein. *Antimicrob. Agents Chemother.* 47, 309–316. doi: 10.1128/AAC.47.1.309-316.2003.

Hopper, M., Yun, J., Zhou, B., Le, C., Kehoe, K., Le, R., et al. (2016). Auranofin inactivates Trichomonas vaginalis thioredoxin reductase and is effective against trichomonads in vitro and in vivo. *Int. J. Antimicrob. Agents* 48, 690–694. doi: 10.1016/j.ijantimicag.2016.09.020.

Huynh, M.-H., and Carruthers, V. B. (2009). Tagging of endogenous genes in a Toxoplasma gondii strain lacking Ku80. *Eukaryot. Cell* 8, 530–539. doi: 10.1128/EC.00358-08.

Ilari, A., Baiocco, P., Messori, L., Fiorillo, A., Boffi, A., Gramiccia, M., et al. (2012). A gold-containing drug against parasitic polyamine metabolism: the X-ray structure of trypanothione reductase from Leishmania infantum in complex with auranofin reveals a dual mechanism of enzyme inhibition. *Amino Acids* 42, 803–811. doi: 10.1007/s00726-011-0997-9.

Kafsack, B. F. C., Beckers, C., and Carruthers, V. B. (2004). Synchronous invasion of host cells by Toxoplasma gondii. *Mol. Biochem. Parasitol.* 136, 309–311. doi: 10.1016/j.molbiopara.2004.04.004.

Kobayashi, H., Takeno, M., Saito, T., Takeda, Y., Kirino, Y., Noyori, K., et al. (2006). Regulatory role of heme oxygenase 1 in inflammation of rheumatoid arthritis. *Arthritis Rheum.* 54, 1132–1142. doi: 10.1002/art.21754.

Lee, D., Xu, I. M.-J., Chiu, D. K.-C., Leibold, J., Tse, A. P.-W., Bao, M. H.-R., et al. (2019). Induction of Oxidative Stress Through Inhibition of Thioredoxin Reductase 1 Is an Effective Therapeutic Approach for Hepatocellular Carcinoma. *Hepatol. Baltim. Md* 69, 1768–1786. doi: 10.1002/hep.30467.

Leitsch, D. (2017). Drug susceptibility testing in microaerophilic parasites: Cysteine strongly affects the effectivities of metronidazole and auranofin, a novel and promising antimicrobial. *Int. J. Parasitol. Drugs Drug Resist.* 7, 321–327. doi: 10.1016/j.ijpddr.2017.09.001.

Lourido, S., Tang, K., and Sibley, L. D. (2012). Distinct signalling pathways control Toxoplasma egress and host-cell invasion. *EMBO J.* 31, 4524–4534. doi: 10.1038/emboj.2012.299.

Lüder, C. G., Giraldo-Velásquez, M., Sendtner, M., and Gross, U. (1999). Toxoplasma gondii in primary rat CNS cells: differential contribution of neurons, astrocytes, and microglial cells for the intracerebral development and stage differentiation. *Exp. Parasitol.* 93, 23–32. doi: 10.1006/expr.1999.4421.

Ma, C. I., Tirtorahardjo, J. A., Jan, S., Schweizer, S. S., Rosario, S. A. C., Du, Y., et al. (2020). Auranofin resistance in Toxoplasma gondii decreases the accumulation of reactive oxygen species but does not target parasite thioredoxin reductase. *BioRxiv*. doi: 10.1101/2020.04.23.058842.

Ma, C., Tran, J., Li, C., Ganesan, L., Wood, D., and Morrissette, N. (2008). Secondary Mutations Correct Fitness Defects in Toxoplasma gondii With Dinitroaniline Resistance Mutations. *Genetics* 180, 845–856. doi: 10.1534/genetics.108.092494.

MacRae, J. I., Sheiner, L., Nahid, A., Tonkin, C., Striepen, B., and McConville, M. J. (2012). Mitochondrial Metabolism of Glucose and Glutamine Is Required for Intracellular Growth of Toxoplasma gondii. *Cell Host Microbe* 12, 682–692. doi: 10.1016/j.chom.2012.09.013.

Martínez-González, J. J., Guevara-Flores, A., Álvarez, G., Rendón-Gómez, J. L., and del Arenal, I. P. (2010). In vitro killing action of auranofin on Taenia crassiceps metacestode (cysticerci) and inactivation of thioredoxin–glutathione reductase (TGR). *Parasitol. Res.* 107, 227–231. doi: 10.1007/s00436-010-1867-1.

Myers, J. M., and Myers, C. R. (2009). The effects of hexavalent chromium on thioredoxin reductase and peroxiredoxins in human bronchial epithelial cells. *Free Radic. Biol. Med.* 47, 1477–1485. doi: 10.1016/j.freeradbiomed.2009.08.015.

Nagamune, K., Moreno, S. N. J., and Sibley, L. D. (2007). Artemisinin-Resistant Mutants of Toxoplasma gondii Have Altered Calcium Homeostasis. *Antimicrob. Agents Chemother.* 51, 3816–3823. doi: 10.1128/aac.00582-07.

Nagel, S. D., and Boothroyd, J. C. (1989). The major surface antigen, P30, of Toxoplasma gondii is anchored by a glycolipid. *J. Biol. Chem.* 264, 5569–5574.

Parsonage, D., Sheng, F., Hirata, K., Debnath, A., McKerrow, J. H., Reed, S. L., et al. (2016). X-ray structures of thioredoxin and thioredoxin reductase from Entamoeba histolytica and prevailing hypothesis of the mechanism of Auranofin action. *J. Struct. Biol.* 194, 180–190. doi: 10.1016/j.jsb.2016.02.015.

Peroutka-Bigus, N., and Bellaire, B. H. (2019). Antiparasitic Activity of Auranofin against Pathogenic Naegleria fowleri. *J. Eukaryot. Microbiol.* 66, 684–688. doi: 10.1111/jeu.12706.

Pfefferkorn, E. R., and Pfefferkorn, L. C. (1979). Quantitative Studies of the Mutagenesis of Toxoplasma gondii. *J. Parasitol.* 65, 364–370. doi: 10.2307/3280274.

Saccoccia, F., Angelucci, F., Boumis, G., Carotti, D., Desiato, G., Miele, A. E., et al. (2014). Thioredoxin reductase and its inhibitors. *Curr. Protein Pept. Sci.* 15, 621–646. doi: 10.2174/1389203715666140530091910.

Sannella, A. R., Casini, A., Gabbiani, C., Messori, L., Bilia, A. R., Vincieri, F. F., et al. (2008). New uses for old drugs. Auranofin, a clinically established antiarthritic metallodrug, exhibits potent antimalarial effects in vitro: Mechanistic and pharmacological implications. *FEBS Lett.* 582, 844–847. doi: 10.1016/j.febslet.2008.02.028.

Schultz, A. J., and Carruthers, V. B. (2018). Toxoplasma gondii LCAT Primarily Contributes to Tachyzoite Egress. *mSphere* 3. doi: 10.1128/mSphereDirect.00073-18.

Selenius, M., Rundlöf, A.-K., Olm, E., Fernandes, A. P., and Björnstedt, M. (2010). Selenium and the selenoprotein thioredoxin reductase in the prevention, treatment and diagnostics of cancer. *Antioxid. Redox Signal.* 12, 867–880. doi: 10.1089/ars.2009.2884.

Sharlow, E. R., Leimgruber, S., Murray, S., Lira, A., Sciotti, R. J., Hickman, M., et al. (2014). Auranofin Is an Apoptosis-Simulating Agent with in Vitro and in Vivo Anti-leishmanial Activity. *ACS Chem. Biol.* 9, 663–672. doi: 10.1021/cb400800q.

Shaulov, Y., Nagaraja, S., Sarid, L., Trebicz-Geffen, M., and Ankri, S. (2020). Formation of oxidised (OX) proteins in Entamoeba histolytica exposed to auranofin and consequences on the parasite virulence. *Cell. Microbiol.* 22, e13174. doi: 10.1111/cmi.13174.

Shen, B., Brown, K. M., Lee, T. D., and Sibley, L. D. (2014). Efficient Gene Disruption in Diverse Strains of Toxoplasma gondii Using CRISPR/CAS9. *mBio* 5, 10.1128/mbio.01114-14. doi: 10.1128/mbio.01114-14.

Stokkermans, T. J., Schwartzman, J. D., Keenan, K., Morrissette, N. S., Tilney, L. G., and Roos, D. S. (1996). Inhibition of Toxoplasma gondii replication by dinitroaniline herbicides. *Exp. Parasitol.* 84, 355–370. doi: 10.1006/expr.1996.0124.

Sweeney, K. R., Morrissette, N. S., LaChapelle, S., and Blader, I. J. (2010). Host cell invasion by Toxoplasma gondii is temporally regulated by the host microtubule cytoskeleton. *Eukaryot. Cell* 9, 1680–1689. doi: 10.1128/EC.00079-10.

Tahara, E. B., Navarete, F. D. T., and Kowaltowski, A. J. (2009). Tissue-, substrate-, and site-specific characteristics of mitochondrial reactive oxygen species generation. *Free Radic. Biol. Med.* 46, 1283–1297. doi: 10.1016/j.freeradbiomed.2009.02.008.

Thomas, M. P., Liu, X., Whangbo, J., McCrossan, G., Sanborn, K. B., Basar, E., et al. (2015). Apoptosis Triggers Specific, Rapid, and Global mRNA Decay with 3’ Uridylated Intermediates Degraded by DIS3L2. *Cell Rep.* 11, 1079–1089. doi: 10.1016/j.celrep.2015.04.026.

Wilson, C. B., Tsai, V., and Remington, J. S. (1980). Failure to trigger the oxidative metabolic burst by normal macrophages: possible mechanism for survival of intracellular pathogens. *J. Exp. Med.* 151, 328–346. doi: 10.1084/jem.151.2.328.

CHAPTER THREE: Elucidating the role of *Toxoplasma gondii*‘s mitochondrial superoxide dismutase

Abstract

Toxoplasma gondii is the only apicomplexan parasite that possesses a well-developed reactive oxygen species (ROS) scavenging system which includes an endogenous catalase and complete glutathione and thioredoxin pathways. Our previous studies generating auranofin resistant *T. gondii* parasites, led to mutations in *T. gondii*'s mitochondrial superoxide dismutase (TgSOD2). These parasites showed reduced accumulation of ROS upon exposure to auranofin. TgSOD2 is an essential gene as evidenced by its low phenotype index and non-viability of constitutive knockouts. To understand the essential role of TgSOD2 throughout the parasite's life, we generated knockdown mutants using an auxin-inducible degron system that allowed us to explore the role of TgSOD2 in parasite replication and replication fitness. During stages of extracellular stress, TgSOD2 is upregulated as the parasite attempts to survive. Its depletion leads to reduction in replication fitness as these parasites showed decreased plaque formation when compared to their parental line. TgSOD2 depletion led to a reduced number of parasites per parasitophorous vacuole. At the mitochondrial level, depletion of TgSOD2 results in aberrancies in the parasite's mitochondrion as well as reduction of the parasite's mitochondrial membrane potential. Through a proximal biotinylation approach, we found that TgSOD2 localizes adjacent to complexes IV and V of *T. gondii* mitochondrial electron transport chain, suggesting that these may be sites of ROS generation or ROS sensitive enzyme subunits. Our studies illuminate the role of TgSOD2 in parasite life and mitochondrion maintenance.

Introduction

Intracellular parasites are vulnerable to not only endogenous reactive oxygen species (ROS), but also those generated by their host cell; controlling these short-lived but highly reactive compounds is critical to their survival. *Toxoplasma gondii* has evolved a highly developed and redundant ROS scavenging system to contend with this challenge. *T gondii* also encodes both thioredoxin and glutaredoxin systems, a pair of parallel pathways which regulate the redox status of critical proteins and other biomolecules (Holmgren, 1979; Ahsan et al., 2009). Additionally, *T. gondii* encodes three distinct superoxide dismutases (SOD); these critical enzymes are solely responsible for the dismutation of superoxide anions into hydrogen peroxide (Odberg-Ferragut et al., 2000; Brydges and Carruthers, 2003; Kwok et al., 2004). Downstream of the SODs are peroxiredoxins and catalase, which catalyze the breakdown of hydrogen peroxide to less reactive forms. It is among the few apicomplexans to express catalase (Kaasch and Joiner, 2000). This highly developed system of ROS scavengers allows the parasite to occupy a wide range of different host cells; it has been observed to infect any nucleated host cell, including macrophages and other phagocytic cells capable of producing ROS bursts (Mordue et al., 1999). These factors contribute to *T. gondii*'s success as a human pathogen; current estimates suggest that a third of the world population has been infected (Rahmanian et al., 2020), and toxoplasmosis remains one of the leading causes of death by foodborne disease in the United States (Scallan et al., 2011). Despite its prevalence, treatments for toxoplasmosis are dated. The current standard of care: pyrimethamine and sulfadiazine, was initially proposed in 1953 with few modifications since (Eyles and Coleman, 1953).

Here, we focus on the role of TgSOD2, to identify potential targets for future therapeutics. TgSOD2 is critical to parasite survival as deletion of the gene is lethal to parasites and disruption of the gene reduces parasite survival *in vitro* (Odberg-Ferragut et al., 2000; Sidik et al., 2016), but its specific role in *T. gondii* has not been evaluated. TgSOD2 is reported to localize to the mitochondrion (Pino et al., 2007) and disruption of mitochondrial homeostasis

results in parasite death (Ghosh et al., 2012; Charvat and Arrizabalaga, 2016). Thus, to better guide anti-parasitic development, it is crucial to understand the basic biology of mitochondrial proteins and homeostasis. Here we found that TgSOD2 responds to changes in parasite environment and depletion of TgSOD2 results in both decreased fitness and mitochondrial abnormalities; thereby indicating an association between TgSOD2 and the apicomplexan-specific parts of the electron transport chain.

Results

Superoxide Dismutase Expression Increases in Extracellular Parasites

Using qRT-PCR, we quantified transcription of various reactive oxygen scavenging genes in both intracellular and extracellular parasites (RH). Of the ROS scavengers surveyed, TgSOD1 and TgSOD2 are the most highly transcribed (**Figure 3.1B**). Extracellular parasites showed elevated ROS scavenger transcription, which increased further after 4 hours of remaining outside of host cells. Relative to intracellular parasites, there is a 2-fold increase in TgSOD1 transcription and a 3-fold increase in TgSOD2 transcription 4 hours after leaving host cells. Of the surveyed ROS scavengers, peroxiredoxin 2 experienced the greatest increase in transcription after 4 hours (5.4-fold increase). Transcription levels of thioredoxin reductase, glutaredoxin, and glutathione reductase in extracellular parasites were similar to that of intracellular parasites (**Figure 3.1B**).

While the qPCR survey showed peroxiredoxin 2 as the most responsive ROS scavenger to extracellular stress, it is not predicted to be fitness conferring (Sidik et al., 2016). TgSOD1 and TgSOD2 also showed modest increases in transcription, and are predicted to be highly fitness conferring (Sidik et al., 2016). As TgSOD2 is localized to the parasite mitochondrion, we focused our analysis on that gene. To supplement the transcriptional measurements, we quantified the protein translation of TgSOD2 in intracellular and extracellular parasites via western blot. There was a dramatic 70% decrease in TgSOD2 protein quantities after parasites

were held extracellular in a host cell-free environment for 4 hours (**Figure 3.2A**). Together, these results suggest that TgSOD2 increases transcription as a response to dropping TgSOD2 protein quantities.

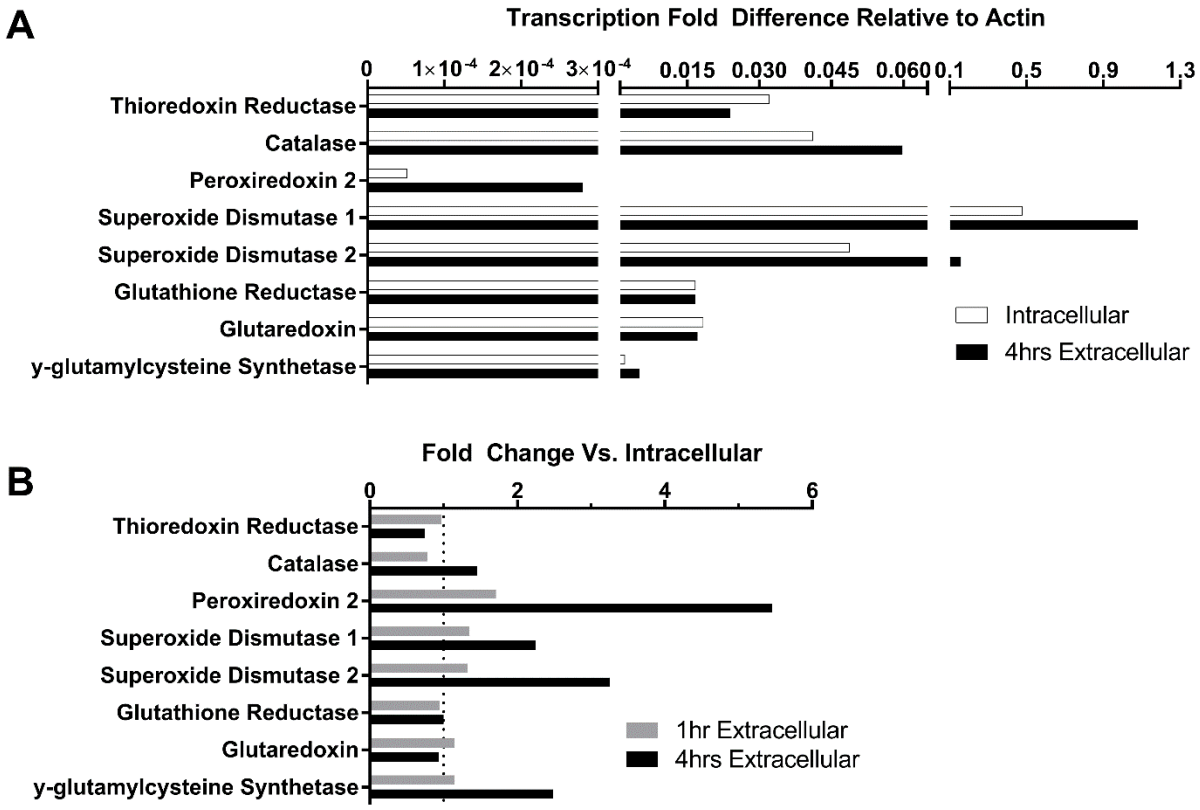

Figure 3.1 qPCR survey of ROS scavengers in intracellular and extracellular parasites. For intracellular parasites, confluent monolayers of fibroblasts infected with RH parasites were collected after washing with PBS. For extracellular stages, filtered parasites were collected after 1 and 4 hours. At each time point, RNA was harvested for cDNA synthesis and real-time qPCR of *T. gondii* ROS scavengers. Data normalized to *T. gondii* actin and presented as **A)** transcription fold difference relative to actin or **B)** average fold change against intracellular parasites. n=3 independent experiments.

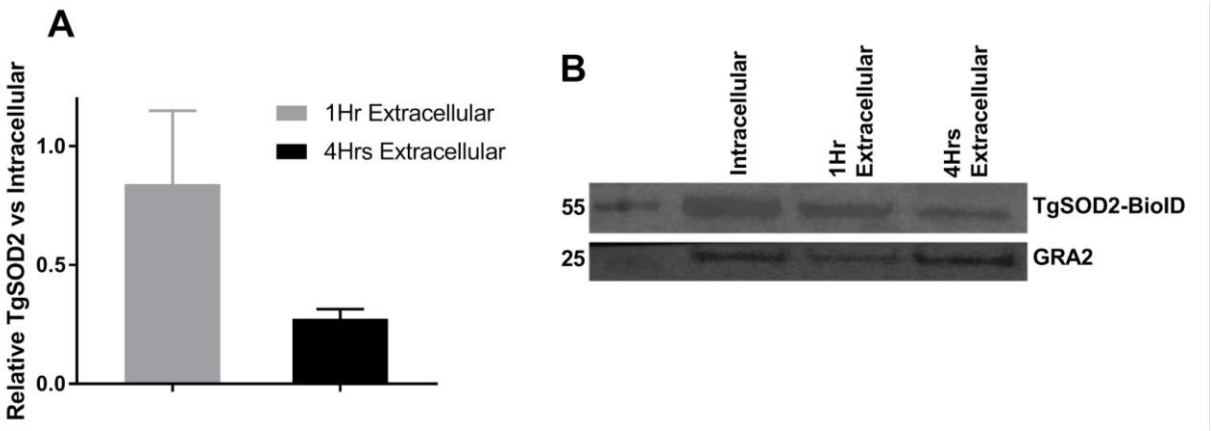

Figure 3.2 Western blot quantification of TgSOD2 in intracellular and extracellular parasites. For intracellular parasites, confluent monolayers of fibroblasts infected with TgSOD2-BioID parasites were collected after washing with PBS. For extracellular stages, filtered parasites were collected after 1 and 4 hours. **A)** Relative TgSOD2 quantification after normalizing to a GRA2 loading control, compared against intracellular band thickness. n=3 independent experiments. Error bars for standard deviation are shown. **B)** Representative western blot.

Validation of Inducible TgSOD2 Knockdown

To directly investigate TgSOD2, we generated an auxin-inducible knockdown strain of RH parasites. Using CAS9-directed homologous recombination, we appended an YFP tag and mini auxin inducible degron (mAID) tag onto the 3' end of the TgSOD2 gene (**Figure 3.3A**). The resulting parasite strain (TgSOD2-mAID) should undergo proteasomal degradation of TgSOD2 upon exposure to indoleacetic acid (IAA). Western blots showed a reduction of TgSOD2 levels in the TgSOD2-maid line in response to IAA treatment (**Figure 3.3B**). Dense granule protein 1 (GRA1) is a highly expressed *T. gondii* protein and was used as a loading control for this blot. Fluorescent microscopy confirmed this decrease of expression and a retention of mitochondrial localization patterns (**Figure 3.3C**).

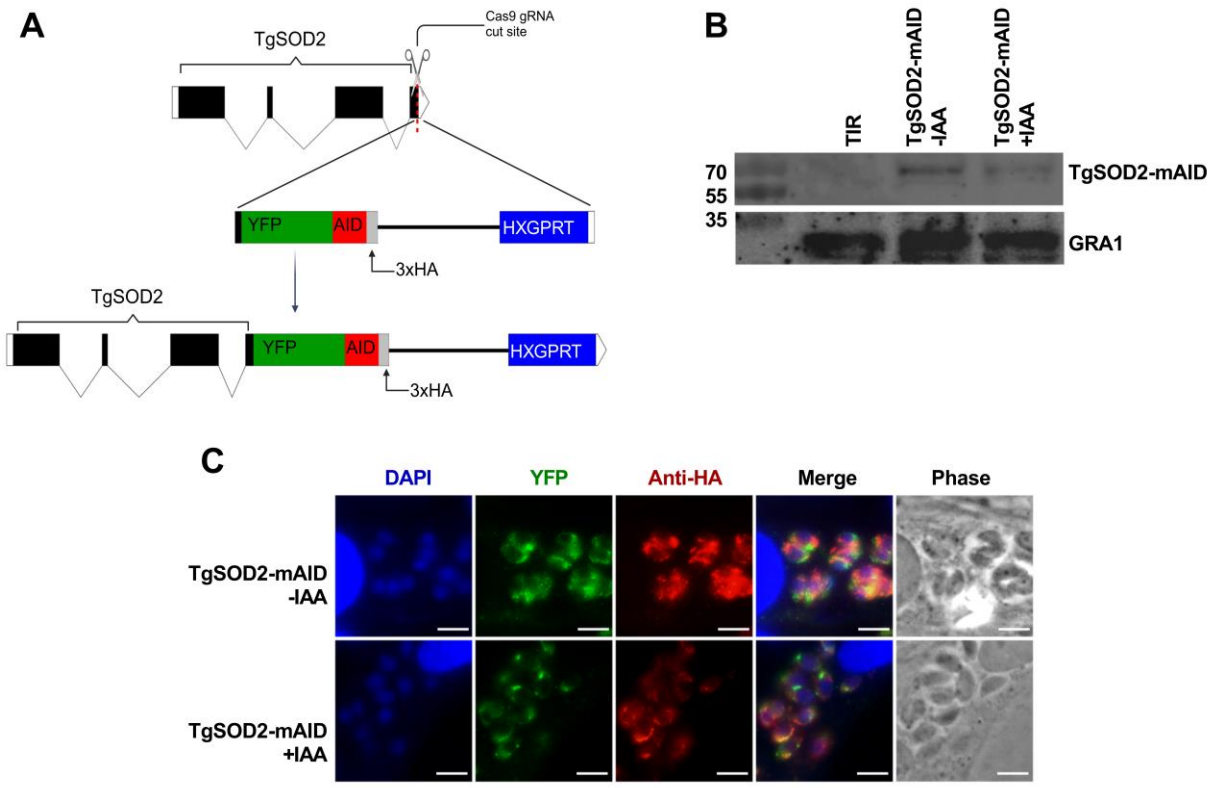

Figure 3.3 Generation and verification of TgSOD2-mAID mutant parasites A) Insertion of the YFP-mAID-HXGPRT cassette via CRISPR/CAS9 **B)** Representative western blot, GRA1 was included as a loading control. **C)** Microscopy validation of YFP fluorescence, HA tags, and mAID mediated TgSOD2 knockdown in IAA media. 5µm scale bars. Created with BioRender.com

Superoxide Dismutase 2 depletion impairs parasite fitness

Following validation of the auxin-inducible degron mutant, we assessed the phenotype of TgSOD2 depletion. First, plaque assays were performed to determine the overall changes to parasite fitness following depletion of TgSOD2. After 8 days of IAA exposure, the TgSOD2-mAID mutants exhibited a baseline decrease in fitness compared against the transport inhibitor response 1 (TIR1) parental line (**Figure 3.4A**). Parasite replication assays also demonstrate a decrease in replication speed of the TgSOD2-mAID line (**Figure 3.4C**).

Inducible knockdown systems also introduce a degree of “leakiness” or baseline target protein knockdown in the absence of the knockdown signal. To evaluate the leakiness of the mAID system when applied to a mitochondrial protein, we used Western blots to quantify

TgSOD2 under a non-knockdown system (TgSOD2-BioID) and under mAID, both with and without IAA exposure. Because TgSOD2-BioID and TgSOD2-mAID retain the same endogenous promoter for TgSOD2, the expression of TgSOD2 between the two mutants should be similar in the absence of unintended knockdown. However, there was a significant reduction in the quantity of TgSOD2 in the mAID line compared against the BioID line, this reduction was enhanced by the addition of IAA (**Figure 3.5**). Given the near complete loss of TgSOD2 expression in the mAID line at baseline, any phenotypic differences between TgSOD2-mAID and its parental line could be an effect of TgSOD2 depletion.

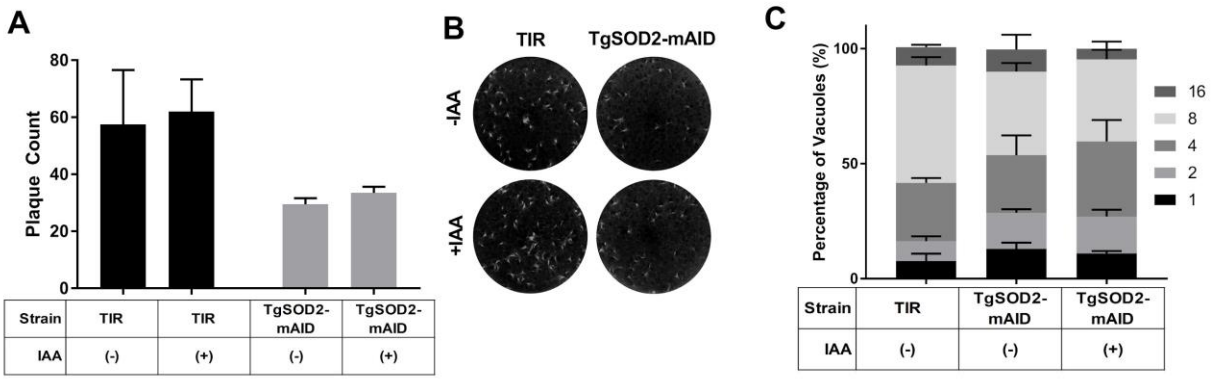

Figure 3.4 TgSOD2-mAID parasites show reduced growth and replication. A) Plaque assay quantification following 8 days of incubation ±IAA. n=2 independent experiments. Error bars for standard deviation are shown. **B)** Representative picture of TIR1 and TgSOD2-mAID plaques. **C)** Replication assay following 24 hours of incubation ±IAA. n=3 independent experiments. Error bars for standard deviation are shown.

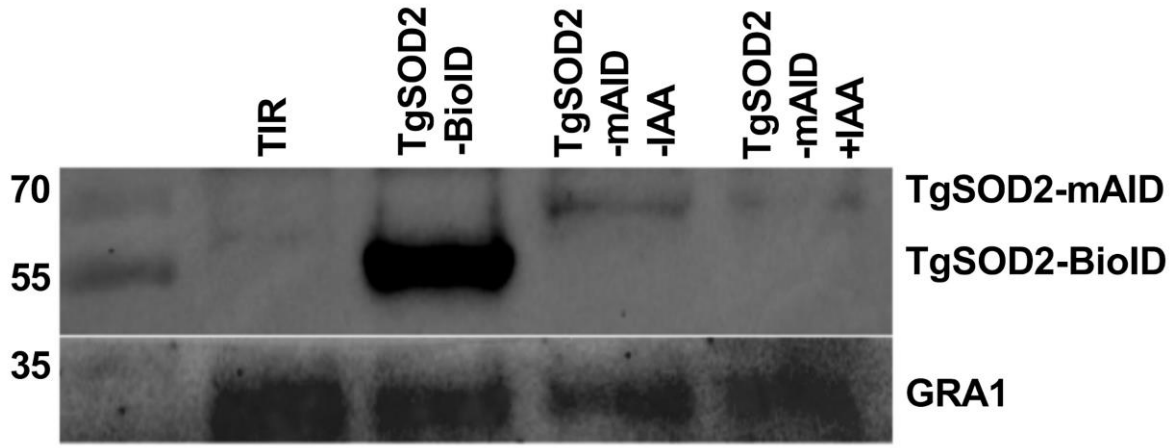

.

Figure 3.5 Western blot of TgSOD2 expression across mutant lines. Western blots are stained with anti-HA antibodies to bind the 3x HA epitopes found on both TgSOD2-BioID and TgSOD2-mAID constructs. GRA1 was used as a loading control. Representative blot of n=3 independent replicates.

Superoxide Dismutase 2 is closely associated with the mitochondrial electron transport chain

Given the importance of TgSOD2 to *T. gondii* survival, we evaluated possible interacting partners using proximal biotin ligation. In brief, BioID, a promiscuous biotin ligase, was appended onto the N-terminus of TgSOD2 via homologous recombination at the 3' end of the TgSOD2 gene. Microscopy verification identified BioID via HA tagging, then verified biotin ligase activity through incubating parasites with 150uM biotin containing media for 24 hours then staining with YFP conjugated streptavidin. These assays showed that the TgSOD2-BioID mutants are properly localized to the mitochondria of the *T. gondii* and are capable of proximal biotin ligation (**Figure 3.6A-B**).

With biotin ligase activity confirmed, we moved onto biotin labeled protein capture via streptavidin conjugated magnetic beads. Mass spectrometry analysis of the streptavidin captured protein revealed that, compared to a parental control protein harvest, TgSOD2-BioID biotin ligation enriched capture of several proteins of the electron transport chain (**Table 3.1**). Namely, the following proteins were enriched in the TgSOD2-BioID sample: TgApiCox18,

TgApiCox26, TgApiCox30, TgApiCox35, and ATP synthase beta subunit 5. The TgApiCox proteins are components of cytochrome C oxidase (Complex IV), and the ATP synthase beta subunit 5 is part of ATP synthase (Complex V). All but one of the captured proteins from this biotin pulldown were parasitic mitochondrial proteins. To validate these findings, we captured proteins again, this time using anti-HA beads instead of streptavidin beads on the TgSOD2-BioID fusion protein. Unlike the prior pulldown which captured biotinylated proteins, using anti-HA beads should capture TgSOD2-BioID and any closely associated proteins in direct contact with the target. This swap in pulldown methodology should result in a more stringent capture of possible interacting proteins. Mass spectrometry revealed that only ATP synthase beta subunit 5 was shared during this anti-HA protein pulldown and the previous streptavidin pulldown (**Table 3.2**). Overall, these pulldowns suggest an association between TgSOD2 and the electron transport chain, but TgSOD2 likely does not bind directly to any of these members as they were not retrieved in the anti-HA pulldown.

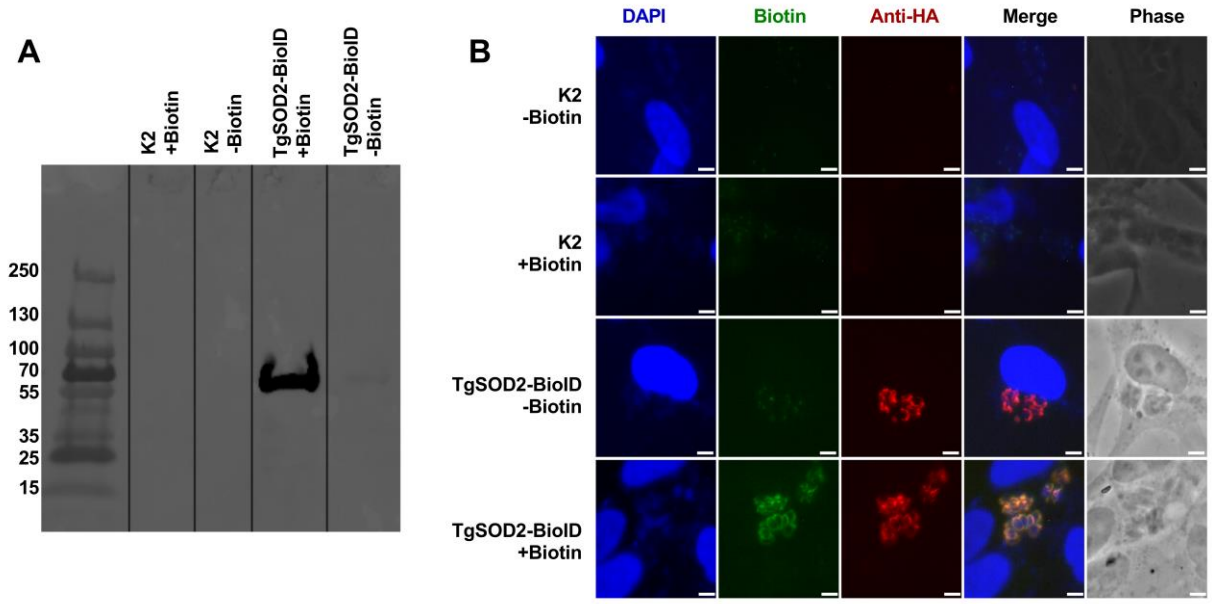

Figure 3.6 Western blot and microscopy validation of TgSOD2-BioID line. A) Streptavidin pulldown of TgSOD2-BioID or parental (K2) lysates after culture in biotin containing media shows capture of an expected ~70kDa band in the TgSOD2-BioID lysates. **B)** Fluorescence microscopy shows mitochondrial localization of the TgSOD2-BioID fusion protein. TgSOD2 identified via anti-HA tag staining, Biotin staining via streptavidin-FITC (green), nuclear staining via DAPI (blue). 5µm scale bars.

ToxoDB GeneID	Protein Annotation	Predicted protein mass (kDa)	Predicted Localization	Phenotype score (Sidik et al., 2016)	Human Homolog Similarity
TGME49_316330	superoxide dismutase TgSOD2 (SOD2)	31.47	Mitochondrion	-4.09	38.97%
TGME49_221510	Tg ApiCox18	17.92	Mitochondrion	-3.28	0.00%
TGME49_306670	Tg ApiCox26	25.84	Mitochondrion	-3.68	0.00%
TGME49_297810	Tg ApiCox30	29.57	Mitochondrion	-3.64	0.00%
TGME49_229920	Tg ApiCox35	34.96	Mitochondrion	-3.84	0.00%
TGME49_261950	ATP synthase beta subunit ATP-B (ATPB)	59.93	Mitochondrion	-4.84	79.45%
TGME49_209260	cytochrome c oxidase subunit 5b	34.71	Mitochondrion	-3.07	38.60%
TGME49_260170	elongation factor EF-G, putative	96.63	Mitochondrion	-4.87	51.36%
TGME49_257730	methionine aminopeptidase, type i, putative	52.24	Mitochondrion	-3.51	50.00%
TGME49_202680	peptidase M16, alpha subunit, putative	62.21	Mitochondrion	-4.30	32.96%
TGME49_236210	peptidase M16 family potein, putative	56.92	Mitochondrion	-4.74	44.15%
TGME49_216530	ribosome recycling factor protein	51.08	Mitochondrion	-3.81	0.00%

Table 3.1 Mass spectrometry identification of streptavidin captured proteins from TgSOD2-BioID and parental lines. Liquid chromatography–mass spectrometry analysis used an UltiMate 3000 RSLC system (Thermo Fisher Scientific) coupled in-line to an Orbitrap Fusion Lumos mass spectrometer (Thermo Fisher Scientific). Proteins were identified by alignment to a toxoplasma proteome and shown here are the 12 mitochondrial proteins which were enriched in the SOD2-BioID sample.

ToxoDB GeneID	Protein Annotation	Predicted protein mass (kDa)	Predicted Localization	Phenotype score (Sidik et al., 2016)	Human Homolog Similarity
TGME49_316330	superoxide dismutase SOD2 (SOD2)	31.47	Mitochondrion	-4.09	38.97%
TGME49_261950	ATP synthase beta subunit ATP-B (ATPB)	59.93	Mitochondrion	-4.84	79.45%
TGME49_247550	heat shock protein HSP60	60.92	Mitochondrion	-5.1	55.51%
TGME49_288500	FAD Malate-dehydrogenase (MDH-FAD)	60.39	Mitochondrion	-0.79	0.00%
TGME49_243950	prohibitin, putative	30.23	Mitochondrion	-5.18	51.49%
TGME49_219550	dihydrolipoyllysine-residue succinyltransferase component of oxoglutarate dehydrogenase	50.13	Mitochondrion	-4.25	60.26%
TGME49_215590	flavoprotein subunit of succinate dehydrogenase	72.76	Mitochondrion	-3.96	65.70%
TGME49_319920	2-oxo acid dehydrogenases acyltransferase (catalytic domain) domain-containing protein	70.30	Mitochondrion	-1.92	40.60%
TGME49_204400	ATPase synthase subunit alpha, putative	62.16	Mitochondrion	-3.84	74.11%

Table 3.2 Mass spectrometry identification of anti-HA captured proteins from TgSOD2-BioID and parental lines. Liquid chromatography–mass spectrometry analysis used an UltiMate 3000 RSLC system (Thermo Fisher Scientific) coupled in-line to an Orbitrap Fusion Lumos mass spectrometer (Thermo Fisher Scientific). Proteins were identified by alignment to a toxoplasma proteome and shown here are the 9 mitochondrial proteins which were enriched in the SOD2-BioID sample.

ApiCox Transcription Patterns Mirror TgSOD2 Transcription

In wild-type parasites, we evaluated the previously generated cDNA to test if the transcription patterns of various TgApiCox genes were also upregulated in extracellular parasites. Extracellular parasites showed increases in TgApiCox26 and TgApiCox35 transcription following 4 hours of being forcefully egressed from host cells. This pattern mirrors the transcription pattern and response in TgSOD2 (**Figure 3.7**).

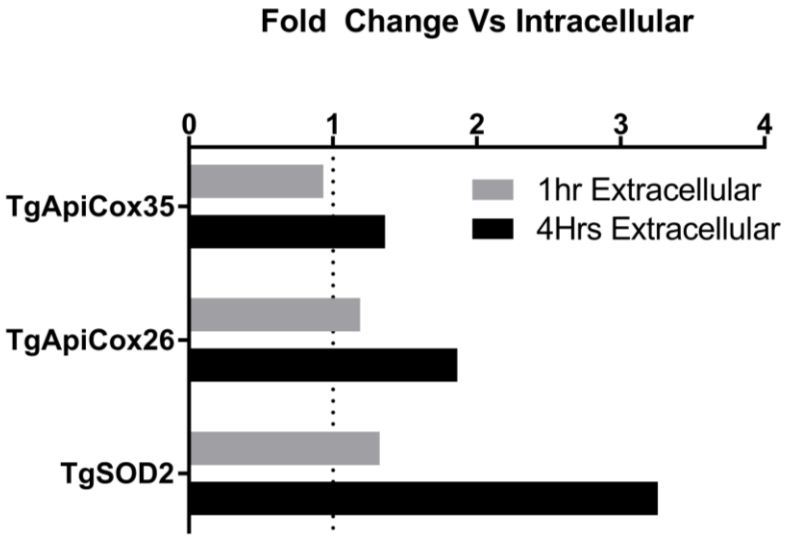

Figure 3.7 qPCR survey of TgApiCox in intracellular and extracellular parasites. For intracellular parasites, confluent monolayers of fibroblasts infected with RH parasites were collected after washing with PBS. For extracellular stages, filtered parasites were collected after 1 and 4 hours. At each time point, RNA was harvested for cDNA synthesis and real-time qPCR of *T. gondii* ROS scavengers. Data normalized to *T. gondii* actin and presented as average fold change against intracellular parasites. n=3 independent experiments.

TgApiCox35 likely interacts with multiple components of the mitochondrial electron transport chain

To confirm this possible association between TgSOD2 and TgApiCox, we generated another biotin ligase expressing mutant parasite line by fusing biotin ligase to TgApiCox35 instead of TgSOD2. If there is a direct interaction between these proteins, streptavidin pulldown of proteins labeled by TgApiCox35-BioID would capture TgSOD2, along with other TgApiCox

components. We verified these mutant parasites by fluorescence microscopy and Western blot following streptavidin pulldown (**Figure 3.8A**). Microscopic verification identified TgApiCox35-BioID via HA tagging, and biotin ligase activity was confirmed through staining with YFP conjugated streptavidin. This microscopy panel demonstrated that the TgApiCox35-BioID mutants properly localized to the mitochondria of the *T. gondii* and are capable of proximal biotin ligation (**Figure 3.8B**).

With biotin ligase activity confirmed, we moved onto biotinylated protein capture and identification via mass spectrometry. Mass spectrometry of the streptavidin captured proteins revealed an enrichment of other TgApiCox proteins: TgApiCox 16, 18, 19, 24, 25, 26, and 30 were retrieved during this pulldown. Cytochrome C and ATP synthase B subunits were also retrieved (**Table 3.3**). However, TgSOD2 was absent from this pulldown, indicating that TgSOD2 does not form strong interactions with or directly bind to TgApiCox35.

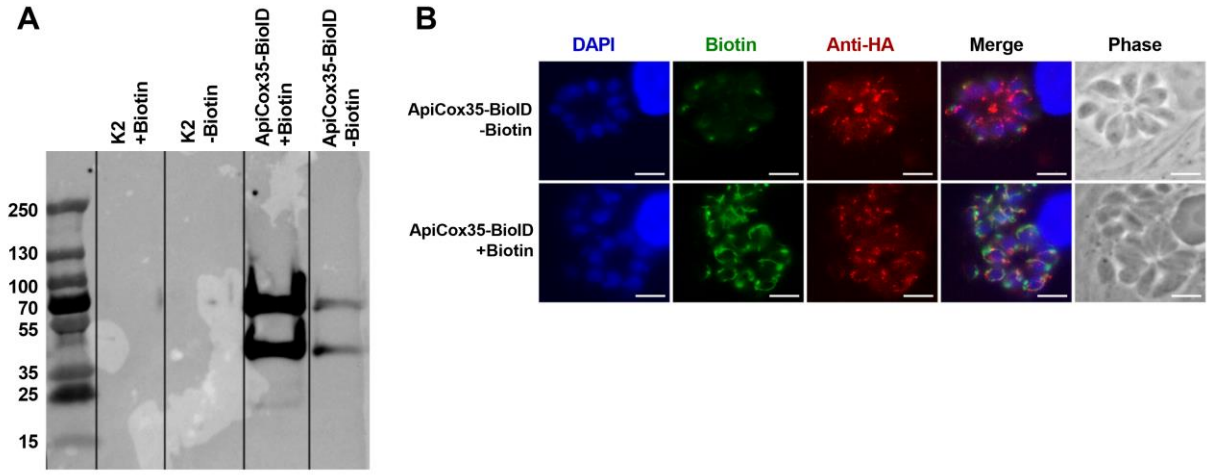

Fig 3.8 Western blot and microscopy validation of TgApiCox35-BioID mutant line. A) Streptavidin pulldown of TgApiCox35-BioID or parental (K2) lysates after culture in biotin containing media shows capture of an expected ~70kDa band in the TgApiCox35-BioID lysates. **B)** Fluorescence microscopy shows mitochondrial localization of the TgApiCox35-BioID fusion protein. TgApiCox35 identified via anti-HA tag staining, Biotin staining via streptavidin-FITC (green), nuclear staining via DAPI (blue). 5µm scale bars.

ToxoDB GeneID	Protein Annotation	Predicted protein mass (kDa)	Predicted Localization	Phenotype score (Sidik et al., 2016)	Human Homolog Similarity
TGME49_229920	Tg ApiCox35	34.96	Mitochondrion	-3.84	0.00%
TGME49_265370	Tg ApiCox16	16.03	Mitochondrion	1.56	0.00%
TGME49_221510	Tg ApiCox18	17.92	Mitochondrion	-3.28	0.00%
TGME49_247770	Tg ApiCox19	19.27	Mitochondrion	-2.61	0.00%
TGME49_286530	Tg ApiCox24	25.4	Mitochondrion	-2.82	0.00%
TGME49_264040	Tg ApiCox25	24.6	Mitochondrion	-2.54	0.00%
TGME49_306670	Tg ApiCox26	25.84	Mitochondrion	-3.68	0.00%
TGME49_297810	Tg ApiCox30	29.57	Mitochondrion	-3.64	0.00%
TGME49_234420	ATPase, AAA family protein	66.82	Mitochondrion	-5.08	38.83%
TGME49_262640	Cg8 family protein	23.76	Mitochondrion	-3.49	0.00%
TGME49_209260	cytochrome c oxidase subunit 5b	34.71	Mitochondrion	-3.07	38.60%
TGME49_210790	dihydroorotate dehydrogenase	65.07	Mitochondrion	-2.84	47.51%
TGME49_251780	heat shock protein	78.27	Mitochondrion	-5.09	66.67%
TGME49_257730	methionine aminopeptidase, type i	52.24	Mitochondrion	-3.51	42.96%
TGME49_236210	peptidase M16 family protein	56.92	Mitochondrion	-4.74	44.15%
TGME49_255910	PfMNL-2 CISD1 family iron-sulfur protein	24.96	Mitochondrion	1.64	48.72%
TGME49_207620	pyridine nucleotide-disulfide oxidoreductase domain-containing protein	71.17	Mitochondrion	-1.15	34.94%
TGME49_284580	ribose-phosphate diphosphokinase subfamily protein	69.12	Mitochondrion	-0.72	29.10%
TGME49_216530	ribosome recycling factor protein	51.08	Mitochondrion	-3.81	0.00%
TGME49_319730	YOU2 family C2C2 zinc finger protein	17.13	Mitochondrion	0.02	0.00%
TGME49_229420	cytochrome c	18.10	Cytoplasm	0.61	33.93%
TGME49_231350	glucosamine-fructose-6-phosphate aminotra	96.73	Plastid	-4.57	31.11%
TGME49_312160	hypothetical protein	22.26	Mitochondrion	-1.29	0.00%

Table 3.3. Mass spectrometry identification of streptavidin captured proteins from TgApiCox35-BioID and parental lines. Liquid chromatography–mass spectrometry analysis used an UltiMate 3000 RSLC system (Thermo Fisher Scientific) coupled in-line to an Orbitrap Fusion Lumos mass spectrometer (Thermo Fisher Scientific). Proteins were identified by alignment to a toxoplasma proteome and shown here are a subset of the proteins which were enriched in the SOD2-BioID sample.

TgSOD2 depletion alters parasite mitochondrion homeostasis

Considering that TgSOD2-mAID mutants have generally impaired fitness, and TgSOD2 associates with the electron transport chain as evidenced by the TgSOD2-BioID results, we suspected abnormalities with the mitochondria in TgSOD2-mAID mutants. To test this prediction, we used mitoTracker staining and flow cytometry to measure mitochondrial membrane potential (MMP) in the mutant lines. Analyses showed MMP is decreased in TgSOD2-mAID mutants compared to the TIR1 parental line, and this effect in mutants was not further altered with IAA exposure (**Figure 3.9**). This observation is suggestive of defects in mitochondrial function in the TgSOD2-mAID line.

Immunofluorescence assays of TgSOD2-mAID parasites showed abnormalities in ATP synthase distribution within the parasite mitochondrion. Although TgSOD2-mAID parasites retained their mitochondrial localization and lasso-like mitochondrial morphology, parasite ATP synthase did not show spatial overlap with TgSOD2 (**Figure 3.10A**). ATP synthase was disrupted in roughly 50% of mutant parasites (**Figure 3.10B**), instead of localizing to the entire mitochondrion, ATP synthase staining either displayed punctate/discontinuous localization or was completely absent. There did not appear to be any differences upon treatment with IAA. These observations link depletion of TgSOD2 to the depletion of ATP synthase localization or assembly of the multi-subunit complex.

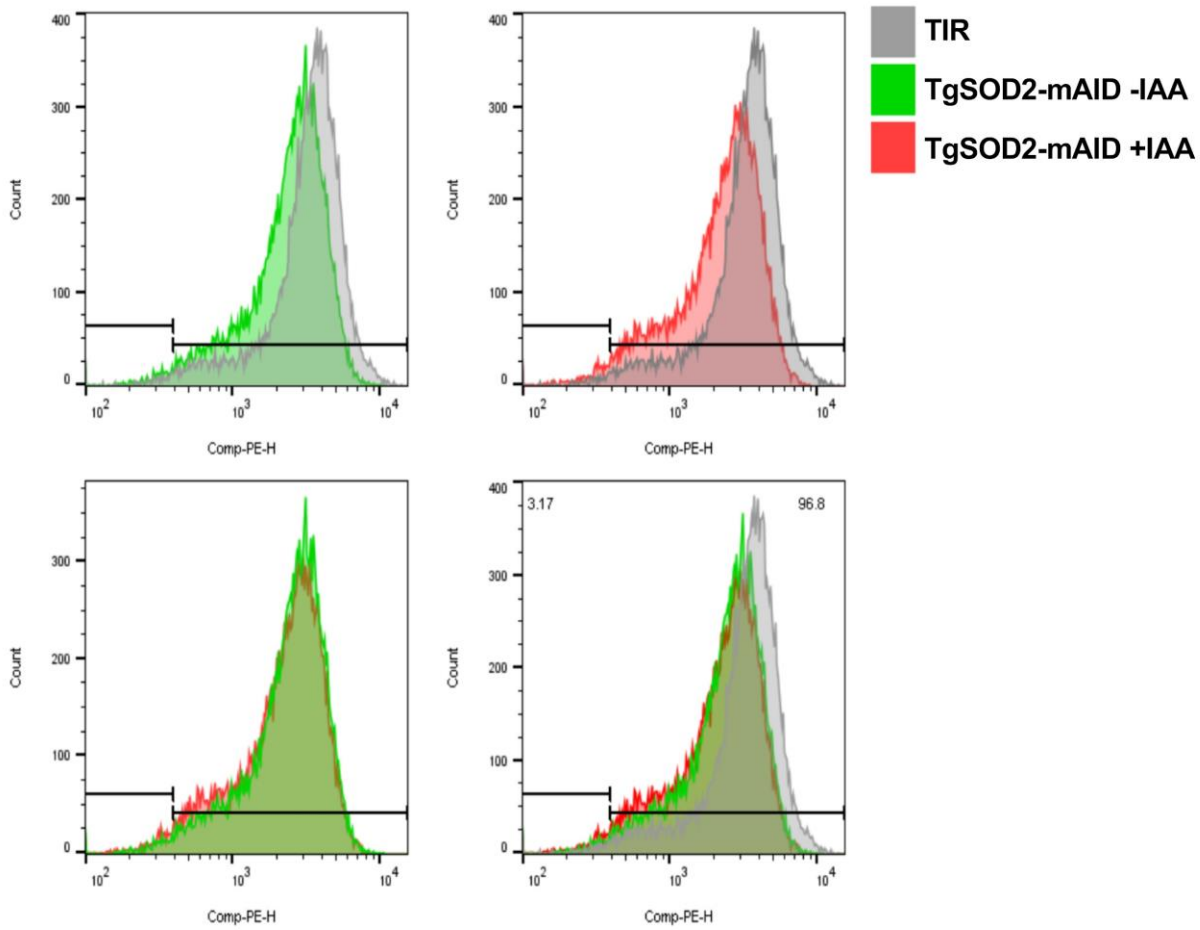

Figure 3.9 Mitochondrial membrane potential of TgSOD2-mAID and parental lines. Mitochondrial membrane potential measured via mitoTracker staining and flow cytometry after 24 hours of IAA treatment. Representative flow histograms shown.

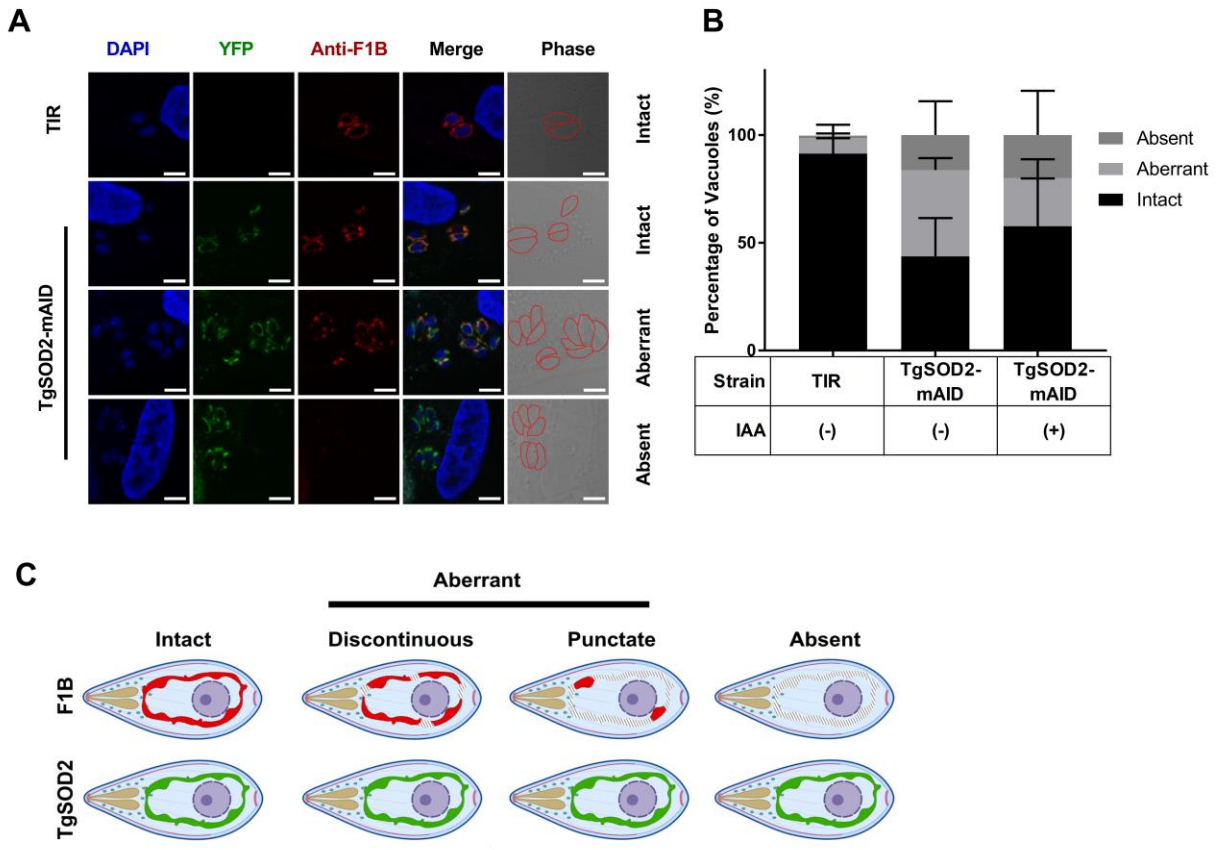

Figure 3.10 Evaluation of mitochondrial morphology by microscopy and western blot. A) Parasites stained with anti-F1B ATPase antibodies, 5µm scale bars. **B)** Phenotypic scoring classified vacuoles based on the observed F1B ATPase staining pattern. Aberrant group includes both discontinuous and punctate staining signals. FITC channel shows TgSOD2-mAID fluorescent signal. **C)** schematic examples of observed staining patterns. n=3 independent experiments. Error bars for standard deviation are shown. Created with BioRender.com

Discussion

In summation, this chapter shows that depletion of TgSOD2 leads to decreased parasite fitness and mitochondrial membrane potential. Due to TgSOD2 proximity to both complexes IV and V of *T. gondii's* mitochondrial electron transport chain, TgSOD2 may be relevant for ATP synthase maintenance within the parasite mitochondrion. Our results suggest that TgSOD2 plays a protective role in maintaining the function of the parasite's mitochondrial electron transport chain by localizing adjacent to ROS-generating proteins or ROS-sensitive proteins. Our qPCR survey showed that ROS scavenger transcription increases as parasites remain

outside of host cells (**Figure 3.1**). Notably, TgSOD2 is highly transcribed when forcefully egressed from host cells. This elevated TgSOD2 transcription is in accord with previous reports comparing transcriptomics prior to and during host cell invasion (Gaji et al., 2011). Despite increases in the TgSOD2 transcripts, the generation of *de novo* TgSOD2 does not occur within the first 2-4 hours of their extracellular stage. (**Figure 3.2**). Thus, the increased transcription of TgSOD2 observed on qPCR surveys is likely a response to decreasing TgSOD2 protein levels.

Previous attempts to knock out TgSOD2 rendered non-viable parasites, indicating that TgSOD2 is essential for parasite survival (Odberg-Ferragut et al., 2000). Therefore, we approached depleting mitochondrial TgSOD2 by using an auxin inducible degron system via CRISPR/CAS9 (**Figure 3.3A**). This methodology introduces a smaller insertion, limiting disruptions to other proximal genes. This has been previously applied in *T. gondii* (Brown et al., 2017; Long et al., 2017; Hu et al., 2020), but we show that this methodology is also effective for depletion of mitochondrial matrix proteins. This subcellular compartment would be a challenging target due to the multiple membranes sequestering it from the cytoplasm. Application of the AID system incorporates ligases TIR1 and Skp1–Cul1–F-box (SCF). They mediate poly-ubiquitination of AID-tagged proteins, which are typically cytoplasmically localized, (Natsume et al., 2016) and may not have access to mitochondrial proteins. Thus, AID tag mediated depletion of mitochondrial targets would need to rely upon degrading nascent protein following cytoplasmic translation (Daniel et al., 2018). Furthermore, the parasites were kept in dialyzed media to minimize unintended knockdown from auxin-like compounds present in tissue culture media (Natsume and Kanemaki, 2017). These optimizations were successful: the resulting mutant line displayed the intended insertion and TgSOD2 was depleted upon addition of IAA to culture media (**Figure 3.3**). Thus, depletion of a *T. gondii* mitochondrial protein via auxin inducible degron tagging is possible. Our resulting parasite, TgSOD2-mAID showed a reduction in parasite fitness as measured by plaque assays (**Figure 3.4**). This finding was expected, considering TgSOD2's low phenotype score (Sidik et al., 2016). Surprisingly, exposure to IAA

did not inhibit plaque formation or exacerbate fitness loss in the TgSOD2-mAID mutants. Prior works using AID tags in the cytoplasm have also demonstrated baseline reductions of the tagged protein (Sepers et al., 2022); this uninduced knockdown may underlie the loss of fitness in the TgSOD2-mAID line.

As with other conditional knockdown systems, some degree of leakiness, or unintentional knockdown, is to be expected with the AID system. We determined the degree of leakiness in the TgSOD2-mAID line by comparing the inducible knockdown TgSOD2-mAID line with the TgSOD2-BioID mutant line in Western blots. Analysis of lysates showed dramatic reductions in TgSOD2 levels in the TgSOD2-mAID line, which is further depleted following IAA exposure (**Figure 3.5**). Therefore, the reduced fitness observed in the TgSOD2-mAID line is likely attributed to baseline decreases in TgSOD2 levels. This would also explain the lack of difference in fitness level following IAA addition (**Figure 3.4**). Thus, this novel application of the auxin inducible degron tags can be used to deplete mitochondrially localized proteins. Despite the high degree of unintentional target knockdown, this mediated knockdown of genomically encoded mitochondrial proteins has potential for many avenues of future research.

Notably, TgSOD2 is localized to the matrix of the parasite's mitochondrion. To evaluate if TgSOD2 has a homeostatic role, we assessed whether TgSOD2 interacts with any neighboring mitochondrial proteins. We generated a TgSOD2-BioID mutant (**Figure 3.7**), for proximal biotinylation of TgSOD2's adjacent proteins. Mass spectrometry of the streptavidin captured proteins identified several members of the electron transport chain complexes, specifically the TgApiCox subunits and ATP synthase B-subunit (**Table 3.1**). Interestingly, the captured proteins were all predicted to have a CRISPR fitness score of <-3, indicating that they were likely highly fitness conferring (Sidik et al., 2016). As TgSOD2-BioID also contains an HA tag, we performed pulldown and mass spectrometry using anti-HA magnetic beads instead of streptavidin beads. Unlike the previous capture, which relied on BioID's activity as a promiscuous biotin ligase to label all proteins within 10nm, this anti-HA capture relied on proteins forming stronger

interactions with TgSOD2-BioID, which was the only HA-tagged protein in the sample. An anti-HA pulldown would not capture all proximal proteins; rather, it would capture proteins which form more direct interactions with the bait protein. For example, an anti-HA pulldown could capture multi-subunit complex members if given a single subunit as its HA-tagged target. This more stringent anti-HA pulldown captured ATP synthase B-subunit in addition to other mitochondrial proteins not shared with the original streptavidin pulldown (**Table 3.2**). These findings are in line with previous reports that iron-dependent SODs form homodimers for function, but had not identified any other stable protein-protein interactions involving TgSOD (Odberg-Ferragut et al., 2000). Thus, it is unlikely that TgSOD2 would form covalent bonds with complexes IV or V, rather, this data suggests that TgSOD2 is found in proximity to those complexes. It may be the case that TgSOD2 is a necessary bystander which maintains electron transport chain function by neutralizing generated superoxide anions in the vicinity. This is supported by BioID's nature as a promiscuous proximal biotin ligase; it biotinylates all proteins within a 10nm radius of itself, regardless of whether or not said protein is bound to it (Roux et al., 2012). Notably, this study is the first to suggest a relationship between TgSOD2 and ATP synthase B-subunit.

Seeing that multiple TgApiCox subunits were captured in the streptavidin pulldown, a TgApiCox35-BioID mutant was generated (**Figure 3.8**) to test for reciprocal tagging with TgSOD2. Reciprocal biotinylation and pulldown would be indicative of direct interactions between the two proteins. Unlike the TgSOD2-BioID pulldown, TgApiCox35 pulldown captured proteins associated with complex III in addition to complex IV. This pulldown also isolated additional TgApiCox subunits not captured through the TgSOD2-BioID pulldown, such as TgApiCox25 (**Table 3.3**). Prior BioID pulldown assays with a TgApiCox25-BioID mutant line captured TgApiCox35 in addition to other TgApiCox subunits (Seidi et al., 2018). No reciprocal pulldown of TgSOD2 was identified from the TgApiCox35-BioID streptavidin captured proteins (**Table 3.3**). This lack of reciprocity may be a result of TgApiCox's nature as a multi-subunit

membrane-bound protein. While TgSOD2 is found in the mitochondrial matrix, TgSOD2 may not be on the same side of the inner mitochondrial membrane as TgApiCox35 or the BioID tag appended onto it. TgApiCox35 may have been pulled down during the TgSOD2-BioID streptavidin capture as it could have been covalently bound to a biotinylated subunit, while remaining unbiotinylated itself. This lack of reciprocity does not rule out the TgApiCox complex as a proximal protein to TgSOD2.

Considering the possible association between TgSOD2 and members of the electron transport chain, it may be the case that mitochondrial dysfunction is underlying the fitness defect present in TgSOD2-mAID. Measurements of MMP show that it is reduced in the TgSOD2-mAID, even in the absence of IAA (**Figure 3.9**). Decreased MMP is indicative of mitochondrial stress and predictive of parasite apoptosis (Charvat and Arrizabalaga, 2016). Surveying mitochondrial morphology via immunofluorescence assay revealed that, while TgSOD2-mAID retained mitochondrial localization and distribution, stains against ATP synthase B-subunit displayed an abnormal variety of localization patterns (**Figure 3.10**). Some TgSOD2-mAID parasites displayed ATP synthase B-subunit localization with intact mitochondrial signal, but there were a significant proportion of parasites with completely absent ATP synthase B-subunit signal. To our knowledge, this is the first demonstration showing the loss of ATP synthase signal following TgSOD2 depletion. This result suggests that a decrease in TgSOD2 leads to increased superoxide dismutation mediated damage of ATP synthase, explaining the loss of ATP synthase signal. Thus, the interaction between TgSOD2 and ATP synthase likely contributes to *T. gondii* survival.

Although a direct interaction between TgSOD2 and TgApiCox35 is unlikely, many of these TgApiCox subunits are viable therapeutic targets for treating toxoplasmosis. The TgApiCox subunits observed in this work are highly fitness conferring (Sidik et al., 2016) and interference of these fitness conferring subunits could either make treated parasites susceptible to other therapeutic strategies or result in outright parasite death. Additionally, these TgApiCox

subunits lack human homologs, as amino acid sequence alignment showed no sequence similarity to human proteins. A lack of human orthologs should minimize side effects of a potential TgApiCox-targeting drug. Thus, these features make TgApiCox a highly attractive therapeutic target. This strategy of inhibiting mitochondrial electron transport at cytochrome C oxidase has been successfully applied in: antifungal antibiotics (Tripathi and Gottlieb, 1969), antibiotics against gram-positive bacteria (Irschik et al., 2007), and antiparasitics for *Leishmania* promastigotes (Luque-Ortega and Rivas, 2007). Furthermore, miltefosine has been effective in treating both acute and chronic toxoplasmosis(Eissa et al., 2015), further bolstering the argument that cytochrome C oxidase inhibition is a valid therapeutic strategy. Further investigation could evaluate the viability of a multi-target approach; coordinating inhibition of TgSOD2 alongside one or more of these highly fitness conferring respiratory enzymes would likely be a potent therapeutic strategy. Fortunately, there are existing drugs which target various members of the electron transport chain: miltefosine (Luque-Ortega and Rivas, 2007), sodium hydrosulfide (Nicholls et al., 2013), and potassium cyanide (Antonini et al., 1971) are all potent complex IV inhibitors, while aurovertin (Johnson et al., 2009) and oligomycin (Shchepina et al., 2002) are ATP synthase inhibitors. Refinements or derivatives of these drugs could offer greater specificity for parasite complex IV or ATP synthase, sparing host cells and widening the therapeutic window of a given treatment. Thus, complex IV and ATP synthase inhibition should be strongly considered during anti-parasitic drug development.

In addition to establishing an interaction between TgSOD2 and the TgApiCox complex, we also found a possible relationship between TgSOD2 and ATP synthase. Work in other organisms identified loss of SOD as a contributing factor to decreased ATP production, low membrane potential, and general mitochondrial dysfunction (Singh et al., 2021). Future testing should assess a reciprocal relationship between ATP synthase B-subunit and TgSOD2; given that ATP synthase B-subunit was also captured during the anti-HA pulldown of TgSOD2-BioID, there is a higher likelihood of a reciprocal pulldown under this proposed study. There is

evidence that TgSOD2 does not directly bind of TgSOD2 to ATP synthase (Sibley et al., 1986); it is likely the case that TgSOD2 preferentially localized adjacent to either ROS generation points, or ROS sensitive proteins. Superoxide anion generation studies in other eukaryotes have identified complexes I and III as the key generators of superoxide anions within the mitochondria (St-Pierre et al., 2002). It should be noted that apicomplexan electron transport chains are radically different from those of other eukaryotes. Apicomplexans lack a discrete membrane bound complex I, opting for free NADH dehydrogenases (Lin et al., 2011). They also have generally larger membrane bound electron transport proteins, boasting more subunits, leading to higher molecular weight complexes (Maclean et al., 2022). The above features may shift ROS generation to different members of the electron transport chain or render different components vulnerable to ROS-mediated damage. Considering the evidence above and the present work, it is likely that ATP synthase is sensitive to superoxide anions and TgSOD2's preferential localization adjacent to ATP synthase prevents damage from superoxide anion accumulation.

Our results point to the conclusion that TgSOD2 maintains mitochondrial function by protecting the electron transport chain from oxidative damage. The interaction between TgSOD2 and electron transport chain maintenance is not yet elucidated but there is reason to expect that loss of TgSOD2 would result in oxidative damage to complexes IV and V. Further experimentation could interrogate the link between specific electron transport chain members and TgSOD2 or examine the function of specific electron transport chain members of TgSOD2-mAID mutants following TgSOD2 depletion. Loss of TgSOD2 in the TgSOD2-mAID mutant may also sensitize parasites to antiparasitic treatments; possible sensitizations should be investigated as well with priority given to electron transport chain disruptors. Loss of TgSOD2 may also affect the parasite's wide host cell tropism or general virulence (Mittra et al., 2017); thus virulence of TgSOD2-mAID parasites should be assessed. Further studies could also

determine whether the identified proteins are superoxide anion generators or susceptible to spontaneous superoxide oxidation.

Materials and Methods

Host Cell and Parasite Cultures

Parasite clones and human foreskin fibroblasts (HFF) were grown and maintained in Dulbecco's modified Eagle's medium supplemented with 10% fetal bovine serum (Hyclone), penicillin and streptomycin (50 mg/ml each) and 200 µM L-glutamine. This complete medium is referred to as D10. We also used media containing dialyzed fetal bovine serum (Gibco #A3382001), which consisted of the same components and ratios as D10, but with dialyzed serum instead of standard fetal bovine serum. *T. gondii* were maintained by serial passage in HFF monolayers at 37°C in a humid 5% CO_2 atmosphere, including RH parasites (National Institutes of Health AIDS Reference and reagent Repository, Bethesda, MD), RH tachyzoites expressing cytoplasmic yellow fluorescent protein (YFP) (kindly provided by M.J. Gubbels, Boston College, Boston, Massachusetts) (Gubbels et al., 2003) RHΔku80Δhpt parasites (DKu80, kindly provided by V. Carruthers, University of Michigan Medical School Dexter, Michigan) (Fox et al., 2009; Huynh and Carruthers, 2009), and RH-TIR1 parasites (obtained through BEI Resources, NIAID, NIH: *Toxoplasma gondii*, Strain RH TIR1-3FLAG, NR 51145).

Transcription Quantification of ROS Scavenger Genes in Parasites

Quantitative PCR (qPCR) was used to quantify the expression level of various ROS scavenger genes in RH parasites. For intracellular parasites, an infected T175 was scraped, filtered, and immediately lysed with TRIzol. For extracellular parasites, the infected monolayer was scraped, filtered into a sterile centrifuge tube to remove host cell debris, then placed back into the incubator for 1 or 4 hours prior to lysis. Parasite lysis used TRIzol (Invitrogen) and chloroform. The aqueous phase was then used for RNA extraction via the RNeasy Mini Kit

(Qiagen) and subjected to DNAse I treatment to remove gDNA. The resulting RNA was then used for cDNA synthesis via iScript cDNA Synthesis Kit (Bio-Rad).

The resulting cDNA samples were used in qPCR with iTaq Universal SYBR Green Supermix (Bio-Rad) with the following gene targets: actin (TGGT1_209030, ToxoDB.org), catalase (TGGT1_232250, ToxoDB.org), peroxiredoxin 2 (TGGT1_266130, ToxoDB.org), thioredoxin reductase (TGGT1_309730, ToxoDB.org), superoxide dismutase 1 (TGGT1_316310, ToxoDB.org), superoxide dismutase 2 (TGGT1_316330, ToxoDB.org), glutaredoxin (TGGT1_227150, ToxoDB.org), glutathione reductase (TGGT1_246920, ToxoDB.org), and γ-glutamylcysteine synthetase (TGGT1_232590, ToxoDB.org). Primer sequences can be found in supplementary table 1. The selected primers amplify 100-150bp regions of the selected genes. To quantify the amount of target transcript present, target CT values were normalized against actin CT values. The resulting DCT values were then compared between different intracellular parasite populations in order to determine DDCT values.

Generation of TgSOD2-mAID-YFP tagged mutants

TgSOD2-BioID mutants were generated using CAS9 directed homologous recombination. Guide RNA were selected based on the Eukaryotic Pathogen CRISPR guide RNA/DNA Design Tool (http://grna.ctegd.uga.edu/) (Peng and Tarleton, 2015). For tagging TgSOD2, gRNA were targeted at the 3' end of the respective genes (Synthesized as primers 1 & 2, supplementary table 2). Once designed, gRNA must be inserted into a plasmid (pU6, courtesy of the Bradley lab) containing both CAS9 and a gRNA expression cassette allowing for the transient expression and direction of CAS9. pU6 was linearized with BsaI-Hf to allow for insertion of new gRNA sequences. These gRNA sequences were synthesized as two complementary oligos (IDT) including BsaI compatible overhangs. The primers were hybridized into a double stranded oligo by heating a 1:1 mixture of 10μM of each primer to 100ºC for 10 min. The hybridized oligo was ligated onto the linear pU6 using NEB T4 ligase with the following

reaction mixture: 50ng linear pU6, 3µL gRNA oligo, 1µL NEB ligase buffer, 0.5µL T4 ligase, and water to 10µL for 2 hours at room temperature. After ligation, T4 ligase was heat-inactivated at 65°C for 10 minutes, then used in *E. coli* transformation for plasmid amplification.

In addition to generating a gRNA/CAS9 plasmid, homologous recombination inserts specific for TgSOD2 were also generated. Each insert contained YFP, mAID and 3x HA tags along with a HXGPRT expression cassette for xanthine and mycophenolic acid selection. Inserts were generated by PCR using primers 3 and 4 (supplementary table 2) on the pTUB1_YFP-mAID-3HA HPT plasmid. These homologous recombination inserts were purified via QiaQuick PCR purification kit (Qiagen) prior to use in transfection. Once both the homologous recombination inserts and CAS9/gRNA plasmids were generated, TIR1 parasites were transfected with both to insert the BioID sequence into the target genes. As before, 10^7 freshly lysed TIR1 parasites were filtered and spun down at 400xG and 18ºC for 10 min. The pellet was resuspended with Cytomix buffer (10 mM KH_2PO_4, 120 mM KCl, 5 mM MgCl2, 25 mM HEPES, 2 mM EDTA, 2µM ATP and 5µM glutathione). Transfections included 10^7 parasites and 7.5µg of the ligated gRNA-pU6 plasmid and 1.5µg of the homologous recombination insert suspended in a total volume of 800µL Cytomix. The mixture was transfected using the ECM 630 Electro Cell Manipulator (BTX) at 2000V, 25 ohm resistance, and 50 µF capacitance. Parasites were incubated in non-selective D10 media after electroporation and switched to 2 µM pyrimethamine selection 24 h later.

The resulting transfectant pools were subjected to selection with 2µM mycophenolic acid and xanthine for at least 3 passages prior to single cell cloning. Clones were screened by both PCR and microscopy. PCR screening used a forward primer situated upstream of the homologous recombination target, and a reverse primer within the inserted HA tag encoding region. Screening via microscopy was used to identify clones which both expressed an HA tagged fusion protein and bore a YFP tag. HA tagged fusion proteins were identified with an anti-HA antibody, YFP was identified via fluorescence microscopy.

Verification of mAID activity

After generation of the mAID tagged mutant parasite lines, the activity of the mAID construct was verified through microscopy and western blots. Tagged parasites were cultured in D10 with dialyzed serum to ensure removal of auxin-like compounds in media which may induce unwanted protein degradation. Prior to protein collection, fresh parasites were used to infect flasks containing either fresh media with dialyzed serum, or fresh media supplemented with 500µM indoleacetic acid (IAA) to initiate tagged protein knockdown. Collected parasites were then spun down at 2500 RPM at 4℃ for 10 minutes, then rinsed with cold PBS. This process was repeated for a total of 2 PBS washes. After the 2nd wash, parasites were spun down again, then resuspended in 100µL of RIPA buffer supplemented with EDTA-free protease inhibitors (cOmplete™ 11836170001 Roche) and were lysed on ice for 30 minutes. Insoluble cell components were then collected via centrifugation at 10,000xG at 4°C for 10 minutes. Proteins were measured via Bradford assay. 10µg of protein were loaded for each lane. Gel electrophoresis, transfer, and blotting were carried out as previously described. TgSOD2 was identified via HA staining, GRA1 was used for loading controls and identified via anti-GRA1 antibodies (Monoclonal Anti-*Toxoplasma gondii* Dense Granule Antigen 1, Clone T5 2B4).

Parasite Plaque Assay

Plaque assays were used to assess the holistic fitness of mutant parasites. Briefly, a confluent 6-well plate coverslip in D10 media containing dialyzed serum or 500µM IAA supplemented media was infected with 100 parasites. Once infected, the 6 well plate was left undisturbed in normal tissue culture conditions for 8 days. To visualize plaques, the 6 well plates were washed with PBS, fixed with methanol, then stained with crystal violet (Roos et al., 1994). Plaques were manually counted, and the area of each identified plaque was quantified via ImageJ (Schneider et al., 2012).

Parasite Replication Assay

Replication assays were used to assess the ability of mutant parasites to replicate following host cell invasion. Briefly, a confluent 18mm coverslip in D10 media containing dialyzed serum was infected with 1,000,000 parasites (MOI of 5). Invasion was allowed to take place over the course of 1 hour, at 37℃, under standard tissue culture conditions. Following invasion, the monolayer was washed with PBS to remove uninvaded parasites, then replaced with either fresh dialyzed D10, or 500µM IAA containing media, then returned to the incubator for 24 hours for replication. To quantify replication, coverslips were stained with an anti-SAG1 antibody to identify parasites. Fluorescent microscopy images were taken, and the number of parasites per vacuole were counted. Vacuoles were tallied as containing: 1, 2, 4, 8 or 16+ parasites. Images of 20 random fields of view per experimental condition per experiment were quantified in this manner.

Generation of TgSOD2-BioID tagged mutants

TgSOD2-BioID mutants were generated via homologous recombination of a BioID-HA3x plasmid to a RHΔku80Δhpt parasite strain. This tagging plasmid was generated by ligation independent cloning of a homologous recombination arm from TgSOD2 onto the BioID_HA3x.LIC plasmid provided as a generous gift from the Bradley lab (Chen et al., 2015). Homologous recombination arms were generated by PCR amplification of the sequence of interest from isolated RH parasite genomes using the PCR primers described in Supplementary Table 2 (Primers: 5 and 6). The ligated plasmids were then used for parasite transfection into K2 strain *T. gondii*. Ten million freshly lysed K2 parasites were filtered and spun down at 400xG and 18ºC for 10 min. The pellet was resuspended with Cytomix buffer. Transfections included 10^7 parasites and 7.5µg of the ligated TgSOD2-YFP-HXGPRT.LIC plasmid suspended in a total volume of 800µL Cytomix. The mixture was transfected using the ECM 630 Electro Cell

Manipulator (BTX) at 2000V, 25 ohm resistance, and 50 µF capacitance. Parasites were incubated in non-selective D10 media after electroporation and switched to 2 µM mycophenolic acid/xanthine selection 24 h later. Following transfection, parasites were incubated in non-selective D10 media after electroporation and switched to 2 µM pyrimethamine selection 24 hours later.

The resulting transfectant pools were subjected to selection with 2µM pyrimethamine for at least 3 passages prior to single cell cloning. Following isolation and expansion of distinct clones, clones were screened by PCR to ensure integration of the BioID tagging plasmid. As with the prior mutants, a dual PCR verification strategy was deployed. Clones were screened for the absence of the wild-type 3' UTR (Primers: 7 and 8) and the presence of the BioID_HA3x insertion (Primers: 9 and 10); clones which were positive for insertion and negative for the wild-type 3' UTR would be screened for BioID ligase activity via microscopy.

Generation of TgApiCox-BioID tagged mutants

TgApiCox-BioID mutants were generated using CAS9 directed homologous recombination. Guide RNA were selected based on the Eukaryotic Pathogen CRISPR guide RNA/DNA Design Tool (http://grna.ctegd.uga.edu/) (Peng and Tarleton, 2015). For tagging TgApiCox35, gRNA was targeted at the 3' end of the gene of interest (Synthesized as primers 11 & 12, supplementary table 2). Once designed, gRNA must be inserted into a plasmid (pU6, courtesy of Dr. Peter Bradley) containing both CAS9 and a gRNA expression cassette allowing for the transient expression and direction of CAS9. pU6 was linearized with BsaI-Hf to allow for insertion of new gRNA sequences. These gRNA sequences were synthesized as two complementary oligos (IDT) including BsaI compatible overhangs. The primers were hybridized into a double stranded oligo by heating a 1:1 mixture of 10µM of each primer to 100ºC for 10 min. The hybridized oligo was ligated onto the linear pU6 using NEB T4 ligase with the following reaction mixture: 50ng linear pU6, 3µL gRNA oligo, 1µL NEB ligase buffer, 0.5µL T4 ligase, and

water to 10µL for 2 hours at room temperature. After ligation, T4 ligase was heat-inactivated at 65°C for 10 minutes, then used in *E. coli* transformation for plasmid amplification.

In addition to generating a gRNA/CAS9 plasmid, a homologous recombination insert specific for TgApiCox35 also needed to be generated. Each insert contained BioID and 3x HA tags along with a DHFR expression cassette for pyrimethamine selection. Inserts were generated by PCR using primers 13 and 14 (supplementary table 2) on the BioID_HA3x.LIC plasmid. These homologous recombination inserts were purified via QiaQuick PCR purification kit (Qiagen) prior to use in transfection. Once both the homologous recombination inserts and CAS9/gRNA plasmids were generated, K2 parasites were transfected with both to insert the BioID sequence into the target genes. As before, 10^7 freshly lysed K2 parasites were filtered and spun down at 400xG and 18ºC for 10 min. The pellet was resuspended with Cytomix buffer. Transfections included 10^7 parasites and 7.5µg of the ligated gRNA-pU6 plasmid and 1.5µg of the homologous recombination insert suspended in a total volume of 800µL Cytomix. The mixture was transfected using the ECM 630 Electro Cell Manipulator (BTX) at 2000V, 25 ohm resistance, and 50µF capacitance. Parasites were incubated in non-selective D10 media after electroporation and switched to 2 µM pyrimethamine selection 24 h later.

As before, the resulting transfectant pools were subjected to selection with 2-4µM pyrimethamine for at least 3 passages prior to single cell cloning in 96 well plates. Clones were screened by both PCR and microscopy. PCR screening used a forward primer situated upstream of the homologous recombination target, and a reverse primer within the inserted HA tag encoding region. Screening via microscopy was used to identify clones which both expressed an HA tagged fusion protein, and also displayed active biotin ligase. HA tagged fusion proteins were identified with an anti-HA antibody, active biotin ligase was identified by staining with YFP conjugated streptavidin.

Verification of integration of BioID activity: Microscopy

Following genomic verification of the clones, parasites were screened via microscopy to ensure that the integrated BioID was both present and active. For this microscopy assay, 12mM coverslips were seeded with HFF. Once confluent, these coverslips were then infected with ~10^4 parasites of either the BioID expressing clonal line, or a parental control strain. The parasites were cultured in either 150µM biotin containing media or standard media without the added biotin for 24 hours, then processed for imaging. The infected coverslips were fixed with 4% paraformaldehyde for 10 minutes at room temperature, permeabilized with 0.25% triton in PBS for 10 minutes at room temperature, blocked with 5% bovine serum albumin for 1 hour at room temperature, then labeled with a mix of antibodies and fluorophore conjugated streptavidin. To identify BioID localization, the coverslip was incubated in mouse anti-HA antibodies (1:2,500 dilution BioLegend Cat# 901514) in blocking buffer for 1 hour at room temperature. Then the coverslips were incubated in a PBS solution containing Alexa Fluor™ 594 goat anti-mouse antibodies (1:5,000 dilution Invitrogen #A11005) and of streptavidin-FITC (1:50 dilution Invitrogen #SA1001) for biotin labeling for 1 hour at room temperature. Slides were imaged on Zeiss Axioskop with Axiovision camera and software.

Isolation of proteins for mass spectrometry

Capture of biotinylated or HA-tagged proteins was achieved through use of Streptavidin Magnetic Beads (NEB #S1420S) or Pierce Anti-HA Magnetic Beads (Thermo Fisher Scientific #88836). Briefly, either BioID tagged parasites or K2 parental strain parasites were used to infect 3 T175 flasks of HFF. 24 hours after infection, the media in the flasks was swapped to 150µM biotin containing media, and the parasites were allowed to incubate for another 24 hours. For anti-HA capture, fresh, non-biotin supplemented media was used instead. A total of 48 hours after infection, the parasites had fully lysed the fibroblast monolayer and were collected by scraping the flask. Collected parasites were then spun down at 2500 RPM at 4℃

for 15 minutes, then rinsed with cold PBS twice to remove free biotin and debris. After the 2nd wash, parasites were spun down again, then resuspended in 2mL of RIPA buffer supplemented with EDTA-free protease inhibitors (cOmplete™ 11836170001 Roche) and were lysed on ice for 30 minutes. Insoluble cell components were then collected via centrifugation at 10,000xG at 4°C for 10 minutes. 1.8mL of protein containing supernatants was added to 200µL of washed magnetic bead slurry in RIPA buffer. Protein and beads were incubated at 4°C with constant agitation overnight to allow for protein binding.

Following protein binding, the beads were washed with RIPA buffer to remove non-specific proteins which may have been captured. Beads are washed 3 times in total, transferring the bead-protein slurry to a new microcentrifuge tube following each wash. After washing, the beads are resuspended in 100µL 8M urea dissolved in tris-HCl. Beads in urea were then used for either mass spectrometry, or western blots for protein capture verification.

Verification of integration of BioID activity: Western Blots

Following protein harvest and isolation of biotinylated proteins, biotin ligase activity of the mutant BioID expressing lines was verified by Western blot. 30µl of total isolated proteins were loaded onto a 12% polyacrylamide gel for electrophoresis. This gel was run at 100V for 100 minutes in a chilled TRIS/glycine running buffer (BioRad). Following transfer onto a nitrocellulose membrane, the blot was blocked with a mixture of 5% skim milk powder, 5% goat serum, and 0.1% TWEEN-20 in Tris-buffered saline for 1 hour. It was then stained with a mouse anti-HA antibody overnight at 4℃ in order to verify successful biotinylation of the tagged mutant protein (diluted at 1:2,500 in blocking buffer). Lastly, the blot was stained with a goat anti-mouse HRP conjugated antibody (1:2,500 dilution) for 1 hour. The blot was visualized using BioRad's Clarity ECL solution.

Mass spectrometry

Mass spectrometry was performed by UCI's High-end Mass Spectrometry Facility managed by the Huang Lab. Briefly, the collected magnetic bead-protein slurry in 8M urea was subjected to on bead digestion with trypsin. Resulting peptides were then used for liquid chromatography–mass spectrometry analysis with an UltiMate 3000 RSLC system (Thermo Fisher Scientific) coupled in-line to an Orbitrap Fusion Lumos mass spectrometer (Thermo Fisher Scientific).

Following mass spectrometry of the captured peptides, raw data files needed to be analyzed to identify proteins specifically enriched in the BioID parasite lines. MaxQuant was used to database search and quantify the relative composition in purified proteins. Raw files were aligned against an Me49 proteome (Toxodb: PA.ToxoDB-10.0_TgondiiME49_20140131) to identify which protein each peptide belongs to. To determine which proteins were enriched, we focused on the peptide counts. Enrichment was defined as having at least 4 peptides recovered and a mutant strain peptide count:parental strain peptide count ratio greater than 3.

Mitochondrial Membrane Potential

Confluent HFFs in T25 flasks were infected with parasites in D10 media with or without 500 µM IAA for ~24 hours. After infection, infected HFFs were scraped and syringe lysed with a 20G needle and filtrated through 3.0 µm pore-size membrane filters (Whatman) to remove host cell debris. Released parasites were centrifuged at 400 g for 10 minutes, and incubated with D10 media with 200 nM MitoTracker Red CMXRos (Life Technologies) for 25 minutes in a 37 °C incubator at 5% CO_2. After staining, cultures were pelleted at 500 g for 5 minutes and resuspended in PBS to assess mitochondrial membrane potential. Parasites were analyzed using a NovoCyte flow cytometer (Agilent) and FlowJo V10 software (Tree Star Inc., Ashland, OR). The threshold for MitoTracker positive and negative parasites in the PE (FL2) channel was determined by non-MioTracker stained controls.

Mitochondrial Morphology Microscopy

Mitochondrial morphology was evaluated via fluorescence microscopy. A confluent 18mm coverslip in D10 media containing dialyzed serum was infected with 1,000,000 parasites (MOI of 5). Invasion was allowed to take place over the course of 1 hour, at 37℃, under standard tissue culture conditions. Following invasion, the monolayer was washed with PBS to remove uninvaded parasites, then replaced with either fresh dialyzed D10, or 500µM IAA containing media, then returned to the incubator for 24 hours for replication. Coverslips were stained with an anti-F1B antibody to label parasite mitochondria. Fluorescent microscopy images were taken, and the mitochondria were classified as intact, aberrant, or absent. Images of 20 random fields of view per experimental condition per experiment were quantified in this manner.

Target	Gene ID	Primer Sequence
Actin F	TGGT1_209030	CACGAGAGAGGATACGGCTTC
Actin R	TGGT1_209030	CGATGTCGCTAGAGTCCTCAG
Catalase F	TGGT1_232250	CTCAGGTTCCGCCCGTAACATTC
Catalase R	TGGT1_232250	GCCAGCTTGTCGATGAGATGGAAG
thioredoxin reductase F	TGGT1_309730	CACAAACACGAACAACGGCG
thioredoxin reductase R	TGGT1_309730	GTGGACGGCTGAACAAAGTCG
superoxide dismutase 1 F	TGGT1_316310	GGAGACACTTCAGTTCCATC
superoxide dismutase 1 R	TGGT1_316310	GAAAATGGCTCCAGTAGACG
peroxiredoxin 2	TGGT1_266130	CATTACGAACGTCGCATCGC
peroxiredoxin 2	TGGT1_266130	CAGCGAGGAACGTCTTGATGTC
superoxide dismutase 2 F	TGGT1_316330	GGCACACCGTTCGCTGATAAG
superoxide dismutase 2 R	TGGT1_316330	CGTGGTTCCATGCTTGTGCTG
glutaredoxin F	TGGT1_227150	CTGGAGATTCTCAGGAACGC
glutaredoxin R	TGGT1_227150	GCGTGTAGTCCATCCGATC
glutathione reductase F	TGGT1_246920	CTGCGTGAAAAGCCAGATG
glutathione reductase R	TGGT1_246920	CGCAGTTGTCAAAGTCTGC
γ-glutamylcysteine synthetase F	TGGT1_232590	CGACCACGGTTCTTTACATG
γ-glutamylcysteine synthetase R	TGGT1_232590	GGTAGTCTGGTACTTTCCGTC

Supplementary Table 1: qPCR primers

Number	Gene ID	Primer Sequence
1	TGGT1_316330	AAGTTGCGAAACAATCGTCTTGGTGG
2	TGGT1_316330	AAAACCACCAAGACGATTGTTTCGCA
3	TGGT1_316330	TTTCGCAGCTGAGAACTTGGTGAAAGCACTTGAAAGCAACT CTAAAATGGTGAGCAAGGG
4	TGGT1_316330	GACGCACAAATGACCATCGGCACTGATATAATTATGTTCCGA GAGGAAAACGAGAGACG
5	TGGT1_316330	TACTTCCAATCCAATTTACGAAGGTGAGGAGCATTCG
6	TGGT1_316330	TCCTCCACTTCCAATTTTAGCGTTGCTTTCAAGTGCTTTCAC C
7	TGGT1_316330	GCATTTGTGTCCTCCATCCGC
8	TGGT1_316330	CACGCCTCGGAGCATGTAAAG
9	TGGT1_316330	GAACCACCACATAACAGC
10	BioID_HA3x.LIC	CATAATCTGGAACATCGTAAGG
11	TGGT1_229920	AAGTTGAAGACGCTGTGGATCCAGTG
12	TGGT1_229920	AAAACACTGGATCCACAGCGTCTTCA
13	TGGT1_229920	ACACAAAATCAACTGGGTAGTGCCACGAGGCGACCTCGTTG CTAAAATTGGAAGTGGAGG
14	TGGT1_229920	GCGAAGGACGCCAAACGTTCATCGTTCCTCGTGTTTTGTTTC CTGCAAGTGCATAGAAG

Supplementary Table 2: primers used for parasite genetic engineering

References

Ahsan, Md. K., Lekli, I., Ray, D., Yodoi, J., and Das, D. K. (2009). Redox Regulation of Cell Survival by the Thioredoxin Superfamily: An Implication of Redox Gene Therapy in the Heart. *Antioxid. Redox Signal.* 11, 2741–2758. doi: 10.1089/ars.2009.2683.

Antonini, E., Brunori, M., Rotilio, G. C., Greenwood, C., and MalmstrÖM, B. G. (1971). The Interaction of Cyanide with Cytochrome Oxidase. *Eur. J. Biochem.* 23, 396–400. doi: 10.1111/j.1432-1033.1971.tb01633.x.

Brown, K. M., Long, S., and Sibley, L. D. (2017). Plasma Membrane Association by N-Acylation Governs PKG Function in Toxoplasma gondii. *mBio* 8. doi: 10.1128/mBio.00375-17.

Brydges, S. D., and Carruthers, V. B. (2003). Mutation of an unusual mitochondrial targeting sequence of SODB2 produces multiple targeting fates in Toxoplasma gondii. *J. Cell Sci.* 116, 4675–4685. doi: 10.1242/jcs.00750.

Charvat, R. A., and Arrizabalaga, G. (2016). Oxidative stress generated during monensin treatment contributes to altered Toxoplasma gondii mitochondrial function. *Sci. Rep.* 6, 22997. doi: 10.1038/srep22997.

Chen, C.-T., Kelly, M., Leon, J. de, Nwagbara, B., Ebbert, P., Ferguson, D. J. P., et al. (2015). Compartmentalized Toxoplasma EB1 bundles spindle microtubules to secure accurate chromosome segregation. *Mol. Biol. Cell* 26, 4562–4576. doi: 10.1091/mbc.E15-06-0437.

Daniel, K., Icha, J., Horenburg, C., Müller, D., Norden, C., and Mansfeld, J. (2018). Conditional control of fluorescent protein degradation by an auxin-dependent nanobody. *Nat. Commun.* 9, 3297. doi: 10.1038/s41467-018-05855-5.

Eissa, M. M., Barakat, A. M. A., Amer, E. I., and Younis, L. K. (2015). Could miltefosine be used as a therapy for toxoplasmosis? *Exp. Parasitol.* 157, 12–22. doi: 10.1016/j.exppara.2015.06.005.

Eyles, D. E., and Coleman, N. (1953). Synergistic effect of sulfadiazine and daraprim against experimental toxoplasmosis in the mouse. *Antibiot. Chemother. Northfield Ill* 3, 483–490.

Fox, B. A., Ristuccia, J. G., Gigley, J. P., and Bzik, D. J. (2009). Efficient Gene Replacements in Toxoplasma gondii Strains Deficient for Nonhomologous End Joining. *Eukaryot. Cell* 8, 520–529. doi: 10.1128/ec.00357-08.

Gaji, R. Y., Behnke, M. S., Lehmann, M. M., White, M. W., and Carruthers, V. B. (2011). Cell cycle-dependent, intercellular transmission of Toxoplasma gondii is accompanied by marked changes in parasite gene expression. *Mol. Microbiol.* 79, 192–204. doi: 10.1111/j.1365-2958.2010.07441.x.

Ghosh, D., Walton, J. L., Roepe, P. D., and Sinai, A. P. (2012). Autophagy is a cell death mechanism in Toxoplasma gondii. *Cell. Microbiol.* 14, 589–607. doi: 10.1111/j.1462-5822.2011.01745.x.

Gubbels, M.-J., Li, C., and Striepen, B. (2003). High-Throughput Growth Assay for Toxoplasma gondii Using Yellow Fluorescent Protein. *Antimicrob. Agents Chemother.* 47, 309–316. doi: 10.1128/AAC.47.1.309-316.2003.

Holmgren, A. (1979). Thioredoxin catalyzes the reduction of insulin disulfides by dithiothreitol and dihydrolipoamide. *J. Biol. Chem.* 254, 9627–9632.

Hu, X., O'Shaughnessy, W. J., Beraki, T. G., and Reese, M. L. (2020). Loss of the Conserved Alveolate Kinase MAPK2 Decouples Toxoplasma Cell Growth from Cell Division. *mBio* 11, 10.1128/mbio.02517-20. doi: 10.1128/mbio.02517-20.

Huynh, M.-H., and Carruthers, V. B. (2009). Tagging of endogenous genes in a Toxoplasma gondii strain lacking Ku80. *Eukaryot. Cell* 8, 530–539. doi: 10.1128/EC.00358-08.

Irschik, H., Reichenbach, H., Höfle, G., and Jansen, R. (2007). The thuggacins, novel antibacterial macrolides from Sorangium cellulosum acting against selected Gram-positive bacteria. *J. Antibiot. (Tokyo)* 60, 733–738. doi: 10.1038/ja.2007.95.

Johnson, K. M., Swenson, L., Opipari Jr., A. W., Reuter, R., Zarrabi, N., Fierke, C. A., et al. (2009). Mechanistic basis for differential inhibition of the F1Fo-ATPase by aurovertin. *Biopolymers* 91, 830–840. doi: 10.1002/bip.21262.

Kaasch, A. J., and Joiner, K. A. (2000). Targeting and Subcellular Localization of Toxoplasma gondii Catalase: IDENTIFICATION OF PEROXISOMES IN AN APICOMPLEXAN PARASITE *. *J. Biol. Chem.* 275, 1112–1118. doi: 10.1074/jbc.275.2.1112.

Kwok, L. Y., Schlüter, D., Clayton, C., and Soldati, D. (2004). The antioxidant systems in Toxoplasma gondii and the role of cytosolic catalase in defence against oxidative injury. *Mol. Microbiol.* 51, 47–61. doi: 10.1046/j.1365-2958.2003.03823.x.

Lin, S. S., Blume, M., von Ahsen, N., Gross, U., and Bohne, W. (2011). Extracellular Toxoplasma gondii tachyzoites do not require carbon source uptake for ATP maintenance, gliding motility and invasion in the first hour of their extracellular life. *Int. J. Parasitol.* 41, 835–841. doi: 10.1016/j.ijpara.2011.03.005.

Long, S., Brown, K. M., Drewry, L. L., Anthony, B., Phan, I. Q. H., and Sibley, L. D. (2017). Calmodulin-like proteins localized to the conoid regulate motility and cell invasion by Toxoplasma gondii. *PLOS Pathog.* 13, e1006379. doi: 10.1371/journal.ppat.1006379.

Luque-Ortega, J. R., and Rivas, L. (2007). Miltefosine (hexadecylphosphocholine) inhibits cytochrome c oxidase in Leishmania donovani promastigotes. *Antimicrob. Agents Chemother.* 51, 1327–1332. doi: 10.1128/AAC.01415-06.

Maclean, A. E., Hayward, J. A., Huet, D., van Dooren, G. G., and Sheiner, L. (2022). The mystery of massive mitochondrial complexes: the apicomplexan respiratory chain. *Trends Parasitol.* 38, 1041–1052. doi: 10.1016/j.pt.2022.09.008.

Mittra, B., Laranjeira-Silva, M. F., Miguel, D. C., Perrone Bezerra de Menezes, J., and Andrews, N. W. (2017). The iron-dependent mitochondrial superoxide dismutase SODA promotes Leishmania virulence. *J. Biol. Chem.* 292, 12324–12338. doi: 10.1074/jbc.M116.772624.

Mordue, D. G., Håkansson, S., Niesman, I., and David Sibley, L. (1999). Toxoplasma gondii Resides in a Vacuole That Avoids Fusion with Host Cell Endocytic and Exocytic Vesicular Trafficking Pathways. *Exp. Parasitol.* 92, 87–99. doi: 10.1006/expr.1999.4412.

Natsume, T., and Kanemaki, M. T. (2017). Conditional degrons for controlling protein expression at the protein level. *Annu. Rev. Genet.* 51, 83–102. doi: 10.1146/annurev-genet-120116-024656.

Natsume, T., Kiyomitsu, T., Saga, Y., and Kanemaki, M. T. (2016). Rapid Protein Depletion in Human Cells by Auxin-Inducible Degron Tagging with Short Homology Donors. *Cell Rep.* 15, 210–218. doi: 10.1016/j.celrep.2016.03.001.

Nicholls, P., Marshall, D. C., Cooper, C. E., and Wilson, M. T. (2013). Sulfide inhibition of and metabolism by cytochrome c oxidase. *Biochem. Soc. Trans.* 41, 1312–1316. doi: 10.1042/BST20130070.

Odberg-Ferragut, C., Renault, J. P., Viscogliosi, E., Toursel, C., Briche, I., Engels, A., et al. (2000). Molecular cloning, expression analysis and iron metal cofactor characterisation of a superoxide dismutase from Toxoplasma gondii. *Mol. Biochem. Parasitol.* 106, 121–129. doi: 10.1016/S0166-6851(99)00211-X.

Peng, D., and Tarleton, R. (2015). EuPaGDT: a web tool tailored to design CRISPR guide RNAs for eukaryotic pathogens. *Microb. Genomics* 1. doi: 10.1099/mgen.0.000033.

Pino, P., Foth, B. J., Kwok, L.-Y., Sheiner, L., Schepers, R., Soldati, T., et al. (2007). Dual targeting of antioxidant and metabolic enzymes to the mitochondrion and the apicoplast of Toxoplasma gondii. *PLoS Pathog.* 3, e115. doi: 10.1371/journal.ppat.0030115.

Rahmanian, V., Rahmanian, K., Jahromi, A. S., and Bokaie, S. (2020). Seroprevalence of toxoplasma gondii infection: An umbrella review of updated systematic reviews and meta-analyses. *J. Fam. Med. Prim. Care* 9, 3848–3855. doi: 10.4103/jfmpc.jfmpc_753_20.

Roos, D. S., Donald, R. G., Morrissette, N. S., and Moulton, A. L. (1994). Molecular tools for genetic dissection of the protozoan parasite Toxoplasma gondii. *Methods Cell Biol.* 45, 27–63. doi: 10.1016/s0091-679x(08)61845-2.

Roux, K. J., Kim, D. I., Raida, M., and Burke, B. (2012). A promiscuous biotin ligase fusion protein identifies proximal and interacting proteins in mammalian cells. *J. Cell Biol.* 196, 801–810. doi: 10.1083/jcb.201112098.

Scallan, E., Hoekstra, R., Angulo, F., Tauxe, R., Widdowson, M., Roy, S., et al. (2011). Foodborne illness acquired in the United States-major pathogens. *Emerg. Infect. Dis.* 17, 7–15. doi: 10.3201/eid1701.091101p1.

Schneider, C. A., Rasband, W. S., and Eliceiri, K. W. (2012). NIH Image to ImageJ: 25 years of image analysis. *Nat. Methods* 9, 671–675. doi: 10.1038/nmeth.2089.

Seidi, A., Muellner-Wong, L. S., Rajendran, E., Tjhin, E. T., Dagley, L. F., Aw, V. Y., et al. (2018). Elucidating the mitochondrial proteome of Toxoplasma gondii reveals the presence of a divergent cytochrome c oxidase. *eLife* 7. doi: 10.7554/eLife.38131.

Sepers, J. J., Verstappen, N. H. M., Vo, A. A., Ragle, J. M., Ruijtenberg, S., Ward, J. D., et al. (2022). The mIAA7 degron improves auxin-mediated degradation in Caenorhabditis elegans. *G3 GenesGenomesGenetics* 12, jkac222. doi: 10.1093/g3journal/jkac222.

Shchepina, L. A., Pletjushkina, O. Y., Avetisyan, A. V., Bakeeva, L. E., Fetisova, E. K., Izyumov, D. S., et al. (2002). Oligomycin, inhibitor of the F0 part of H+-ATP-synthase, suppresses the TNF-induced apoptosis. *Oncogene* 21, 8149–8157. doi: 10.1038/sj.onc.1206053.

Sibley, L. D., Lawson, R., and Weidner, E. (1986). Superoxide dismutase and catalase in Toxoplasma gondii. *Mol. Biochem. Parasitol.* 19, 83–87. doi: 10.1016/0166-6851(86)90069-1.

Sidik, S. M., Huet, D., Ganesan, S. M., Huynh, M.-H., Wang, T., Nasamu, A. S., et al. (2016). A Genome-wide CRISPR Screen in Toxoplasma Identifies Essential Apicomplexan Genes. *Cell* 166, 1423-1435.e12. doi: 10.1016/j.cell.2016.08.019.

Singh, N., NaveenKumar, S. K., Geethika, M., and Mugesh, G. (2021). A Cerium Vanadate Nanozyme with Specific Superoxide Dismutase Activity Regulates Mitochondrial Function and ATP Synthesis in Neuronal Cells. *Angew. Chem. Int. Ed.* 60, 3121–3130. doi: 10.1002/anie.202011711.

St-Pierre, J., Buckingham, J. A., Roebuck, S. J., and Brand, M. D. (2002). Topology of Superoxide Production from Different Sites in the Mitochondrial Electron Transport Chain *. *J. Biol. Chem.* 277, 44784–44790. doi: 10.1074/jbc.M207217200.

Tripathi, R. K., and Gottlieb, D. (1969). Mechanism of action of the antifungal antibiotic pyrrolnitrin. *J. Bacteriol.* 100, 310–318. doi: 10.1128/jb.100.1.310-318.1969.

CHAPTER FOUR: Summary and Future Directions

Auranofin mediated ROS stress inhibits *T. gondii*

While data from prior works had demonstrated that auranofin is an effective treatment for toxoplasmosis (Andrade et al., 2014), studies in *Chapter Two* elucidated its effects on the parasite lytic cycle, which underlie auranofin's efficacy. These experiments characterized the mechanism by which auranofin inhibits parasite growth, then identified mutations responsible for drug resistance. Treatment with auranofin decreased parasite ability to invade host cells (**Figure 2.1**), induced parasite egress from host cells (**Figure 2.2B**), and triggered apoptosis (**Figure 2.3**). Drug resistant mutant screens showed that mutations decreasing parasite ROS accumulation were common to the development of auranofin resistance (**Figure 2.6**). Additional studies are needed to determine if there are other phenotypic differences which arose alongside auranofin resistance development. We identified TgSOD2 L201P as a consensus mutation in one line (line 8) of auranofin resistant mutants. While this mutation did decrease ROS accumulation, it was not sufficient to confer auranofin resistance (**Figure 2.7**). Therefore, additional compensatory mutations are needed for the development of drug resistance. Overall, these results suggest a route in which auranofin treatment leads to ROS accumulation-induced apoptosis.

Current studies of toxoplasmosis treatments are focused on adapting existing, pre-approved therapeutics for anti-parasitic purposes. The conclusions from *Chapter Two* advocate auranofin as a potential treatment for toxoplasmosis. While auranofin has been previously FDA approved for human use, it does pose the risk of patient bone marrow toxicity, leading to a decline in its clinical use (Roder and Thomson, 2015). Derivatives of auranofin or other gold salt compounds may be able to exert the same effects as auranofin on *T. gondii*. Auranofin derivative compounds may be able to retain or improve upon the presented anti-parasitic effects while minimizing host cell toxicity. More broadly, these data provide further support for redox homeostasis disruption as a treatment strategy.

TgSOD2 maintains the parasite electron transport chain

The experimental design in *Chapter Three* employed inducible knockdown and proximal biotinylation mutants of TgSOD2 to clarify its role within the parasite's mitochondrion. Insertion of a mini-auxin inducible degron (mAID) tag onto the TgSOD2 C-terminal (TgSOD2-mAID) allowed for inducible depletion of the tagged enzyme. This TgSOD2-mAID mutant exhibited decreased replication and generally reduced fitness (**Figure 3.4**). Additionally, they had reduced mitochondrial membrane potential, indicative of ROS stress (**Figure 3.9**). This phenotype is likely attributed to baseline decreases in TgSOD2 quantity in the absence of knockdown induction by IAA (**Figure 3.5**). This data suggest that TgSOD2 has a protective role in mitochondrial homeostasis. To better evaluate this role, TgSOD2-BioID mutants were generated to identify other proteins associated with TgSOD2. Streptavidin capture of proximally biotinylated proteins suggested that TgSOD2 localizes adjacent to the electron transport chain; likely near apicomplexan cytochrome C oxidase (ApiCox) or ATP synthase (**Figure 4.1**, **Table 3.1**). Subsequent microscopy of TgSOD2-mAID probing for ATP synthase revealed abnormalities in ATP synthase localization. While ATP synthase is a reliable mitochondrial marker in control parasites, it failed to completely localize to the parasite mitochondrion in TgSOD2-mAID parasites (**Figure 3.10**). Therefore, TgSOD2 is likely involved with maintaining ATP synthase within the mitochondrion. Disruption of ATP synthase could explain TgSOD2-mAID's growth defect and attenuated mitochondrial membrane potential.

The work discussed above introduced both conceptual and technical novelties. Prior application of proximal biotinylation were used to identify direct, bound interactors via reciprocal pulldown (Chen et al., 2015; Seidi et al., 2018). The TgSOD2-BioID and TgApiCox35-BioID experimental designs employed proximal biotinylation to survey neighboring proteins, not as direct interactors or fellow complex subunits, but as proteins at risk of ROS-mediated damage. This methodology can be applied to other ROS scavengers to identify proteins which require assistance to maintain redox homeostasis. For example, a TgSOD1-BioID mutant streptavidin

pulldown may reveal cytoplasmic proteins which are sensitive to superoxide anion-mediated damage. The TgSOD2-mAID study poses technical novelty by attaching auxin-inducible degron tags to a mitochondrial protein. While this may inhibit the speed and degree of target degradation compared to traditional AID tags to cytoplasmic proteins of interest (15 minutes for 95% target depletion (Brown et al., 2018)), mitochondrial proteins can still be depleted upon addition of IAA (**Figure 3.3**). Auxin-inducible degradation of mitochondrial proteins opens the possibility of depletion studies of these highly fitness conferring proteins.

The mutant parasites generated in *Chapter Three* could be informative in future experimental designs. Previous works have used AID parasites in a murine infection model to examine the tagged protein's role in an *in vivo* infection (Brown and Sibley, 2018). As SODs have been implicated as virulence factors in other parasites (Mittra et al., 2017), it may be the case that TgSOD2 loss affects parasite virulence. Loss of this critical ROS scavenger could limit the variety of host cells that mutant parasites can effectively colonize. Host cells with higher intracellular ROS concentrations may be uninhabitable for TgSOD2-depleted parasites. Alternatively, further *in vitro* analysis of the TgSOD2-mAID mutants may prove fruitful. Given that this mutant line displays baseline reductions in TgSOD2, it may have developed compensatory mechanisms. Whole genome sequencing or RNA sequencing could shed light on how *T. gondii* is able to acclimate to ROS stress following TgSOD2 depletion. These adaptations are more likely to manifest while the parasite is in an extracellular state; parasites in this state exhibit greater dependence on oxidative phosphorylation (MacRae et al., 2012). Disruptions to the parasite mitochondrial electron transport chain or mitochondrial membrane potential are likely to interfere with oxidative phosphorylation. On the other hand, further investigation of TgSOD2-BioID mutants may reveal alterations in TgSOD2 localization in response to different stressors. The results from *Chapter Three* originated from extracellular parasites, which have shifted their metabolism to favor oxidative phosphorylation (MacRae et al., 2012). It is unclear whether TgSOD2 would still preferentially localize adjacent to the

electron transport chain in different nutritional or environmental scenarios where it is not as engaged. Additionally, it is not clear if TgSOD2 changes upon expression of TgSOD3, the other mitochondrially-localized SOD, which is limited to feline-shed oocysts where the parasite completes its sexual cycle.

While this dissertation explores the effects of TgSOD2 depletion on parasite fitness, it raises the question of whether the loss of TgSOD2 sensitizes parasites to other therapeutics. With the BioID findings, it is conceivable that loss of TgSOD2 would render the parasite especially vulnerable to treatments which affect either TgApiCox or ATP synthase. Given the conserved nature of ATP synthase, it may be more feasible to consider pharmaceuticals which target TgApiCox. Within the electron transport chain, Complex I and III have been shown to produce superoxide anions(Brand et al., 2004). Cytochrome C oxidase, while not a direct producer of superoxide anions, does leak electrons when damaged; these freed electrons reduce molecular oxygen into superoxide anions (Srinivasan and Avadhani, 2012). If allowed to undergo spontaneous dismutation, superoxide anions can oxidize mitochondrial membrane lipids, permeabilizing the membrane (Halliwell and Gutteridge, 2015, 1.10). Ideally, a combination strategy of impairing TgSOD2 in conjunction with damaging TgApiCox may be applicable to both acute and chronic phases of infection. This strategy would lead to increased superoxide anion generation within parasites and force spontaneous dismutation of the radical, thereby damaging the parasite's mitochondrion. Both TgSOD2 and TgApiCox are present in both tachyzoites and bradyzoites. TgApiCox shares few or no similarities to human host proteins, making them ideal drug targets. Future evaluations of the efficacy of various electron transport chain inhibitors on the TgSOD2-mAID line would simulate this bipartite approach.

Conclusion

Ultimately, this dissertation contributes to the body of knowledge by suggesting that TgSOD2 plays a protective role within the parasite mitochondrion, defending the electron

transport chain from ROS mediated damage. Prior works have defined the biochemical reactions which TgSOD2 catalyzes, its localization, and TgSOD2's necessity to parasite survival. We then further characterized TgSOD2's expression profile, identified proximal proteins, and described the consequences of targeted protein depletion. It would be informative to expand on open-ended concepts such as: the use of auranofin derivatives against toxoplasmosis, the suggested links between TgSOD2 and ATP synthase, or the compensatory mutations which enable survival following TgSOD2 depletion. These fundamental advancements are presented alongside technical advances as well: we demonstrate the first application of auxin-induced depletion of a mitochondrial protein, showing that the AID system could be used to degrade nascent proteins prior to trafficking to their specific target subcellular compartment. We have also applied the BioID proximal biotinylation system to identify adjacent proteins, not as members of an interacting complex, but as ROS sensitive proteins which would require TgSOD2-mediated protection from superoxide anions. Altogether, these conceptual advancements and technical novelties provide a foundation for future studies to augment our understanding of the parasitic mitochondrion.

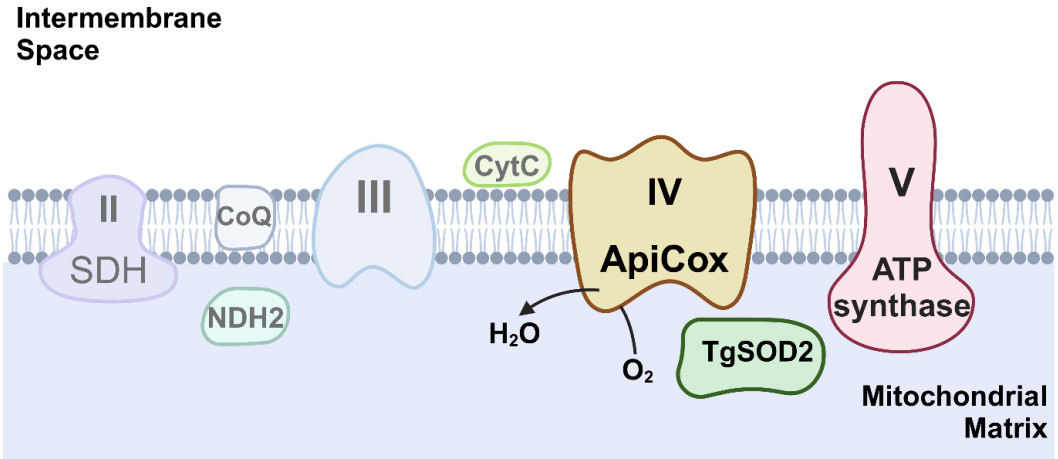

Figure 4.1: Proposed model of TgSOD2 localization within *T. gondii* mitochondrion.
Created with BioRender.com

References

Andrade, R. M., Chaparro, J. D., Capparelli, E., and Reed, S. L. (2014). Auranofin is highly efficacious against Toxoplasma gondii in vitro and in an in vivo experimental model of acute toxoplasmosis. *PLoS Negl. Trop. Dis.* 8, e2973. doi: 10.1371/journal.pntd.0002973.

Brand, M. D., Affourtit, C., Esteves, T. C., Green, K., Lambert, A. J., Miwa, S., et al. (2004). Mitochondrial superoxide: production, biological effects, and activation of uncoupling proteins. *Free Radic. Biol. Med.* 37, 755–767. doi: 10.1016/j.freeradbiomed.2004.05.034.

Brown, K. M., Long, S., and Sibley, L. D. (2018). Conditional Knockdown of Proteins Using Auxin-inducible Degron (AID) Fusions in Toxoplasma gondii. *Bio-Protoc.* 8. doi: 10.21769/BioProtoc.2728.

Brown, K. M., and Sibley, L. D. (2018). Essential cGMP Signaling in Toxoplasma Is Initiated by a Hybrid P-Type ATPase-Guanylate Cyclase. *Cell Host Microbe* 24, 804-816.e6. doi: 10.1016/j.chom.2018.10.015.

Chen, A. L., Kim, E. W., Toh, J. Y., Vashisht, A. A., Rashoff, A. Q., Van, C., et al. (2015). Novel components of the Toxoplasma inner membrane complex revealed by BioID. *mBio* 6, e02357-14. doi: 10.1128/mBio.02357-14.

Halliwell, B., and Gutteridge, J. M. C. (2015). *Free Radicals in Biology and Medicine*. Oxford University Press.

MacRae, J. I., Sheiner, L., Nahid, A., Tonkin, C., Striepen, B., and McConville, M. J. (2012). Mitochondrial Metabolism of Glucose and Glutamine Is Required for Intracellular Growth of Toxoplasma gondii. *Cell Host Microbe* 12, 682–692. doi: 10.1016/j.chom.2012.09.013.

Mittra, B., Laranjeira-Silva, M. F., Miguel, D. C., Perrone Bezerra de Menezes, J., and Andrews, N. W. (2017). The iron-dependent mitochondrial superoxide dismutase SODA promotes Leishmania virulence. *J. Biol. Chem.* 292, 12324–12338. doi: 10.1074/jbc.M116.772624.

Roder, C., and Thomson, M. J. (2015). Auranofin: Repurposing an Old Drug for a Golden New Age. *Drugs RD* 15, 13–20. doi: 10.1007/s40268-015-0083-y.

Seidi, A., Muellner-Wong, L. S., Rajendran, E., Tjhin, E. T., Dagley, L. F., Aw, V. Y., et al. (2018). Elucidating the mitochondrial proteome of Toxoplasma gondii reveals the presence of a divergent cytochrome c oxidase. *eLife* 7. doi: 10.7554/eLife.38131.

Srinivasan, S., and Avadhani, N. G. (2012). Cytochrome c oxidase dysfunction in oxidative stress. *Free Radic. Biol. Med.* 53, 1252–1263. doi: 10.1016/j.freeradbiomed.2012.07.021.